AD_____

Award Number: DAMD17-01-1-0439

TITLE: The Role of the Chk1 Kinase in Cell Cycle Checkpoint Response in Breast Epithelial Cells

PRINCIPAL INVESTIGATOR: Matthew D. Westfall
Jennifer A. Pietenpol, Ph.D.

CONTRACTING ORGANIZATION: Vanderbilt University Medical Center
Nashville, Tennessee 37232-2103

REPORT DATE: August 2003

TYPE OF REPORT: Annual Summary

PREPARED FOR: U.S. Army Medical Research and Materiel Command
Fort Detrick, Maryland 21702-5012

REPORT DOCUMENTATION PAGE

Form Approved
OMB No. 074-0188

1. AGENCY USE ONLY (Leave blank)	2. REPORT DATE	3. REPORT TYPE AND DATES COVERED
	August 2003	Annual Summary (1 Aug 01-31 Jul 03)

4. TITLE AND SUBTITLE
The Role of the Chk1 Kinase in Cell Cycle Checkpoint Response in Breast Epithelial Cells

5. FUNDING NUMBERS
DAMD17-01-1-0439

6. AUTHOR(S)
Matthew D. Westfall, Ph.D.
Jennifer A. Pietenpol, Ph.D.

7. PERFORMING ORGANIZATION NAME(S) AND ADDRESS(ES)
Vanderbilt University Medical Center
Nashville, Tennessee 37232-2103

E-Mail: m.westfall@vanderbilt.edu

8. PERFORMING ORGANIZATION REPORT NUMBER

9. SPONSORING / MONITORING AGENCY NAME(S) AND ADDRESS(ES)
U.S. Army Medical Research and Materiel Command
Fort Detrick, Maryland 21702-5012

10. SPONSORING / MONITORING AGENCY REPORT NUMBER

11. SUPPLEMENTARY NOTES
Original contains color plates. All DTIC reproductions will be in black and white.

12a. DISTRIBUTION / AVAILABILITY STATEMENT
Approved for Public Release; Distribution Unlimited

12b. DISTRIBUTION CODE

13. ABSTRACT (Maximum 200 Words)

p63 is a recently identified homolog of p53 that is found in the basal layer of several epithelial tissues such as the epidermis, oral mucosa, prostate, urogenital tract, and **mammary gland**. Studies with p63-/-mice and analysis of several human autosomal dominant disorders with germline p63 mutations suggest p63 involvement in maintaining epithelial stem cell populations. However, the biochemical mechanisms by which p63 functions are not well understood. The goals of the current study were to determine the splice variants that are expressed in primary human mammary epithelial cells (HMECs) and the biochemical activity p63 has in these epithelial cell populations. Progress to date includes (i) Cloning of p63 splice variants and development of assay systems in primary epidermal cell cultures to analyze p63 expression and biochemical activity; (ii) determining that p63 represses transcription and binds directly to p53 consensus sites in the p21 and 14-3-3σ promoters *in vitro* and *in vivo* in HEKs and HMECs; (iii) development of optimal growth conditions for primary human mammary epithelial cells; (iv) determining that ΔNp63α is the predominant splice variant expressed in HMECs; (v) determining that ΔNp63α is a phosphoprotein and how phosphorylation affects p63 function. It is critical to obtain a more thorough understanding of how p63 works at the molecular level in HMECs to better understand the role of p63 in breast cancer development.

14. SUBJECT TERMS
No subject terms provided.

15. NUMBER OF PAGES
67

16. PRICE CODE

17. SECURITY CLASSIFICATION OF REPORT	18. SECURITY CLASSIFICATION OF THIS PAGE	19. SECURITY CLASSIFICATION OF ABSTRACT	20. LIMITATION OF ABSTRACT
Unclassified	Unclassified	Unclassified	Unlimited

Table of Contents

INTRODUCTION:

The importance of p63 to mammalian epithelia cells was first noticed with generation of p63-/- mice. **The p63-/- mice are born, but die shortly after birth, and are completely deficient in mammary gland development (2, 5).** Subsequent studies showed p63 expressed in breast myoepithelial cells and certain subsets of breast neoplasias (1, 3, 4). Because p63 has been implicated in the maintenance of the stem cell population in the basal layer of stratified epithelium, we hypothesize that p63 may function as a dominant negative in suppressing p53 signaling in numerous epithelial tissues, including the mammary gland. In support of this, we found several splice variants of p63 RNA expressed in normal keratinocytes and tumor cells of the head and neck, but only one of these splice variants (ΔNp63α), which lacks a transactivation domain, was found to be expressed at the protein level. Several studies have suggested this role for p63 regulation of p53 signaling, but conclusive data demonstrating p63 binding to p53 consensus DNA sites *in vivo*, and negative regulation of p53 mediated transcription, has only recently been shown.

Current work is now focused on evaluating the effect of p63 on p53 signaling, as well as identifying novel p63 regulated genes, in normal and tumor derived mammary epithelium. Elucidation of the p63 mechanism of action in this model system should provide a better understanding of the development of epithelial tumors in tissues that express p63 such as breast, cervix, prostate, and skin.

BODY:

Specific Aim#1 from the revised statement of work (submitted at the midterm report) has been completed. The goals and conditions were accomplished in both human epidermal keratinocytes (HKs) and human mammary epithelial cells (HMECs). See attached manuscript published in "Molecular and Cellular Biology" and attached manuscript submitted to "Journal of Biological Chemistry"

Specific Aim#2 from the revised statement of work focused on 1) determining p63 splice variants expressed in HMECs and how expression changes during senescence and after genotoxic stress and 2) determining if p63 binds directly to p53 consensus sites in HMECs *in vivo*. Similar to results with the HKs we determined that ΔNp63α is the predominant splice variant expressed in HMECs and using chromatin

immunoprecipitation assays we also determined that ΔNp63α binds p53 consensus sites *in vivo* (see attached manuscript submitted to Journal of Biological Chemistry). Additionally, we have determined changes to ΔNp63α protein levels in HMECs after genotoxic stress (see attached manuscript submitted to Journal of Biological Chemistry). However, we are continuing experiments to examine regulation of p63 during senescence and have not completed this portion of the aim at this time.

Specific Aim#3 from the revised statement of work focused on examining the role of p63 phosphorylation in HMECs. Much of this section of work has been completed (see attached manuscript submitted to Journal of Biological Chemistry). Briefly, we have determined by one-dimensional gel electrophoresis that ΔNp63α is phosphorylated in rapidly proliferating HMECs and after certain genotoxic stresses. Additionally, we have determined that phosphorylation of ΔNp63α after Taxol treatment, a chemotherapeutic commonly used to treat breast cancer, does not affect ΔNp63α subcellular localization, DNA binding, or stability. These results suggest that phosphorylation affects ΔNp63α activity directly or alters association with other transcriptional regulatory factors. Additional experiments are currently being performed to further analyze phosphorylation of ΔNp63α by two-dimensional electrophoresis and mass spectrometry (see attached manuscript to Virology for previous work with two-dimensional electrophoresis of p53).

KEY RESEARCH ACCOMPLISHMENTS:

- Cloned and subsequently analyzed p63 expression in a primary epithelial cell model system.

- Determined that ΔNp63α functions as a transcriptional repressor.

- Determined through *in vitro* and *in vivo* DNA binding assays that ΔNp63α bound to both p53 consensus binding sites in the 14-3-3σ and p21 promoters in human epidermal keratinocytes and **human mammary epithelial cells.**

- Optimized growth conditions for human mammary epithelial cells.

- Determined that ΔNp63α is a phospho-protein in human epidermal keratinocytes and **human mammary epithelial cells.**

•Determined that altered phosphorylation of ΔNp63α does not affect subcellular localization, DNA binding, or short-term stability in human epidermal keratinocytes and **human mammary epithelial cells.**

REPORTABLE OUTCOMES:

•Westfall, M.D., Mays, D.J., Sniezek, J.C., Pietenpol, J.A. (2003) The ΔNp63α phosphoprotein binds the p21 and 14-3-3σ promoters *in vivo* and has transcriptional repressor activity that is reduced by Hay-Wells syndrome-derived mutations.
Molecular and Cellular Biology, 2003. 23(7) 2264-2276.

• Westfall M.D., Pietenpol, J.A. (2003) Microtubule disruption causes phosphorylation of ΔNp63α but does not alter ΔNp63α subcellular localization or DNA binding ability. Journal of Biological Chemistry (submitted)

CONCLUSIONS:

The main objective of this research is to test the hypothesis that **that p63 sustains the proliferative capacity of the basal cells in normal human mammary epithelium through sequence-specific DNA binding to promoter regions of select growth regulatory genes.** Primarily, our research goal is to determine the biochemical activity in human mammary epithelial cells and determine if this activity contributes to breast cancer development. The results described above and in the attached manuscripts suggest that ΔNp63α functions to repress growth inhibitory genes which are upregulated by the tumor suppressor p53 in response to genotoxic stress. Because evidence exists that breast tumor cells with defective DNA damage checkpoint function (usually due to mutation or loss of the p53 gene) have increased sensitivity to anticancer agents, it is critical to understand the molecular basis for ΔNp63α function and regulation since ΔNp63α may function to repress growth inhibitory genes in breast cancer cells. This will be important in determining whether p63 activity dictates the type of therapy for breast cancer patients. Highlighting this point, we have determined that certain chemotherapeutic agents modify ΔNp63α post-translationally and thus may further complicate the choice of therapy.

Additionally, the results from our studies will have to be evaluated in the context of p53 status. Since p53 is the most frequent genetic alteration in breast cancer, it will be important to determine if p63 activity is involved in the development of breast cancer in cells with or without wild-type p53.

References:

1. **Barbareschi, M., L. Pecciarini, M. G. Cangi, E. Macri, A. Rizzo, G. Viale, and C. Doglioni.** 2001. p63, a p53 homologue, is a selective nuclear marker of myoepithelial cells of the human breast. Am J Surg Pathol **25:**1054-60.
2. **Mills, A. A., B. H. Zheng, X. J. Wang, H. Vogel, D. R. Roop, and A. Bradley.** 1999. *p63* is a *p53* homologue required for limb and epidermal morphogenesis. Nature **398:**708-713.
3. **Reis-Filho, J. S., and F. C. Schmitt.** 2002. Taking advantage of basic research: p63 is a reliable myoepithelial and stem cell marker. Adv Anat Pathol **9:**280-9.
4. **Wang, X., I. Mori, W. Tang, M. Nakamura, Y. Nakamura, M. Sato, T. Sakuri, and K. Kakudo.** 2002. p63 Expression in Normal, Hyperplastic and Malignant Breast Tissues. Breast Cancer **9:**216-219.
5. **Yang, A., R. Schweitzer, D. Sun, M. Kaghad, N. Walker, R. Bronson, C. Tabin, A. Sharpe, D. Caput, C. Crum, and F. McKeon.** 1999. p63 is essential for regenerative proliferation in limb, craniofacial and epithelial development. Nature **398:**714-718.

Appendices:

See Attached

List of Personnel:

Matthew Westfall

Matthew D. Westfall

Curriculum Vitae

PERSONAL INFORMATION

Laboratory Address:
652 Preston Research Building
2220 Pierce Avenue
Vanderbilt University
Nashville, TN 37232-6838
Phone: (615) 936-1513
Fax: (615) 936-1790
E-mail: m.westfall@vanderbilt.edu

Home Address:
205 Acklen Park Dr. Apt#9
Nashville, TN 37203
Phone: (615) 460-9804

EDUCATION

1990	**B.S.**, Biology, Rhodes College, Memphis, TN
2003	**Ph.D.**, Vanderbilt University-Department of Biochemistry, Nashville, TN

HONORS AND AWARDS

1990-1994	Academic Sholarship, Rhodes College

RESEARCH/WORK EXPERIENCE

1994-1997	**Cytometry Associates**, Brentwood, TN; Project director for Biopharmaceutical Support Services. Performed antibody research and development for fluorescent activated cell sorting applications. Gained extensive experience with cell surface markers and cell sorting using the FACStar, FACSCalibur, and Orthocytoron instrumentation.
1997-2003	**Ph.D. Dissertation,** Vanderbilt University -Department of Biochemistry, Nashville, TN (Mentor: Jennifer A. Pietenpol, Ph. D.) Analysis of p63 in Keratinocyte Growth and Differentiation: Identification of ΔNp63α as a Transcritptional Repressor

FELLOWSHIPS/GRANTS

1998-2000	National Cancer Institute (2T32CA09385), Virus, Nucleic Acids, and Cancer; Institutional Training Grant (P.I. Ruley, E.)
2001-2003	Department of Defense Breast Cancer Research (DAMD17-01-1-0439); Predoctoral Traineeship Award The Role of the Chk1 Kinase in Cell Cycle Checkpoint Response in Breast Epithelial Cells

PROFESSIONAL SOCIETY MEMBERSHIP

2001-Present Associate member American Association for Cancer Research (AACR)

PUBLICATIONS

Westfall MD, Mays DJ, Sniezek JC, Pietenpol JA (2003). The ΔNp63α phosphoprotein binds the p21 and 14-3-3σ promoters *in vivo* and has transcriptional repressor activity that is reduced by Hay-Wells syndrome-derived mutations. *Mol Cell Biol.* 23: 2264-76.

Stewart Z, **Westfall MD**, Pietenpol JA (2003). Cell-cycle dysregulation and anticancer therapy. *Trends Pharmacol Sci.* 24: 139-45

Eichten A, **Westfall M**, Pietenpol JA, Munger K (2002). Stabilization and functional impairment of the tumor suppressor p53 by the human papillomavirus type 16 E7 oncoprotein. *Virology.* 295: 74-85.

Flatt PM, Polyak K, Tang LJ, Scatena CD, **Westfall MD**, Rubinstein LA, Yu J, Kinzler KW, Vogelstein B, Hill DE, Pietenpol JA (2000). p53-dependent expression of PIG3 during proliferation, genotoxic stress, and reversible growth arrest. *Cancer Lett.* 156: 63-72.

CONFERENCE ABSTRACTS

Westfall MD, Mays DJ, Sniezek JC, Pietenpol JA (2002). Department of Defense: Era of Hope Meeting, Orlando, FL.
Functional Characterization of the p53 homologue p63

Westfall MD, Mays DJ, Sniezek JC, Pietenpol JA (2001). American Association for Cancer Research: Pathobiology of Cancer, Keystone, CO.
Analysis of the p53 Homologue p63

MOLECULAR AND CELLULAR BIOLOGY, Apr. 2003, p. 2264–2276 Vol. 23, No. 7
0270-7306/03/$08.00+0 DOI: 10.1128/MCB.23.7.2264–2276.2003

The ΔNp63α Phosphoprotein Binds the p21 and 14-3-3σ Promoters In Vivo and Has Transcriptional Repressor Activity That Is Reduced by Hay-Wells Syndrome-Derived Mutations

Matthew D. Westfall, Deborah J. Mays, Joseph C. Sniezek,† and Jennifer A. Pietenpol*

Department of Biochemistry, Center in Molecular Toxicology, The Vanderbilt-Ingram Comprehensive Cancer Center, Vanderbilt University School of Medicine, Nashville, Tennessee 37232

Received 17 July 2002/Returned for modification 21 August 2002/Accepted 2 January 2003

p63 is a recently identified homolog of p53 that is found in the basal layer of several stratified epithelial tissues such as the epidermis, oral mucosa, prostate, and urogenital tract. Studies with $p63^{-/-}$ mice and analysis of several human autosomal-dominant disorders with germ line p63 mutations suggest p63 involvement in maintaining epidermal stem cell populations. The p63 gene encodes six splice variants with reported transactivating or dominant-negative activities. The goals of the current study were to determine the splice variants that are expressed in primary human epidermal keratinocytes (HEKs) and the biochemical activity p63 has in these epithelial cell populations. We found that the predominant splice variant expressed in HEKs was ΔNp63α, and it was present as a phosphorylated protein. During HEK differentiation, ΔNp63α and p53 levels decreased, while expression of p53 target genes p21 and 14-3-3σ increased. ΔNp63α had transcriptional repressor activity in vitro, and this activity was reduced in ΔNp63α proteins containing point mutations, corresponding to those found in patients with Hay-Wells syndrome. Further, we show that ΔNp63α and p53 can bind the p21 and 14-3-3σ promoters in vitro and in vivo, with decreased binding of p63 to these promoters during HEK differentiation. These data suggest that ΔNp63α acts as a transcriptional repressor at select growth regulatory gene promoters in HEKs, and this repression likely plays an important role in the proliferative capacity of basal keratinocytes.

Recently, p63 and p73, two p53 homologues, were identified (2, 27, 39, 54, 57). These proteins exhibit a high sequence and structural homology to the p53 protein. Each gene encodes an amino-transactivating domain, a core DNA-binding domain, and a carboxy-oligomerization domain. However, there are significant differences between these homologues and p53. Both p63 and p73 genes contain two transcriptional start sites that are used to generate transcripts that encode proteins with or without an amino-transactivating domain. Proteins with the transactivating domain are termed TAp63 or TAp73, and proteins lacking the transactivation domain are termed ΔNp63 or ΔNp73. In addition, both genes can be alternatively spliced to generate proteins with different carboxy termini. For example, six splice variants can be generated from the two promoters of the p63 gene with three different C termini termed α, β, and γ (7, 57). The p63α and p73α proteins also contain an additional region not found in p53 known as a sterile alpha motif (SAM) domain. This domain is found in the α form of p63 and p73 (27, 57) and is a protein-protein interaction domain implicated in developmental processes (46, 53).

In addition to the structural differences within the p53 gene family, differing functional properties were discovered. These differences became apparent after analysis of $p63^{-/-}$ and $p73^{-/-}$ mice. Whereas $p53^{-/-}$ mice are developmentally normal but prone to neoplastic disease (14), the $p63^{-/-}$ and $p73^{-/-}$ mice have severe developmental abnormalities. The $p63^{-/-}$ mice are born but die shortly after birth and are deficient in the development of limbs and several epithelial tissues such as skin, prostate, mammary gland, and urothelia (36, 58). The $p73^{-/-}$ mice exhibit neurological, pheromonal, and inflammatory defects (59).

The p63 protein is localized to the nucleus of basal cells of stratified epithelia such as skin, oral mucosa, cervix, vaginal epithelium, urothelium, prostate, breast, and other tissues (12, 13, 57). The ΔNp63α splice variant is the predominant, if not the only, form expressed in these basal epithelial cells (13, 41, 57). Ectopic expression of the ΔN splice variants can decrease p53 target gene promoter activity, suggesting a role for ΔNp63α in maintaining the proliferative capacity of cells by repressing p53 target genes involved in growth arrest (27, 57). This hypothesis is supported by the data of Parsa et al. and Pellegrini et al. showing that a decrease in p63 was associated with a reduced proliferative potential and subsequent terminal differentiation of skin keratinocytes (41, 42).

We analyzed here the role of p63 in primary human epidermal keratinocyte (HEK) differentiation. Our results indicate that ΔNp63α is the predominant form of p63 protein expressed in primary cultures of HEKs and is downregulated during differentiation. We also show that ΔNp63α is a phosphoprotein that can function as a transcriptional repressor and bind consensus p53-binding sites in the $p21^{waf1}$ (p21) and 14-3-3σ promoters in vivo.

* Corresponding author. Mailing address: 652 Medical Research Building II, The Vanderbilt-Ingram Comprehensive Cancer Center, Vanderbilt University School of Medicine, Nashville, TN 37232-6838. Phone: (615) 936-1512. Fax: (615) 936-2294. E-mail: jennifer.pietenpol@vanderbilt.edu.

† Present address: Head and Neck Oncologic Surgery, MCHK-DSH, Tripler Army Medical Center, Honolulu, HI 96859.

MATERIALS AND METHODS

Cell culture and treatment. Second-passage primary HEKs were obtained from the Vanderbilt Skin Disease Research Core. HEKs were isolated as previously described (17) and were cultured in EpiLife M-EPI-500 keratinocyte growth medium (Cascade Biologics, Portland, Oreg.) supplemented with human keratinocyte growth supplement S-001-5 (Cascade Biologics) and 0.06 mM $CaCl_2$. The human colorectal carcinoma cell lines HCT116 and RKO were cultured in Dulbecco modified Eagle medium supplemented with 10% fetal calf serum and 1% penicillin-streptomycin. The human embryonic kidney cell line 293 was kindly provided by S. Hiebert (Vanderbilt University Department of Biochemistry, Nashville, Tenn.) and cultured in Dulbecco modified Eagle medium supplemented with 10% fetal calf serum and 1% penicillin-streptomycin. All cells were cultured at 37°C with 5% CO_2.

p63 cloning. ΔNp63 splice variants, α, β, and γ were cloned from primary human oral mucosa. Tissue was obtained from patient specimens collected at Vanderbilt University School of Medicine. The Access RT-PCR system (Promega, Madison, Wis.) was used with mRNA isolated from the primary human oral keratinocytes. Primers used to generate the splice variants were as follows: ΔNp63 N-terminal 5′-CCCAAGCTTAATACGACTCACTATAGGGA GACCATGGAACAAAAACTCATCTCAGAAGAGGATCTGATGTTGTAC CTGGAAAACAATG-3′, ΔNp63α C-terminal 5′-CGGGATCCTCACTCCCCC TCCTCTTTG-3′, ΔNp63β C-terminal 5′-CGGGATCCTCAGACTTGCCAGA TCCTG-3′, and ΔNp63γ C-terminal 5′-CGGGATCCCTATGGGTACACTGA TCGG-3′. The N-terminal primer also encodes for an in frame myc-epitope tag. p63 splice variants were subsequently cloned into the pCEP4 vector (Invitrogen, Carlsbad, Calif.) for transient transfections.

HEK differentiation assays. HEKs were grown to ~90% confluency, washed twice with phosphate-buffered saline (PBS), and induced to differentiate by the addition of 1 mM $CaCl_2$ in growth factor-deficient medium. Cells were harvested at days 0, 2, 4, 6, and 8 after the induction of differentiation. Culture medium was changed every 2 days. Cells were harvested as described for Western and Northern analyses.

Protein lysate preparation and Western analysis. Dishes (100 mm) of primary HEKs were washed twice with ice-cold PBS, and harvested by scraping into 750 μl of kinase lysis buffer (KLB; 50 mM Tris-HCl [pH 7.4], 150 mM NaCl, 0.1% Nonidet P-40, 0.1% Triton X-100, 4 mM EDTA, 1 mM dithiothreitol [DTT]) containing the phosphatase inhibitors 50 mM NaF, 0.2 mM sodium vanadate, 10 mM *p*-nitrophenyl phosphate, and 10 mM β-glycerophosphate and the protease inhibitors antipain (10 μg/ml), leupeptin (10 μg/ml), pepstatin A (10 μg/ml), chymostatin (10 μg/ml; Sigma), and 4-(2-aminoethyl)-benzenesulfonylfluoride (200 μg/ml; Calbiochem, San Diego, Calif.). Cells were incubated on ice 30 to 45 min, and the protein supernatant was clarified by centrifugation at 13,000 × *g* for 10 min at 4°C. Protein concentration was determined by the Bio-Rad protein quantification kit (Bio-Rad Laboratories, Hercules, Calif.). Western analysis was performed as previously described (17) with the following primary antibodies: α-p63 monoclonal antibody Ab-1 (Oncogene Research Products, Calbiochem), α-p53 monoclonal antibody Ab-2 (Oncogene Research Products, Calbiochem), α-$p21^{Waf1}$ antibody Ab-1 (Oncogene Research Products, Calbiochem), α-14-3-3σ polyclonal antibody N-14 (Santa Cruz Biotechnology, Inc., Santa Cruz, Calif.), α-β-actin polyclonal antibody I-19 (Santa Cruz), and α-Gal4 monoclonal antibody DBD-RK5C1 (Santa Cruz). Uniformity of protein loading was assessed by β-actin analyses, as well as by fast green staining of the membranes.

Northern analysis. Dishes (150 mm) of HEK cells were harvested for mRNA isolation as previously described (18). mRNA (1 to 3 μg) was lyophilized, resuspended in sample buffer (1× morpholinepropanesulfonic acid [MOPS]; 0.1 M MOPS [pH 7.0], 40 mM sodium acetate, 5 mM EDTA [pH 8.0], 50% formamide, 6.5% formaldehyde), and heated at 55°C for 15 min. A 10× loading buffer (50% glycerol, 1 mM EDTA, 0.25% bromophenol blue, 0.25% xylene cyanol, 0.3 mg of ethidium bromide per ml) was added to the sample at a 1× concentration, and mRNA was resolved by gel electrophoresis on a 1% agarose gel containing 2% formaldehyde and 1× MOPS. The gel was washed two times for 40 min each time in 10× SSC buffer (1× SSC is 0.15 M NaCl plus 0.015 M sodium citrate) buffer, and mRNA was transferred to a supported nitrocellulose membrane (Gibco-BRL). ΔNp63, p53, 14-3-3σ, p21, and cyclophilin cDNAs were labeled with [α-^{32}P]dCTP by using Prime-It II (Stratagene, La Jolla, Calif.). After a 2-h prehybridization in Express Hyb (Clontech Laboratories, Inc., Palo Alto, Calif.), membranes were incubated 1 h with 10^6 cpm of labeled cDNA per ml in Express Hyb. Membranes were washed two times for 1 min each time at room temperature in 0.1× SSC–0.1% sodium dodecyl sulfate (SDS), followed by 1 h in 0.3 × SSC–0.1% SDS. Blots were subsequently exposed for autoradiography.

Phosphatase assay. p63 was immunoprecipitated from HEK protein lysates (75 μg of control or 150 μg of differentiation day 4) by rocking at 4°C for 1 h in KLB with a p63 antibody (H-129; Santa Cruz) and 15-μl bed volume of protein A-Sepharose (PAS; Amersham Biosciences Corp., Piscataway, N.J.). Immunoprecipitates were washed once with KLB and twice with phosphatase buffer (50 mM Tris [pH 8.0], 10% glycerol). Samples were resuspended in 20 μl of phosphatase buffer with or without phosphatase inhibitors. A total of 40 U (2 μl of 20 U/μl) of calf intestinal alkaline phosphatase (CIAP; Roche, Indianapolis, Ind.) was added, and samples were incubated 37°C for 3 h. The phosphatase reaction was stopped by the addition of Laemmli SDS sample buffer. The control and phosphatase-treated lysates were analyzed by Western blotting.

Luciferase assays. HCT116 cells were transiently transfected with the p21-luciferase reporter constructs and expression vectors encoding p53, ΔNp63α, or Gal4-ΔNp63α. p21-luciferase was kindly provided by B. Vogelstein (Johns Hopkins Oncology Center, Baltimore, Md.) (15), and p21-lucΔRE1 was kindly provided by S. Hiebert. The p21-lucΔRE1/RE2 was generated by PCR amplification with the full-length p21-luciferase reporter as a template and the following primers: 5′-CGGGATCCGAGATTTCCAGACTCTGAGC-3′ and 5′-CAGCC GGTCCCGGAACC-3′. The PCR product was cloned into the *Bam*HI-*Pst*I-digested luciferase reporter vector. 293 cells were transiently transfected with a Gal4 DNA-binding domain–TK–luciferase reporter construct (kindly provided by S. Hiebert) previously described (47) and Gal4-p63 fusion constructs. Gal4-p63 fusion cDNAs were cloned into the pM2/pY2 vector at the *Sal*I-*Hin*dIII sites. The following primers were used to generate the Gal4-p63 cDNAs: Gal4-ΔNp63 N-terminal 5′-ACGCGTCGACTTGTACCTGGAAAACAATG-3′, ΔNp63α C-terminal 5′-CCCAAGCTTTCACTCCCCCTCCTCTTTG-3′, ΔNp63β C-terminal 5′-CCCAAGCTTTCAGACTTGCCAGATCCTG-3′, ΔNp63γ C-terminal 5′-CCCAAGCTTCTATGGGTACACTGATCGG-3′, Gal4-SAM N-terminal 5′-ACGCGTCGACCCTCCGTATCCCACAGAT-3′, and Gal4-SAM C-terminal 5′-CCCAAGCTTTCAGAATTCGTGGAGCTGCCG-3′. Gal4-ΔNp63α SAM domain point mutants (35) were kindly provided by H. van Bokhoven (Department of Human Genetics, University Hospital, Nijmegen, The Netherlands) and served as templates to generate additional Gal4 fusion cDNAs with the above primers. All transfections were performed with Lipofectamine (Gibco-BRL), and cells were harvested 24 to 48 h after transfection. Luciferase activity measurements were performed by using the dual-luciferase assay kit (Promega).

DNA-binding assay. Radiolabeled oligonucleotide duplexes containing the two p53 DNA-binding sites of p21 and 14-3-3σ were generated by using the following oligonucleotides: p21 site 1, 5′-TGGCCATC AGGAACATGTCCCA ACATGTTGAGCTCTGGCA-3′; p21 site 2, 5′-TAGAGGAAGAAGACTGG GCATGTCTGGGCAGAGATTTCCA-3′; 14-3-3σ site 1, 5′-CTGGGACTACA GGCATGTGCCACCATGCCCGGCTAATTTT-3′; and 14-3-3σ site 2, 5′-TG GAAACCCTGTAGCATTAGCCCAGACATGTCCCTACTCCTCC-3′. For end labeling, 500 ng of each oligonucleotide were incubated with 167 μCi of [γ-^{32}P]ATP and T4 polynucleotide kinase (New England Biolabs, Beverly, Mass.) in kinase buffer (70 mM Tris [pH 7.6], 10 mM $MgCl_2$, 5 mM DTT) for 2 h at 37°C. DNA was ethanol precipitated two times, allowed to air dry, and resuspended in 100 μl of annealing buffer (20 mM Tris [pH 7.5], 2 mM $MgCl_2$, 50 mM NaCl). The complementary oligonucleotides for each binding site were mixed, boiled for 5 min, and allowed to anneal.

The human large cell lung carcinoma cell line H1299, which does not express p53 or p63 protein, was transfected with pCEP4 expression vectors encoding either myc-tagged p53 or myc-tagged p63 proteins or with the empty pCEP4 expression vector (Invitrogen). Western analyses of the transfected cell lysates with α-myc antibody (clone 9E-10) were performed, and p53 and p63 were quantified in triplicate by using a Fluor-S Max MultiImager (Bio-Rad Laboratories). Equivalent amounts of p53 and p63 protein were immunoprecipitated by rocking at 4°C for 1 h in DNA binding buffer (DBB; 20 mM Tris [pH 7.2], 100 mM NaCl, 10% glycerol, 1% Nonidet P-40) with the myc antibody and a 15-μl bed volume of PAS (Amersham Biosciences). Immunoprecipitated proteins were washed twice with DBB and then once in DBB containing 1 mM DTT. The immunopurified protein was rocked for 1 h at 4°C in 100 μl of DBB with 2×10^6 cpm of α-^{32}P-labeled DNA fragments prepared as described above. The protein-DNA complexes were rocked for 1 h at 4°C with 10 μg of poly(dI-dC) (Roche). After three washes with DBB, the proteins were digested with SDS-proteinase K (VWR Scientific Products, West Chester, Pa.) in TE8 (20 mM Tris [pH 8.0], 10 mM EDTA) for 30 min at 55°C prior to electrophoresis on 10% polyacrylamide gels (acrylamide-bisacrylamide [19:1]) at 40 V. Radiolabeled DNA was quantified by using an Instant Imager (Packard Instrument Company, Downers Grove, Ill.).

Formaldehyde cross-linking. Growth medium was aspirated from ~5×10^6 cells, and cell cultures were washed with PBS and incubated with a 1.6% formaldehyde (EM Sciences) solution in PBS for 13 min at room temperature. The cross-linking was terminated by the addition of glycine to a final concentration of 0.144 M for 5 min. Monolayers were washed twice with PBS. Extracts were prepared by scraping cells in 1 ml of radioimmunoprecipitation assay (RIPA)

buffer (150 mM NaCl, 1% Nonidet P-40, 0.5% deoxycholate, 0.1% SDS, 50 mM Tris [pH 8.0], 5 mM EDTA) containing the protease inhibitors antipain (10 μg/ml), leupeptin (10 μg/ml), pepstatin A (10 μg/ml), chymostatin (10 μg/ml), and 4-(2-aminoethyl) benzenesulfonylfluoride (200 μg/ml) and the phosphatase inhibitors 50 mM NaF and 0.2 mM sodium vanadate. Cell lysates were sonicated to yield chromatin fragments of ~600 bp as assessed by agarose gel electrophoresis. Debris was pelleted by centrifugation for 15 min at 13,000 × *g*. The lysate was divided into aliquots, and 0.8 mg of protein extract was precleared with 10 μg of mouse immunoglobulin G bound to PAS for p53 immunoprecipitation or with 20 μg of rabbit immunoglobulin G bound to PAS for p63 immunoprecipitation. Protein lysates were precleared for 1 h at 4°C. After centrifugation for 2 min at 13,000 × *g*, supernatants were transferred to a new tube. A 15-μl bed volume of PAS and 2 μg of α-p53 antibody (Ab-2; Oncogene Research Products) or α-p63 antibody (H129; Santa Cruz) was added to extracts precleared with nonspecific antibodies, and immunoprecipitation was performed by rocking the extracts overnight at 4°C. To control for nonspecific binding during immunoprecipitation, cross-linked lysates were also immunoprecipitated with mouse monoclonal α-cyclin B1 antibody (GNS1; Santa Cruz) or rabbit polyclonal α-Bax antibody (N20; Santa Cruz) that did not cross-react with p53 or p63, respectively.

Immunocomplexes were washed twice with RIPA buffer, four times with immunoprecipitation wash buffer (100 mM Tris [pH 8.5], 500 mM LiCl, 1% Nonidet P-40, 1% deoxycholic acid), and twice more with RIPA buffer. Between washes, samples were rocked for 5 min at 4°C; 200 μl of cross-linking reversal buffer (125 mM Tris [pH 6.8], 10% β-mercaptoethanol, 4% SDS) was added to the washed PAS pellet. Samples were boiled for 30 min to reverse the formaldehyde cross-links. DNA was phenol-chloroform extracted, and the phenol-chloroform phase was back extracted with 10 mM Tris (pH 8.3), ethanol precipitated, allowed to air dry, and dissolved in sterile H_2O.

PCR amplification. p21 site 1 and 14-3-3σ site 1 PCR amplifications were performed in 16.6 mM $(NH_4)_2SO_4$, 0.67 mM Tris (pH 8.8), 6.7 mM $MgCl_2$, 10 mM β-mercaptoethanol, 10% dimethyl sulfoxide, 1.5 mM nucleotides, and 1.25 U of *Taq* polymerase (Promega). A total of 175 ng of each primer was used per 25-μl reaction. Forty-five PCR cycles were performed for p21 site 1, with each cycle consisting of 20 s at 94°C, 45 s at 61°C, and 25 s at 72°C. 14-3-3σ site 1 was amplified by using 45 PCR cycles each consisting of 20 s at 94°C, 45 s at 57.5°C, and 25 s at 72°C. p21 site 2 and 14-3-3σ site 2 PCR amplifications were performed by using Ready-To-Go PCR beads (Amersham Biosciences) according to the manufacturer's directions with a final primer concentration of 0.4 μM. Thirty PCR cycles were performed for p21 site 2. Each cycle consisted of 30 s at 95°C, 45 s at 66°C, and 25 s at 72°C. Thirty-eight PCR cycles were performed for 14-3-3σ site 2. Each cycle consisted of 20 s at 94°C, 45 s at 61°C, and 25 s at 72°C. GAPDH (glyceraldehyde-3-phosphate dehydrogenase) PCR amplification was performed in 10 mM Tris (pH 9.0), 50 mM KCl, 0.1% Triton-X, 0.5 mM $MgCl_2$, 0.25 mM concentrations of nucleotides, and 1.25 U of *Taq* polymerase (Promega). Each primer was used at 0.2 μM per 25-μl reaction. Thirty-five cycles of PCR were performed for GAPDH amplification, each cycle consisted of 20 s at 94°C, 45 s at 62°C, and 25 s at 72°C. The primers used for PCR amplifications were as follows: p21 site 1, 5′-GCTTGGGCAGCAGGCTG-3′ and 5′-AGCCC TGTCGCAAGGATCC-3′; p21 site 2, 5′-GCAGTGGGGCTTAGAGTGGG G-3′ and 5′-CAGGCTTGGAGCAGCTACAATTAC-3′; 14-3-3σ site 1, 5′-CA TTTAGGCAGTCTGATTCC-3′ and 5′-GCTCACGCCTGTCATCTC-3′; and 14-3-3σ site 2, 5′-CTCACTACCTCAAGATACCC-3′ and 5′-CACAGGCCTG TGTCTCCC-3′. GAPDH was amplified with 5′-CACCAGCCATCCTGTCCT CC-3′ and 5′-GTTCCTTCCCAGCCCCCACT-3′ primers. PCR DNA products were resolved by using 8% polyacrylamide gels (acrylamide-bisacrylamide [19:1]) in 1× Tris acetate-EDTA buffer. Gels were stained with ethidium bromide. Relative levels of DNA were determined by using Quantity One software (Bio-Rad Laboratories).

RESULTS

ΔNp63α is the predominant splice variant expressed at the protein level in primary HEKs. To examine the role p63 plays in rapidly growing and differentiating epithelial cells, we analyzed the specific splice variant(s) expressed in the primary cultures of HEKs. Using well-characterized conditions for in vitro keratinocyte growth (31), we generated protein lysates from HEKs that were rapidly growing or induced to differentiate by the removal of growth factors and the addition of 1 mM $CaCl_2$. This differentiation resulted in increased protein levels of keratinocyte differentiation markers loricrin and involucrin (20), as well as the appearance of a differentiated morphology compared to proliferating cells (Fig. 1A and B). In contrast to the increase in differentiation markers, p63 protein levels decreased during differentiation (Fig. 1C). Since p63 expression has been shown to decrease during keratinocyte terminal differentiation in vivo (57), our in vitro culture system replicated this process.

Previous studies have shown p63 expression in the basal layer of numerous epithelial tissues (57) with the predominant p63 splice variant expressed at the transcript level being ΔNp63α (12, 13, 38, 41, 42). Using reverse transcription-PCR, we generated cDNAs representative of all ΔNp63 splice variants from primary human oral keratinocytes (data not shown). However, when we performed Western analysis to determine the p63 levels in protein extracts harvested from rapidly growing and differentiating epidermal keratinocytes, the ΔNp63α splice variant was the predominant form expressed (Fig. 1C).

Expression vectors encoding myc-tagged ΔNp63α, ΔNp63β, ΔNp63γ, and $\Delta Np40^{AIS}$ were generated and transfected into the colon epithelial cell line, RKO, that does not express p63. Protein lysates were generated from transfected RKO cells to serve as controls for the Western analysis. The predominant p63 protein expressed in the HEKs aligned with ectopically expressed myc-tagged ΔNp63α from RKO cells and decreased during differentiation (Fig. 1C). The faster-migrating cross-reactive band on the immunoblot in Fig. 1C, designated with an asterisk, may represent low-level ΔNp63β expression. We also examined the p63 transcript levels by Northern (Fig. 1D). We only detected one 4.5-kb transcript in mRNA isolated in HEKs and, consistent with our Western analysis results, the level of transcript decreased during differentiation. Due to small differences in cDNA lengths of p63 splice variants, it is possible that the p63 transcript in Fig. 1D represents several splice variants not distinguishable by Northern analysis. However, the Western blot results show that ΔNp63α is the predominant protein expressed in primary cultures of HEKs that are either rapidly growing or induced to differentiate.

Western analysis revealed multiple, slower-migrating bands that cross-reacted with the p63-specific antibody, suggesting that p63 may also be a phosphoprotein (Fig. 1C and 2A). To determine whether the differential migration of ΔNp63α was due to phosphorylation, p63 was immunoprecipitated from HEK protein lysates prepared from rapidly growing and differentiated cells (day 4) and then treated with CIAP in the presence or absence of phosphatase inhibitors (Fig. 2B). Twice the amount of protein was used in the immunoprecipitations of the lysates prepared from day 4 differentiated cultures compared to rapidly growing cultures to allow comparison of equal p63 levels. Western analysis revealed a collapse of the slower-migrating ΔNp63α protein form to a faster-migrating form after CIAP treatment, a finding consistent with the conclusion that p63 is a phosphorylated protein.

Changes in expression of cell cycle regulatory proteins and corresponding transcripts in differentiating keratinocytes. As epidermal cells migrate from the basal layer, they begin the process of terminal differentiation characterized by loss of DNA replication and cell cycle arrest, loss of colony-forming ability, and an increase in cell size (3, 4, 51). Upregulation of the p53 target genes p21 and 14-3-3σ is associated with this

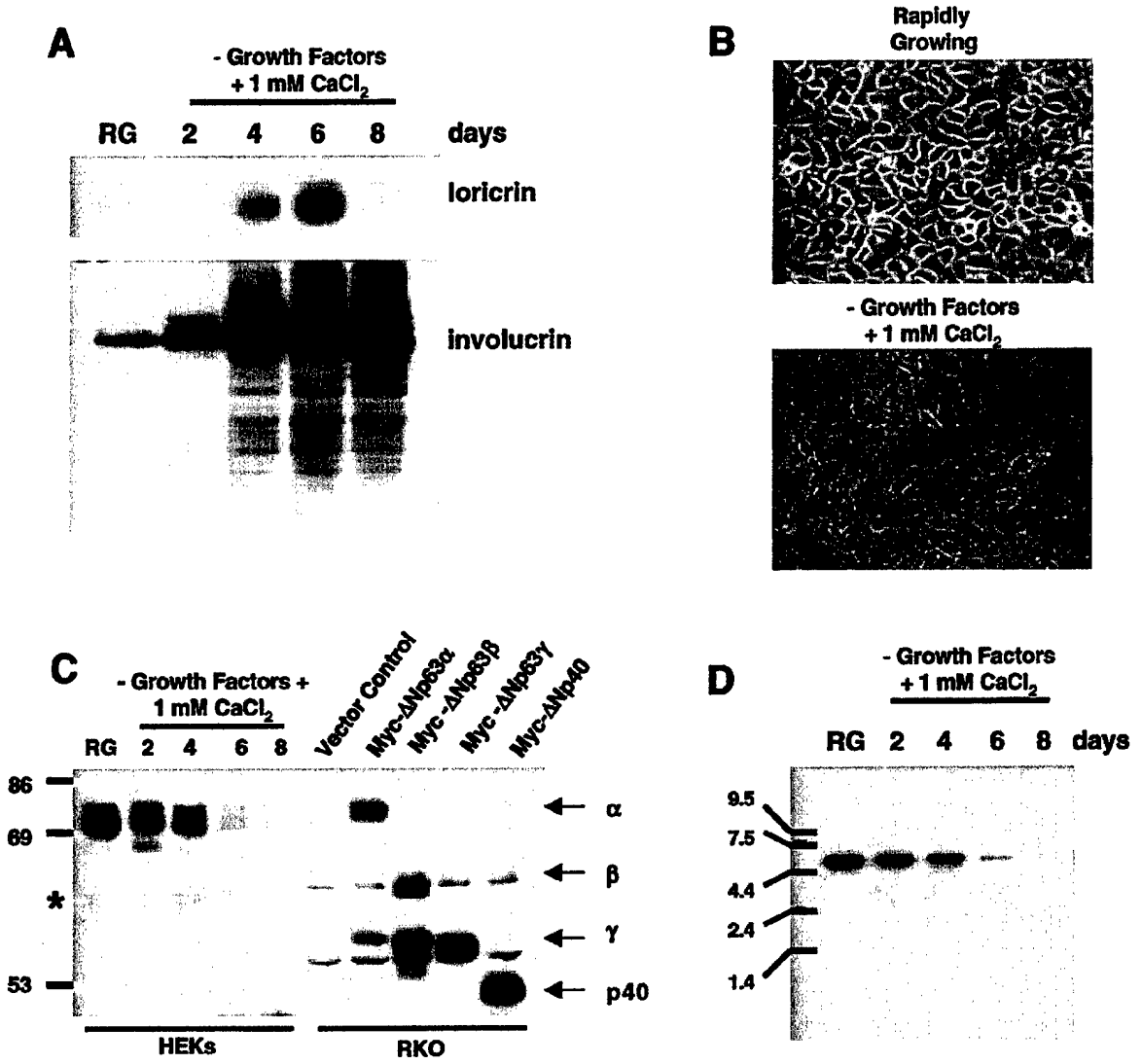

FIG. 1. Differentiation-induced modulation of ΔNp63α protein levels in primary HEKs. HEKs were induced to differentiate as described in Materials and Methods. (A) Western analysis of HEK lysates from rapidly growing and differentiating cells for expression of the terminal differentiation markers loricrin and involucrin. (B) Micrograph of rapidly growing HEKs and HEKs at day 4 after induction of differentiation. (C) Western analysis with antibody Ab-1 for p63 expression in rapidly growing and differentiating HEKs. Myc epitope-tagged ΔNp63 splice variants were ectopically expressed in RKO cells, and lysates were analyzed to serve as molecular weight markers for comparison to HEK p63. The asterisk to the left of the blot aligns with a cross-reactive band that may represent ΔNp63β expression. (D) Northern analysis of p63 transcript expression in HEKs differentiated as in panel A. The results shown are representative of three independent experiments with separate primary cultures of HEKs.

phenomenon (11, 34, 37, 48, 60). p21 is a cyclin-dependent kinase inhibitor originally identified as a p53 target gene and a cyclin/cyclin-dependent kinase-associated protein (15, 22, 23, 56). 14-3-3σ has been linked to p53-dependent regulation of cell cycle progression at the G_2/M transition (6, 24).

We evaluated p21 and 14-3-3σ protein and mRNA levels relative to ΔNp63α and p53 levels during HEK differentiation. Both ΔNp63α and p53 proteins decreased five- and twofold, respectively (Fig. 3A, compare RG and day 8). In contrast, 14-3-3σ and p21 protein levels increased by 2- and 2.8-fold, respectively (Fig. 3A). Similar to the changes in protein levels, ΔNp63α and p53 transcript levels decreased during differentiation (Fig. 3B, compare RG and day 8), and p21 and 14-3-3σ increased as cells differentiated (Fig. 3B). These data suggest that increases in 14-3-3σ and p21 expression during keratinocyte differentiation are due to either increased activity of the remaining p53 protein or loss of ΔNp63α-mediated transcriptional repression resulting from decreased ΔNp63α protein levels.

ΔNp63α represses transcription. Previous studies have shown that ectopic expression of p63 can repress transcription from reporter vectors containing tandem repeats of the p53

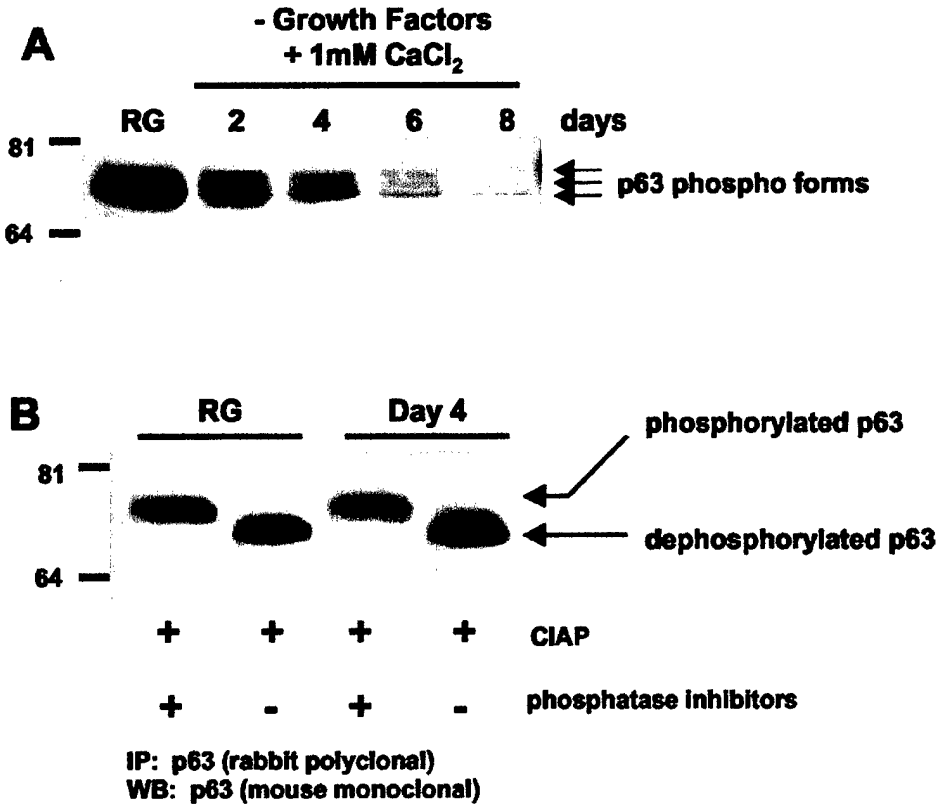

FIG. 2. ΔNp63α is a phosphoprotein. (A) Protein lysates were prepared from rapidly growing and differentiating HEKs and analyzed by Western blotting with mouse monoclonal antibody Ab-1. Arrows denote three differentially migrating ΔNp63α forms. (B) p63 was immunoprecipitated with rabbit polyclonal antibody H129, and immoprecipitates were treated with CIAP in the presence or absence of phosphatase inhibitors. Immunoprecipitated protein was analyzed by Western blotting for p63 by using mouse monoclonal antibody Ab-1. Resolution of the multiple bands by SDS-PAGE in Fig. 2B was not possible due to the percentage of the acrylamide used. The results shown are representative of four independent experiments.

consensus DNA-binding site upstream of a minimal promoter (7, 57). However, the mechanism by which this occurs has not been determined. To explore this mechanism, we analyzed the ability of ΔNp63 splice variants to repress transcription as fusion proteins. We generated expression vectors that encode Gal4-ΔNp63α, -ΔNp63β, and -ΔNp63γ fusion proteins (Fig. 4A). All ΔNp63 splice variants used to generate the fusion proteins were full length. To verify the Gal4 fusion did not impair ΔNp63 activity, we tested the ability of the Gal4-ΔNp63α to repress transcription from a p21-luciferase vector (Fig. 4B). We transiently transfected HCT116 cells with expression vectors encoding ΔNp63α or Gal4-ΔNp63α, as well as the p21-luciferase vector, and found that Gal4-ΔNp63α functions similarly to wild-type ΔNp63α in its ability to inhibit transcription from the p21 promoter (Fig. 4B). Transfection of p53 served as a positive control for activation of the p21 promoter in this assay.

We also determined whether ΔNp63α could function as a dominant-negative inhibitor of p53 transactivation. Cotransfection of expression vectors encoding p53 and ΔNp63α with the p21-luciferase reporter vector resulted in a significant decrease in p53-mediated luciferase expression (Fig. 4B). Further, the ability of ΔNp63α to repress transactivation of the p21 promoter-luciferase vector was dose dependent and was consistent with a dominant-negative activity of ΔNp63α and the previous findings of Yang et al. (57). To determine the necessity of the p53 response elements for the repressive activity of ΔNp63α, we used the assay described above and analyzed p21 promoter deletions that lack either one (p21-lucΔRE1) or both (p21-lucΔRE1/RE2) of the reported p53 response elements in the p21 promoter (15, 16) (Fig. 4C). We transiently transfected the HCT116 cells with an expression vector encoding ΔNp63α and the full-length or deletion mutant p21-luciferase luciferase reporter vectors. Similar to our results in Fig. 4B, ΔNp63α reduced transcriptional activity of the full-length p21-reporter vector by ~45% compared to vector control (Fig. 4D). Loss of one p53 binding site reduced this repression, and loss of both p53 binding sites abrogated the ability of ΔNp63α to repress transcriptional activity from the p21 promoter (Fig. 4D). However, the basal activity of the p21-lucΔRE1/RE2 was significantly lower than that of the full-length p21 promoter reporter.

The results in Fig. 4B established that the Gal4 DNA-binding domain did not impair ΔNp63α function; thus, we analyzed the Gal4-ΔNp63α, -ΔNp63β, and -ΔNp63γ splice variants for their ability to repress transcription. Each Gal4 fusion expression vector was transfected into 293 cells, and the encoded

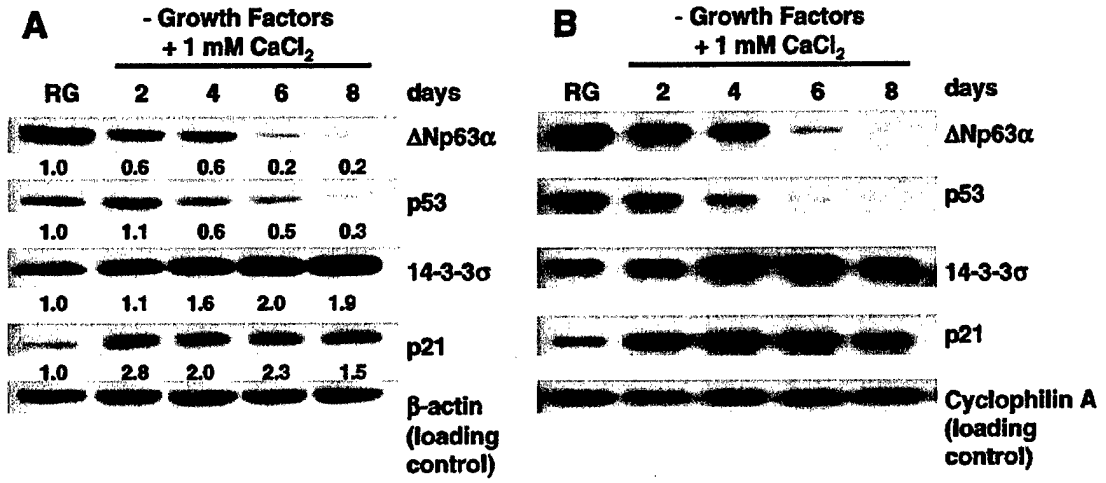

FIG. 3. Differentiation-induced changes in select protein and mRNA levels in primary HEKs. HEKs were induced to differentiate as described in Materials and Methods. (A) Western analysis of p63 (Ab-1), p53 (Ab-2), 14-3-3σ (N-14), and p21 (Ab-1) in rapidly growing and differentiating HEKs with the antibodies listed in Materials and Methods. Note that p63 migrates as a single band due to the use of electrophoresis conditions that allow for analysis of the molecular weight range of proteins shown in panel A. The numbers below the Western panels represent the fold change relative to rapidly growing HEKs. (B) Northern analysis of transcripts for proteins shown in panel A. The results are representative of three independent experiments with independent primary cultures of HEKs.

protein was analyzed for its ability to repress luciferase reporter gene transcription regulated by four Gal4 DNA-binding sites upstream of a thymidine kinase promoter (Fig. 4A). The ΔNp63α splice variant repressed the TK-luciferase reporter construct by ~20-fold, whereas the ΔNp63β did not repress transcription and the ΔNp63γ repressed transcription only by ~5-fold (Fig. 4E). Western analysis of the luciferase assay extracts demonstrated that all ΔNp63 proteins were expressed at similar levels (Fig. 4E, lower panel). These results suggest that the transcriptional repression activity of ΔNp63α is contained within the carboxy terminus of ΔNp63α that contains the SAM domain. All three splice variants bind DNA in in vitro assays (data not shown), indicating that the loss of repression may be due to loss of protein-protein interactions within the carboxy terminus of the ΔNp63α splice variant. Transfection of Gal4-ETO2, a previously described transcriptional corepressor protein (1), served as a positive control for repression of the luciferase reporter vector. These data demonstrate that ΔNp63α can repress transcription directly or through recruitment of transcriptional corepressor molecules.

Analysis of SAM domain mutations. Recent genetic studies link p63 to the proper development of limbs, ectodermal appendages, and the lip and palate in humans (5, 35). Specifically, the autosomal-dominant disorder, ankyloblepharon-ectodermal dysplasia-clefting syndrome or Hay-Wells syndrome, is characterized by point mutations within the SAM domain of p63α splice variants (35). To further explore a potential role of the SAM domain in transcriptional repression, we generated expression vectors encoding Gal4-ΔNp63α fusion proteins containing SAM domain point mutations corresponding to mutations found in the p63 gene of individuals with Hay-Wells syndrome. The four point mutations—L459F, G475V, T478P, and Q481L—and a corresponding wild-type fusion expression vector were generated by using murine p63 (Fig. 4A). Murine p63 was previously used for analysis of SAM domain point mutations by McGrath et al. (35). As before, each vector was transiently transfected into 293 cells and analyzed for its ability to repress transcription from the reporter vector shown in Fig. 4A. Wild-type murine ΔNp63α repressed transcription ~13-fold (Fig. 4F). This level of repression activity is similar to that observed with human ΔNp63α protein (Fig. 4E). In the context of full-length ΔNp63α, the SAM domain point mutants repressed transcription ~7- to 10-fold, suggesting that these mutations led to a reduction of p63 activity rather than complete loss of function. Western analysis of the protein lysates used in this assay demonstrated that all mutant proteins were expressed at relatively equal, if not greater, levels than wild-type ΔNp63α. These results suggest that the difference in activity between wild-type and SAM domain point mutant proteins was not due to differences in protein expression (Fig. 4F, lower panel). Because of the reduced activity of the SAM domain mutant proteins, we generated and analyzed a human Gal4-SAM fusion protein for analysis in the repression assay. The results presented in Fig. 4E indicate that the SAM domain alone is not sufficient to repress transcription but is likely required for repressor activity in the context of the C-terminal domain of ΔNp63α.

Relative binding affinities of ΔNp63α and p53 to p53 consensus DNA-binding sites. The p53 protein binds DNA in a sequence-specific manner and regulates transcription of gene products involved in processes such as growth arrest, DNA repair, and apoptosis (49). To compare the relative affinities of ΔNp63α and p53 binding to known p53-binding sites, in vitro DNA-binding assays were performed with radiolabeled duplex oligonucleotides representing p53-binding sites in the p21 and 14-3-3σ promoters as previously described (15, 24) (Fig. 5A). H1299 cells were transfected with myc-tagged p53 or myc-tagged ΔNp63α, and equal amounts of p53 or ΔNp63α were immunoprecipitated with α-myc epitope antibody. The immunoprecipitates were assayed for their ability to bind the radio-

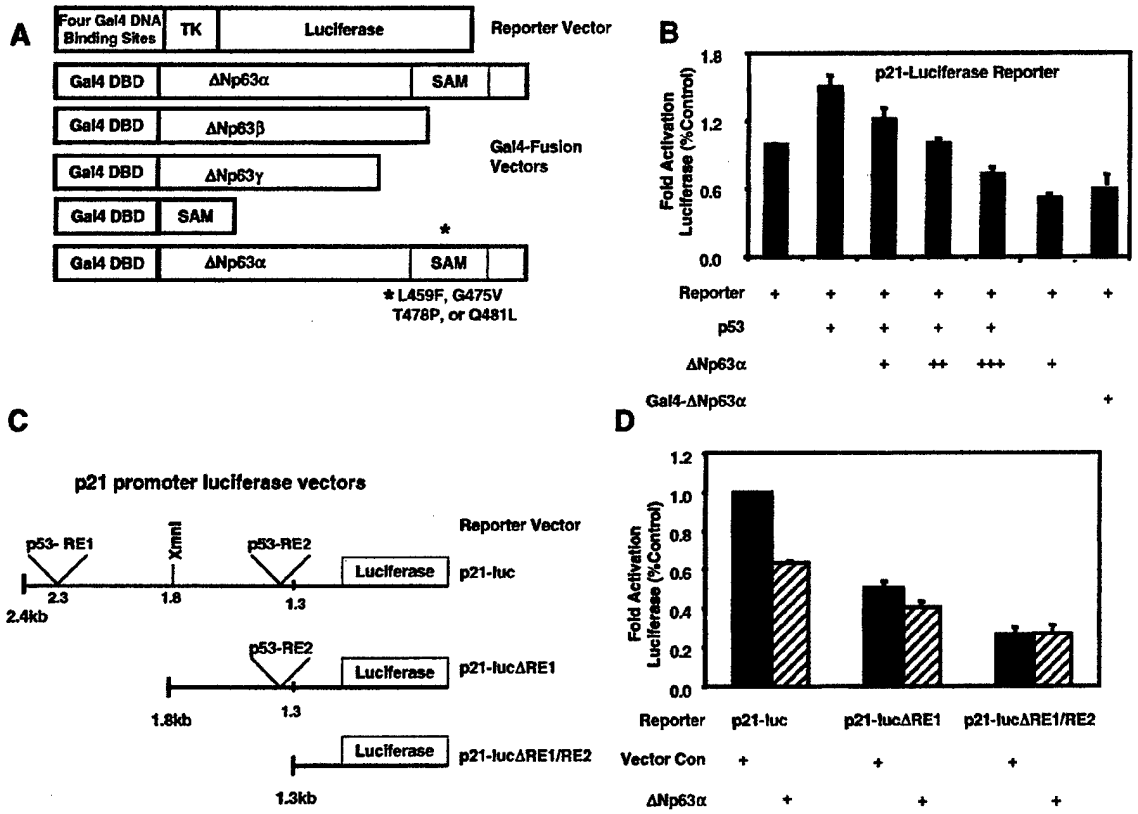

FIG. 4. ΔNp63α represses transcription. (A) Schematic representing vectors used in panels B, D, E, and F. Abbreviations: DBD, DNA-binding domain; TK, thymidine kinase. The SAM mutants were L459F, G475V, T478P, and Q481L. (B) Analysis of ΔNp63α and Gal4-ΔNp63α activity in a p21 promoter-luciferase reporter assay. HCT116 cells were transfected with a p21 promoter-luciferase reporter construct (containing 2,400 bp of p21 promoter sequence) and expression vector encoding either p53, ΔNp63α, or Gal4-ΔNp63α. +, ++, and +++, indicate 1:1, 1:3, and 1:10 ratios of p53 to ΔNp63α expression vectors, respectively. (C) Schematic representing reporter vectors used in panel D. Abbreviations: p53-RE, p53-response element; luc, luciferase. (D) HCT116 cells were transfected as in panel B with the indicated reporter vectors and an empty expression vector (Vector Con) or one expressing ΔNp63α. All values were normalized to those generated with lysates prepared from cells cotransfected with the full-length p21-luciferase reporter vector and the empty expression vector, pCEP4. (E) 293 cells were transfected with the luciferase reporter vector in panel A and the indicated Gal4 fusion vectors. Gal4 alone served as the negative control, and Gal4-ETO2 served as the positive control. (F) 293 cells were transfected with expression vectors encoding murine Gal4-ΔNp63α and Gal4-ΔNp63α proteins containing the indicated SAM domain point mutations. All luciferase assays were normalized for transfection efficiency with a renilla reporter vector. Western analyses with a Gal4-specific antibody were performed to verify protein expression, and results are shown in the lower portions of panels E and F. The results shown are representative of five independent experiments performed each time in triplicate, and error bars indicate the standard deviation.

labeled oligonucleotide duplexes. p53 and ΔNp63α bound to both p53 consensus sites present in the p21 promoter (Fig. 5B). Similarly, ΔNp63α bound to both sites present in the 14-3-3σ promoter, whereas p53 only displayed significant binding to site 2. Quantification of bound radiolabeled DNA illustrated that p53 has ~1.5- and ~2-fold-greater relative binding affinities than ΔNp63α for p21 sites 1 and 2, respectively (Fig. 5C). Similarly, p53 had a ~4-fold-higher relative binding affinity for 14-3-3σ binding site 2. In contrast, ΔNp63α bound to the 14-3-3σ site 1 oligonucleotide with a relative binding affinity that was ca. four- to fivefold greater than that of p53. Similar assays were performed with the myc epitope-tagged SAM mutants analyzed in Fig. 4. However, comparison of SAM mutants to wild-type ΔNp63α showed no significant difference in the relative DNA-binding affinity (data not shown). Thus, the reduction in the transcriptional repression activity of the SAM mutations observed in Fig. 4D was not due to differences in DNA-binding affinity.

p53 and/or p63 occupancy at the p21 and 14-3-3σ and promoters in vivo during HEK differentiation. Since ΔNp63α exhibited significant binding to p53 consensus sites in the p21 and 14-3-3σ promoters, we studied the ability of p63 to bind these consensus sites in vivo by using a chromatin immunoprecipitation (ChIP) methodology previously described in an earlier study from our laboratory (52). Either rapidly growing or differentiated cultures (day 8) of HEKs were cross-linked by exposure to 1.6% formaldehyde as described in Materials and Methods. After cross-linking, p53 and p63 were immunoprecipitated, and the DNA to which the proteins bound was purified. The DNA was PCR amplified with primers specific for sequences that flank the p53 response elements in the promoters studied. To assure that the amplified DNA was the correct

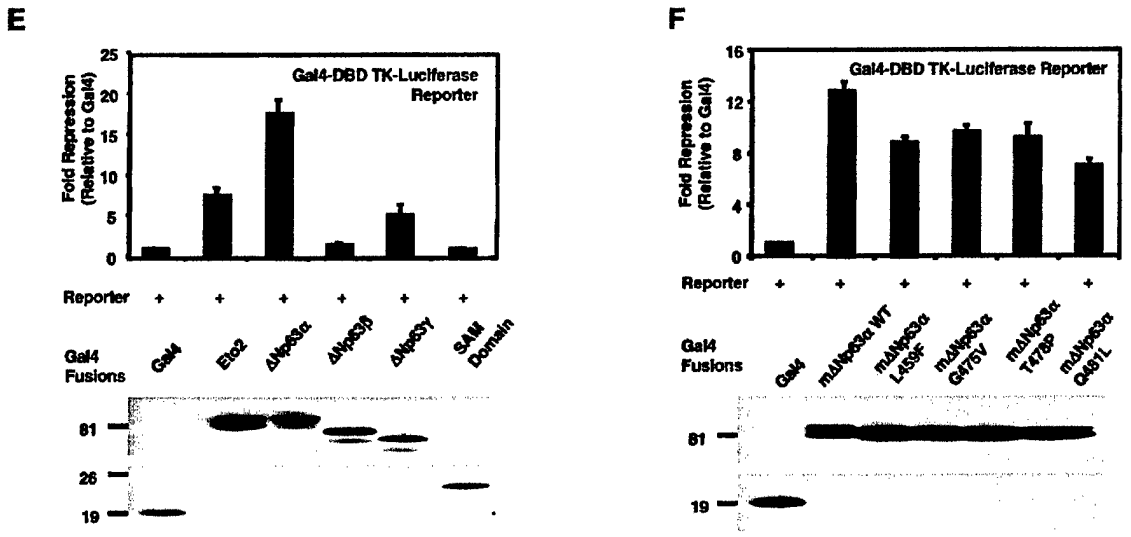

FIG. 4—*Continued.*

size, control PCRs were performed with or without genomic HEK DNA (Fig. 6A, C, E, and G, lanes + or −, respectively). To control for nonspecific binding during immunoprecipitation, cross-linked lysates were immunoprecipitated with mouse monoclonal α-cyclin B1 or rabbit polyclonal α-Bax antibodies that did not cross-react with p53 or p63, respectively (Fig. 6A, C, E, and G, lanes C).

The ChIP experiments revealed that p53 and p63 bind both p21 promoter site 1 and site 2 in rapidly growing (RG) and differentiating (day 8) HEKs (Fig. 6A and C). p53 occupancy at p21 site 1 increased modestly from rapidly growing cells to differentiation day 8 (<1.5-fold), whereas p63 occupancy did not change (Fig. 6B). In contrast to site 1 binding, p53 binding to p21 site 2 did not change and p63 decreased twofold (Fig. 6D). Analysis of the 14-3-3σ promoter showed that p53 binding to site 2 remained unchanged in rapidly growing and differentiated keratinocytes (Fig. 6G and H); however, there was no appreciable binding of p53 to 14-3-3σ site 1 (Fig. 6E and F), a finding consistent with the in vitro DNA-binding results shown in Fig. 5. Like the p21 promoter, p63 bound to both 14-3-3σ site 1 and site 2 in vivo, and by day 8 of differentiation this binding decreased twofold at both site 1 and site 2 (Fig. 6F and H). These data suggest that increased p21 and 14-3-3σ expression are due to the loss of p63 binding and subsequent decreased transcriptional repression of these promoters by p63.

DISCUSSION

Since the identification of the p53 homologue p63, several studies have investigated its function in epithelial cell growth and development. Using HEKs as a model system, we sought to further analyze the biochemical role p63 plays in keratinocyte growth and differentiation. We demonstrated that the primary splice variant of p63 expressed in HEKs is ΔNp63α, and its expression decreases as cells differentiate. Further, the ΔNp63α protein was present in differentiating HEKs as several phosphoforms. In addition to the reduction in p63 transcript and protein levels during differentiation, we also observed a decrease in p53 transcript and protein. The reduction in p53 and p63 expression correlated with an increase in expression of the cell cycle regulatory proteins p21 and 14-3-3σ. Using Gal4 fusion proteins, we determined that the p63 protein represses transcription and that the ΔNp63α splice variant has the highest activity. In addition, in vitro and in vivo DNA-binding assays showed that ΔNp63α binds to both p53 response elements in the p21 and 14-3-3σ promoters with p63 occupancy at p21 site 2 and 14-3-3σ sites 1 and 2 decreasing as cells differentiated.

Consistent with previously published reports (41, 42), we observed a decrease in p63 transcript and protein during differentiation. Analysis of the limited number of keratinocytes in the $p63^{-/-}$ mouse showed expression of epithelial terminal differentiation markers (58), suggesting that epithelial defects were due to the lack of cell survival and/or proliferation and not to impaired terminal differentiation. In support of this, a recent study in zebrafish using antisense oligonucleotides demonstrated that the ΔNp63 splice variant(s) were required for epithelial proliferation (30). These model systems suggest a role for p63 in maintaining the survival or proliferation of basal keratinocytes and, in conjunction with our HEK data, indicate that the loss of ΔNp63α facilitates the growth arrest associated with differentiation.

We determined that p63 migrated as multiple phosphoforms by SDS-polyacrylamide gel electrophoresis (PAGE), suggesting that phosphorylation is a mechanism by which the p63 protein is regulated. This hypothesis is supported by the findings that phosphorylation is a key posttranslational modification for regulation of p53 (49). However, ΔNp63α lacks a transactivation domain where many of the regulatory phosphorylation sites are found in p53. Future studies are required to identify the phosphoresidues in ΔNp63α, upstream kinases, and phosphorylation-dependent associated proteins.

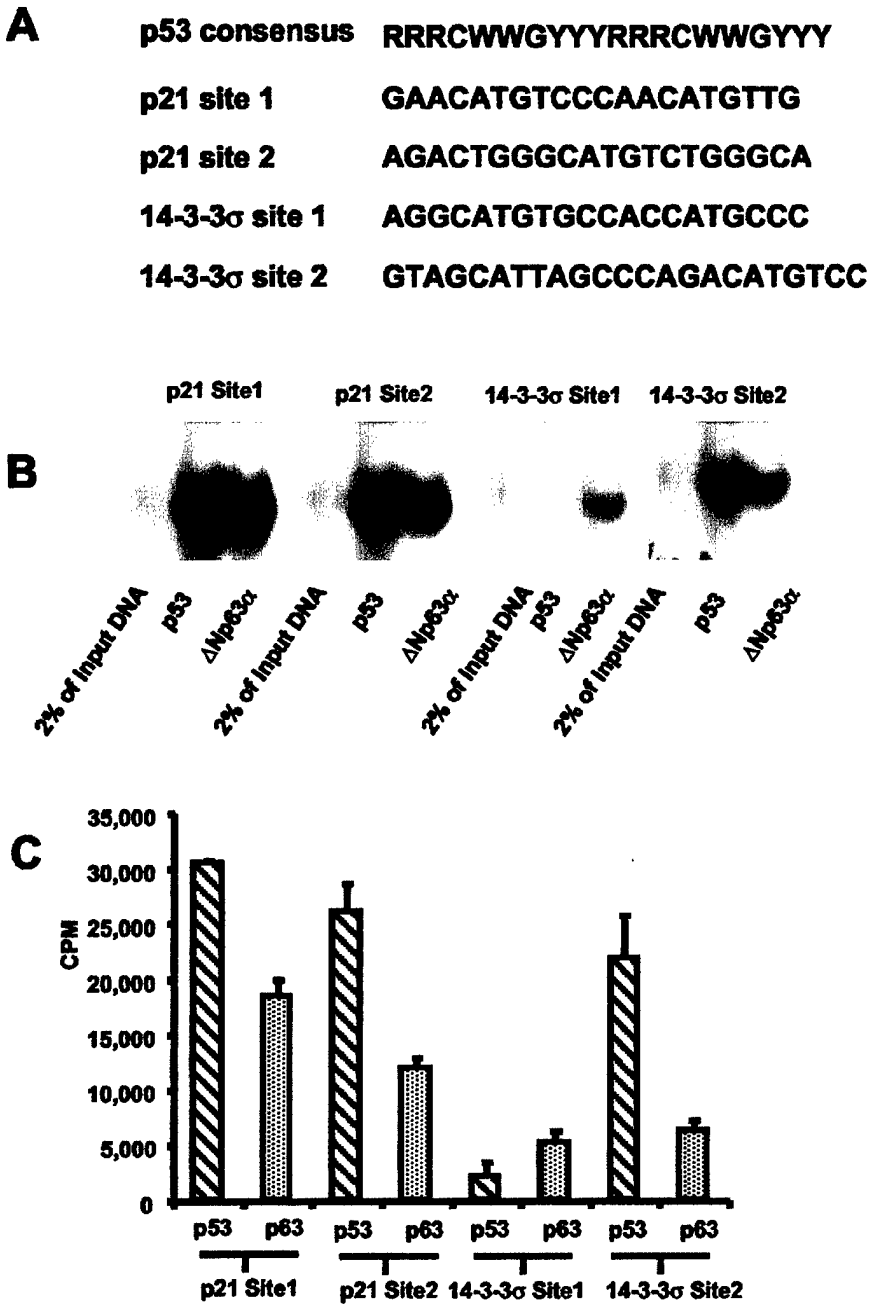

FIG. 5. Relative binding affinities of p53 and ΔNp63α for p53 consensus sites in the p21 and 14-3-3σ promoters. (A) The p53 consensus binding sequence and p53 binding sites in the p21 and 14-3-3σ promoters. Abbreviations: R, purine; Y, pyrimidine; W, adenine or thymine. (B) H1299 cells were transfected with myc-tagged p53 or ΔNp63α, and protein lysates were quantified by using the Fluor-S Max MultiImager. Based on Fluor-S Max quantification, equal amounts of myc-tagged p53 and myc-tagged ΔNp63α were immunoprecipitated with a myc epitope antibody. Immunoprecipitated p53 and ΔNp63α were assayed for their ability to bind radiolabeled oligonucleotides representing p53-binding sites in the p21 and 14-3-3σ promoters as described in Materials and Methods. (C) Bound oligonucleotides were separated on acrylamide gels, exposed for autoradiography, and quantified. Each autoradiograph shows one representative result of at least three independent experiments that are quantified and displayed with the standard deviation.

It has been suggested that ΔNp63α-mediated repression can occur through direct protein-protein interaction, and several groups have examined the association of p63 proteins encoded by the various splice variants with other p53 family members. Davison et al. and Irwin et al. determined that p63 and p73 can form homodimers or have weak heterotypic interactions through their oligomerization domain but do not interact with the p53 oligomerization domain (10, 26). Kojima et al. found

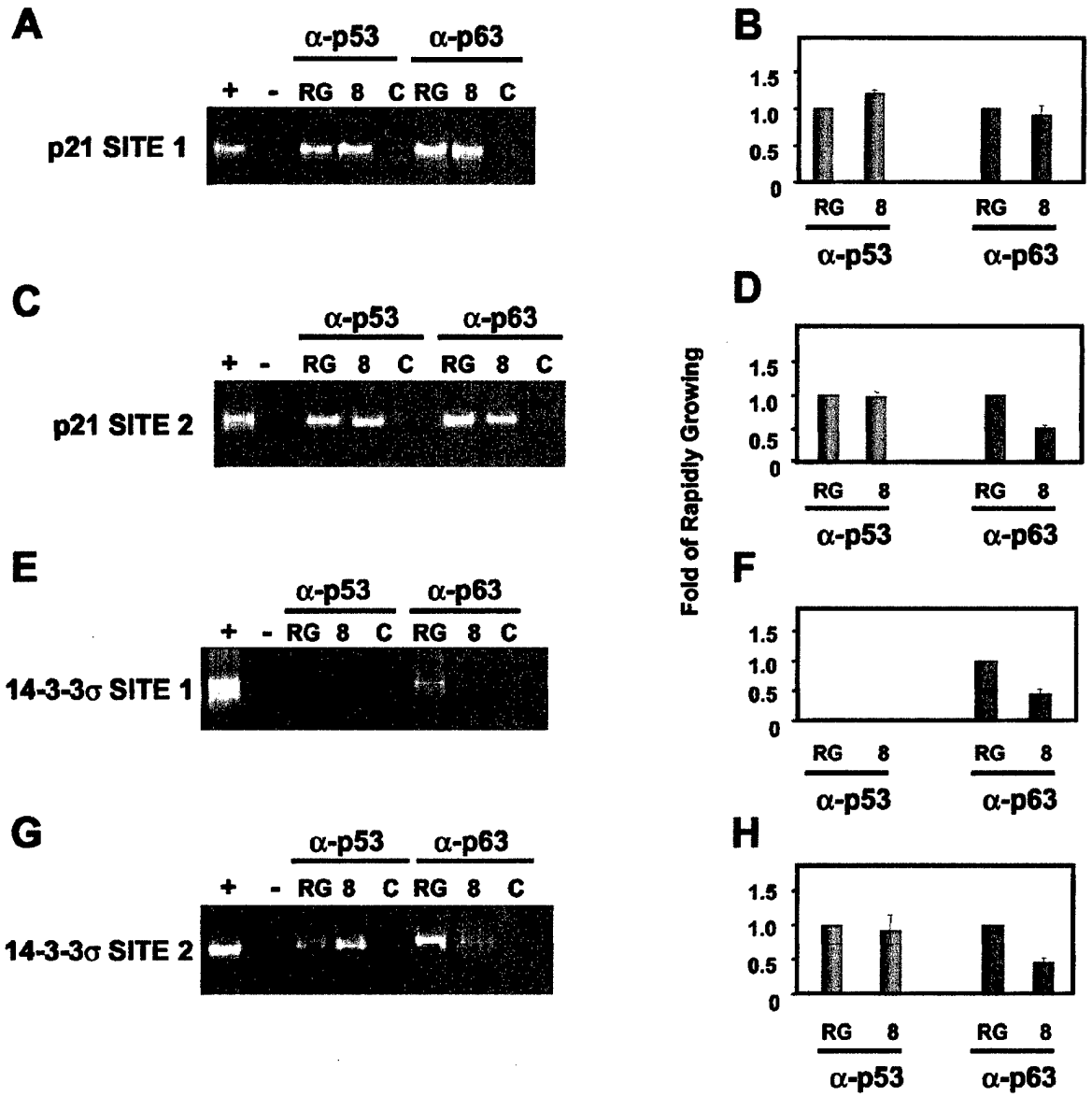

FIG. 6. ChIP analyses for p53 and p63 binding at the 14-3-3σ and p21 promoters during keratinocyte differentiation. Abbreviations: RG, rapidly growing; 8, day 8 after induction of differentiation; C, control. HEKs were induced to differentiate as described in Materials and Methods. At the time of harvest, HEKs were treated with formaldehyde (X-Link) and processed as described in Materials and Methods. The DNA immunoprecipitated with p53- or p63-specific antibodies was PCR amplified by using primers flanking the p53 binding sites in the p21 (A and C) and 14-3-3σ (E and G) promoters. DNA fragments generated by PCR were resolved by PAGE, the gels were stained with ethidium bromide, and the PCR products were quantified by densitometry. Lanes marked "+" indicate PCR products that were generated by using DNA template derived from total genomic DNA harvested from rapidly growing HEKs. Lanes marked "−" indicate the absence of DNA input for the PCR. The lanes marked "C" indicate PCRs performed with templates immunoprecipitated with antibodies specific to cyclin B1 and Bax for p53 and p63 analyses, respectively. Each ethidium bromide-stained gel shows one representative result of at least three independent experiments that are quantified and displayed with standard deviations in the corresponding panels B, D, F, and H.

similar results by using a yeast two-hybrid system (28). Further, several studies have shown that p63 and p53 can interact through the core/DNA-binding domain (21, 44, 50). One consequence of p53 association with ΔNp63α may be caspase-dependent degradation of select ΔNp63 proteins (p40 and ΔNp63α) (44). The significance of these findings remains to be determined in the context of proliferating and differentiating epithelial cells.

Through the use of Gal4 fusion proteins, we determined that the C-terminal domain of ΔNp63α is involved in transcriptional repression. Further, single amino acid substitutions within the SAM domain of ΔNp63α resulted in reduced tran-

scriptional repression. Similar results were obtained for the ΔNp63α proteins containing SAM domain mutations by using a p53-reporter assay and cotransfections of the mutant proteins with p53 or TA-p63γ (35). Chi et al. (8) have shown that the SAM domain of p73 contains a folded, globular α-helical structure and suggest that this domain interacts with additional, as-yet-uncharacterized signaling proteins. However, the SAM domains of p73 and p63 are monomeric and do not interact with one another, leaving the possibility that the p63 SAM domain may play a role in recruiting transcriptional corepressors to select target genes, and these protein-protein interactions are disrupted in individuals with Hay-Wells syndrome (35). Consistent with this hypothesis is our finding that ΔNp63α proteins containing the Hay-Wells mutations bind DNA with the same relative affinity as the wild-type protein. Studies have also demonstrated that a frameshift mutation found in ectrodactyl, ectodermal dysplasia, and cleft lip patients, causing loss of the SAM domain and carboxy-terminal sequence, results in the total loss of transcriptional repressive ability (5). Taken together, the data suggest that the carboxy-terminal region of ΔNp63α containing the SAM domain plays an integral role in ΔNp63α-mediated transcriptional repression.

Since ΔNp63α has been identified as the primary splice variant expressed at the protein level in epithelial cells, several questions remain to be addressed. In particular, what target genes does ΔNp63α regulate and which of these genes are coordinately regulated by p53? Our in vitro DNA-binding assays and ChIP analyses support the hypothesis that p53 and p63 can coordinately bind target genes such as p21 and 14-3-3σ. These results are in agreement with those of Flores et al. showing that increased association of both p53 and p63 with p21, mdm2, PERP, and NOXA promoters in mouse embryo fibroblasts expressing E1A after DNA damage (19).

If ΔNp63α functions as a transcriptional repressor in vivo, as our Gal4 fusion experiments support, then protein levels, promoter binding affinity, and coassociated proteins are likely factors involved in this coordinate regulation of downstream target genes. Similar to our results, Weinberg et al. reported that p53 transcript and protein decreased during differentiation whereas p21 promoter activity increased (55). Does this increase reflect an elevation of p53 activity, an elevation of the activity of other transcriptional activators, or the loss of ΔNp63α repressor activity at the promoter? In support of a role for other transcriptional activators, several studies show that Sp1 and Sp3 can transcriptionally activate the p21 promoter (29, 40, 43, 45) and transcriptional regulators such as these may activate the p21 promoter when p53 levels are decreased during keratinocyte differentiation. In support of the theory that loss of ΔNp63α repressor activity at the p21 promoter allows p53 or other transactivators to act unopposed, Liefer et al. showed a decrease in p63 in mouse keratinocytes in vitro and mouse epidermis in vivo after UV-B exposure (32), a treatment which leads to elevated p53 transcriptional activity (33). Further, ectopic expression of ΔNp63α in the mouse epidermis resulted in decreased UV-B-induced apoptosis (32), a phenotype thought to be primarily dependent on p53 activity (61). Our findings that p63 and p53 can bind the same promoter elements in vivo support the role of ΔNp63α acting coordinately with p53 to regulate select target genes during keratinocyte proliferation and differentiation. Our observations also favor the possibility that p53 and ΔNp63α compete for consensus DNA-binding sites with p53 having a relatively higher binding affinity than ΔNp63α for select promoters, such as p21.

Previous studies and findings reported here support the following model. When rapidly proliferating basal epithelial cells are exposed to cell stress, increased p53 protein combined with the higher binding affinity of p53 for select promoter sites displaces ΔNp63α. Further, as is the case after exposure of keratinocytes to UV radiation, the p63 protein levels decrease. These events lead to subsequent transactivation of genes whose products are involved in growth arrest and apoptosis. In the absence of cell stress, constitutively expressed ΔNp63α protein levels exceed those of p53, and thus select target gene promoters are repressed, allowing for continued proliferation of keratinocytes in the basal layer where ΔNp63α is localized in stratified epithelium. During differentiation, both p53 and ΔNp63α levels decrease; however, it is the loss of ΔNp63α-mediated repression of select target genes that plays a role in differentiation. This model is consistent with the the proposed oncogenic role of p63 overexpression in squamous cell carcinomas of the head and neck (9, 25) and the observations that ectopic expression of the $p40^{AIS}$ splice variant in Rat 1a cells results in increased growth of these cells in soft agar and athymic, nude mice (25). However, as suggested above, it is likely that ΔNp63α also regulates gene expression independently of p53, since mutation of p53 and amplification of p63 both occur during genesis of squamous cell carcinomas (25) (J. Sniezek and J. Pietenpol, unpublished results). Clearly, additional experimentation is required to further link p63 biochemistry to biology and to determine the interplay of p63 and p53 signaling pathways. New technologies, including in vivo DNA-binding assays and mass spectrometry, will aid in the identification of key posttranslational modifications, associated proteins, and novel target genes that are regulated by p63.

ACKNOWLEDGMENTS

This work was supported by the National Institutes of Health grant CA70856 and the Burroughs-Wellcome Fund (J.A.P.), U.S. Army grant DAMD17-01-1-0439 (M.D.W.), and National Institutes of Health grants ES00267 and CA68485 (Core Services).

We thank members of the Pietenpol laboratory for critical reading of the manuscript.

REFERENCES

1. **Amann, J. M., J. Nip, D. K. Strom, B. Lutterbach, H. Harada, N. Lenny, J. R. Downing, S. Meyers, and S. W. Hiebert.** 2001. ETO, a target of t(8;21) in acute leukemia, makes distinct contacts with multiple histone deacetylases and binds mSin3A through its oligomerization domain. Mol. Cell. Biol. **21**:6470–6483.
2. **Augustin, M., C. Bamberger, D. Paul, and H. Schmale.** 1998. Cloning and chromosomal mapping of the human p53-related KET gene to chromosome 3q27 and its murine homolog *Ket* to mouse chromosome 16. Mamm. Genome **9**:899–902.
3. **Barrandon, Y., and H. Green.** 1985. Cell size as a determinant of the clone-forming ability of human keratinocytes. Proc. Natl. Acad Sci. USA **82**:5390–5394.
4. **Barrandon, Y., and H. Green.** 1987. Three clonal types of keratinocyte with different capacities for multiplication. Proc. Natl. Acad. Sci. USA **84**:2302–2306.
5. **Celli, J., P. Duijf, B. Hamel, M. Bamshad, B. Kramer, A. Smits, R. Newbury-Ecob, R. Hennekam, G. Van Buggenhout, A. van Haeringen, C. Woods, A. van Essen, R. de Waal, G. Vriend, D. Haber, A. Yang, F. McKeon, H.**

Brunner, and H. van Bokhoven. 1999. Heterozygous germline muations in the p53 homolog p63 are the cause of EEC syndrome. Cell **99:**143–153.
6. **Chan, T. A., H. Hermeking, C. Lengauer, K. W. Kinzler, and B. Vogelstein.** 1999. 14–3–3σ is required to prevent mitotic catastrophe after DNA damage. Nature **401:**616–620.
7. **Chen, X.** 1999. The p53 family: same response, different signals? Mol. Med. Today **5:**387–392.
8. **Chi, S. W., A. Ayed, and C. H. Arrowsmith.** 1999. Solution structure of a conserved C-terminal domain of p73 with structural homology to the SAM domain. EMBO J. **18:**4438–4445.
9. **Choi, H. R., J. G. Batsakis, F. Zhan, E. Sturgis, M. A. Luna, and A. K. El-Naggar.** 2002. Differential expression of p53 gene family members p63 and p73 in head and neck squamous tumorigenesis. Hum. Pathol. **33:**158–164.
10. **Davison, T. S., C. Vagner, M. Kaghad, A. Ayed, D. Caput, and C. H. Arrowsmith.** 1999. p73 and p63 are homotetramers capable of weak heterotypic interactions with each other but not with p53. J. Biol. Chem. **274:**18709–18714.
11. **Dellambra, E., O. Golisano, S. Siviero Bondanza, E. P. Lacal, M. Molinari, S. D'Atri, and M. DeLuca.** 2000. Downregulation of 14–3–3σ prevents clonal evolution and leads to immortalization of primary human keratinocytes. J. Cell Biol. **149:**1117–1129.
12. **Dellavalle, R. P., T. B. Egbert, A. Marchbank, L. J. Su, L. A. Lee, and P. Walsh.** 2001. CUSP/p63 expression in rat and human tissues. J. Dermatol. Sci. **27:**82–87.
13. **Di Como, C. J., M. J. Urist, I. Babayan, M. Drobnjak, C. V. Hedvat, J. Teruya-Feldstein, K. Pohar, A. Hoos, and C. Cordon-Cardo.** 2002. p63 expression profiles in human normal and tumor tissues. Clin. Cancer. Res. **8:**494–501.
14. **Donehower, L. A., M. Harvey, B. L. Slagle, M. J. McArthur, C. A. Montgomery, Jr., J. S. Butel, and A. Bradley.** 1992. Mice deficient for p53 are developmentally normal but susceptible to spontaneous tumours. Nature **356:**215–221.
15. **El-Deiry, W. S., T. Tokino, V. E. Velculescu, D. B. Levy, R. Parsons, J. M. Trent, D. Lin, W. E. Mercer, K. W. Kinzler, and B. Vogelstein.** 1993. *WAF1*, a potential mediator of p53 tumor suppression. Cell **75:**817–825.
16. **El-Deiry, W. S., T. Tokino, T. Waldman, J. D. Oliner, V. E. Velculescu, M. Burrell, D. E. Hill, E. Healy, J. L. Rees, S. R. Hamilton, K. W. Kinzler, and B. Vogelstein.** 1995. Topological control of $p21^{WAF1/CIP1}$ expression in normal and neoplastic tissues. Cancer Res. **55:**2910–2919.
17. **Flatt, P. M., J. O. Price, A. Shaw, and J. A. Pietenpol.** 1998. Differential cell cycle checkpoint response in normal human keratinocytes and fibroblasts. Cell Growth Differ. **9:**535–543.
18. **Flatt, P. M., L. J. Tang, C. D. Scatena, S. T. Szak, and J. A. Pietenpol.** 2000. p53 Regulation of G_2 checkpoint is retinoblastoma protein dependent. Mol. Cell. Biol. **20:**4210–4223.
19. **Flores, E. R., K. Y. Tsai, D. Crowley, S. Sengupta, A. Yang, F. McKeon, and T. Jacks.** 2002. p63 and p73 are required for p53-dependent apoptosis in response to DNA damage. Nature **416:**560–564.
20. **Fuchs, E., and C. Byrne.** 1994. The epidermis: rising to the surface. Curr. Opin. Genet. Dev. **4:**725–736.
21. **Gaiddon, C., M. Lokshin, J. Ahn, T. Zhang, and C. Prives.** 2001. A subset of tumor-derived mutant forms of p53 downregulate p63 and p73 through a direct interaction with the p53 core domain. Mol. Cell. Biol. **21:**1874–1887.
22. **Gu, Y., C. W. Turck, and D. O. Morgan.** 1993. Inhibition of CDK2 activity in vivo by an associated 20K regulatory subunit. Nature **366:**707–710.
23. **Harper, J. W., G. R. Adami, N. Wei, K. Keyomarsi, and S. J. Elledge.** 1993. The p21 Cdk-interacting protein Cip1 is a potent inhibitor of G1 cyclin-dependent kinases. Cell **75:**805–816.
24. **Hermeking, H., C. Lengauer, K. Polyak, T.-C. He, L. Zhang, S. Thiagalingam, K. W. Kinzler, and B. Vogelstein.** 1997. 14–3–3σ is a p53-regulated inhibitor of G_2/M progression. Mol. Cell **1:**3–11.
25. **Hibi, K., B. Trink, M. Patturajan, W. Westra, O. Caballero, D. Hill, E. Ratovitski, J. Jen, and D. Sidransky.** 2000. AIS is an oncogene amplified in squamous cell carcinoma. Proc. Natl. Acad. Sci. USA **97:**5462–5467.
26. **Irwin, M., M. C. Marin, A. C. Phillips, R. S. Seelan, D. I. Smith, L. Wanguo, E. R. Flores, K. Y. Tsai, T. Jacks, K. H. Vousden, and W. G. Kaelin.** 2002. Role for the p53 homologue p73 in E2F-1-induced apoptosis. Nature **407:**642–645.
27. **Kaghad, M., H. Bonnet, A. Yang, L. Creancier, J. Biscan, A. Valent, A. Minty, P. Chalon, J. Lelias, X. Dumont, P. Ferrara, F. McKeon, and D. Caput.** 1997. Monoallelically expressed gene related to p53 at 1p36, a region frequently deleted in neuroblastoma and other human cancers. Cell **90:**808–819.
28. **Kojima, T., Y. Ikawa, and I. Katoh.** 2001. Analysis of molecular interactions of the p53-family p51(p63) gene products in a yeast two-hybrid system: homotypic and heterotypic interactions and association with p53-regulatory factors. Biochem. Biophys. Res. Commun. **281:**1170–1175.
29. **Koutsodontis, G., I. Tentes, P. Papakosta, A. Moustakas, and D. Kardassis.** 2001. Sp1 plays a critical role in the transcriptional activation of the human cyclin-dependent kinase inhibitor $p21^{WAF1/Cip1}$ gene by the p53 tumor suppressor protein. J. Biol. Chem. **276:**29116–29125.
30. **Lee, H., and D. Kimelman.** 2002. A dominant-negative form of p63 is required for epidermal proliferation in zebrafish. Dev. Cell **2:**607–616.
31. **Leigh, I., E. Lane, and F. Watt.** 1994. The keratinocyte handbook. Cambridge University Press, Cambridge, United Kingdom.
32. **Liefer, K., M. Koster, X. Wang, A. Yang, F. McKeon, and D. Roop.** 2000. Down-regulation of p63 is required for epidermal UV-B-induced apoptosis. Cancer Res. **60:**4016–4020.
33. **Liu, M., and J. C. Pelling.** 1995. UV-B/A irradiation of mouse keratinocytes results in p53-mediated WAF1/CIP1 expression. Oncogene **10:**1955–1960.
34. **Macleod, K. F., N. Sherry, G. Hannon, D. Beach, T. Tokino, K. Kinzler, B. Vogelstein, and T. Jacks.** 1995. p53-dependent and independent expression of p21 during cell growth, differentiation, and DNA damage. Genes Dev. **9:**935–944.
35. **McGrath, J. A., P. H. G. Duijf, V. Doetsch, A. D. Irvine, R. de Waal, K. R. J. Vanmolkot, V. Wessagowit, A. Kelly, D. J. Atherton, W. A. D. Griffiths, S. J. Orlow, A. van Haeringen, M. G. E. M. Ansems, A. Yang, F. McKeon, M. A. Bamshad, H. G. Brunner, B. C. J. Hamel, and H. van Bokhoven.** 2001. Hay-Wells syndrome is caused by heterozygous missense mutations in the SAM domain of p63. Hum. Mol. Genet. **10:**221–229.
36. **Mills, A. A., B. H. Zheng, X. J. Wang, H. Vogel, D. R. Roop, and A. Bradley.** 1999. *p63* is a *p53* homologue required for limb and epidermal morphogenesis. Nature **398:**708–713.
37. **Missero, C., E. Calautti, R. Eckner, J. Chin, L. H. Tsai, D. M. Livingston, and G. P. Dotto.** 1995. Involvement of the cell-cycle inhibitor *Cip1/WAF1* and the E1A-associated p300 protein in terminal differentiation. Proc. Natl. Acad. Sci. USA **92:**5451–5455.
38. **Nylander, K., P. J. Coates, and P. A. Hall.** 2000. Characterization of the expression pattern of p63α and ΔNp63α in benign and malignant oral epithelial lesions. Int. J. Cancer **87:**368–372.
39. **Osada, M., M. Ohba, C. Kawahara, C. Ishioka, R. Kanamaru, I. Katoh, Y. Ikawa, Y. Nimura, A. Nakagawara, M. Obinata, and S. Ikawa.** 1998. Cloning and functional analysis of human *p51*, which structurally and functionally resembles *p53*. Nat. Med. **4:**839–843.
40. **Paglinca, A., G. Pasquale, and L. Lania.** 2000. Differential role for Sp1/Sp3 transcription factors in the regulation of the promoter activity of multiple cyclin-dependent kinase inhibitor genes. J. Cell Biochem. **76:**360–367.
41. **Parsa, R., A. Yang, F. McKeon, and H. Green.** 1999. Association of p63 with proliferative potential in normal and neoplastic human keratinocytes. J. Investig. Dermatol. **113:**1099–1105.
42. **Pellegrini, G., E. Dellambra, O. Golisano, E. Martinelli, I. Fantozzi, S. Bondanza, D. Ponzin, F. McKeon, and M. De Luca.** 2001. p63 identifies keratinocyte stem cells. Proc. Natl. Acad. Sci. USA **98:**3156–3161.
43. **Prowse, D. M., L. Bolgan, A. Molnar, and G. P. Dotto.** 1997. Involvement of the Sp3 transcription factor in induction of $p21^{Cip1/WAF1}$ in keratinocyte differentiation. J. Biol. Chem. **272:**1308–1314.
44. **Ratovitski, E. A., M. Patturajan, K. Hibi, B. Trink, K. Yamaguchi, and D. Sidransky.** 2001. p53 associates with and targets ΔNp63 into a protein degradation pathway. Proc. Natl. Acad. Sci. USA **98:**1817–1822.
45. **Santini, M. P., C. Talora, T. Seki, L. Bolgan, and G. P. Dotto.** 2001. Cross talk among calcineurin, Sp1/Sp3, and NFAT in control of $p21^{WAF1/CIP1}$ expression in keratinocyte differentiation. Proc. Natl. Acad. Sci. USA **98:**9575–9580.
46. **Schultz, J., C. P. Ponting, K. Hofmann, and P. Bork.** 1997. SAM as a protein interaction domain involved in developmental regulation. Protein Sci. **6:**249–253.
47. **Shibata, H., Z. Nawaz, S. Y. Tsai, B. W. O'Malley, and M. J. Tsai.** 1997. Gene silencing by chicken ovalbumin upstream promoter-transcription factor I (COUP-TFI) is mediated by transcriptional corepressors, nuclear receptor-corepressor (N-CoR) and silencing mediator for retinoic acid receptor and thyroid hormone receptor (SMRT). Mol. Endocrinol **11:**714–724.
48. **Steinman, R. A., B. Hoffman, A. Iro, C. Guillouf, D. A. Liebermann, and M. E. el-Houseine.** 1994. Induction of $p21^{WAF-1/CIP1}$ during differentiation. Oncogene **9:**389–396.
49. **Stewart, Z. A., and J. A. Pietenpol.** 2001. p53 signaling and cell cycle checkpoints. Chem. Res. Toxicol. **14:**243–263.
50. **Strano, S., G. Fontemaggi, A. Costanzo, M. G. Rizzo, O. Monti, A. Baccarini, G. Del Sal, M. Levrero, A. Sacchi, M. Oren, and G. Blandino.** 2002. Physical interaction with human tumor-derived p53 mutants inhibits p63 activities. J. Biol. Chem. **277:**18817–18826.
51. **Sun, T. T., and H. Green.** 1976. Differentiation of the epidermal keratinocyte in cell culture: formation of the cornified envelope. Cell **9:**511–521.
52. **Szak, S. T., D. Mays, and J. A. Pietenpol.** 2001. Kinetics of p53 binding to promoter sites in vivo. Mol. Cell. Biol. **21:**3375–3386.
53. **Thanos, C. D., and J. U. Bowie.** 1999. p53 Family members p63 and p73 are SAM domain-containing proteins. Protein Sci. **8:**1708–1710.
54. **Trink, B., K. Okami, L. Wu, V. Sriuranpong, J. Jen, and D. Sidransky.** 1998. A new human p53 homologue. Nat. Med. **4:**747–748.
55. **Weinberg, W. C., C. G. Azzoli, K. Chapman, A. J. Levine, and S. H. Yuspa.** 1995. p53-mediated transcriptional activity increases in differentiating epidermal keratinocytes in association with decreased p53 protein. Oncogene **10:**2271–2279.
56. **Xiong, Y., G. J. Hannon, H. Zhang, D. Casso, R. Kobayashi, and D. Beach.** 1993. p21 is a universal inhibitor of cyclin kinases. Nature **366:**701–704.
57. **Yang, A., M. Kaghad, Y. Wang, E. Gillet, M. Fleming, V. Dotsch, N. An-**

drews, D. Caput, and F. McKeon. 1998. p63, a p53 homolog at 3q27–29, encodes multiple products with transactivating, death-inducing, and dominant-negative activities. Mol. Cell **2**:305–316.

58. **Yang, A., R. Schweitzer, D. Sun, M. Kaghad, N. Walker, R. Bronson, C. Tabin, A. Sharpe, D. Caput, C. Crum, and F. McKeon.** 1999. p63 is essential for regenerative proliferation in limb, craniofacial and epithelial development. Nature **398**:714–718.
59. **Yang, A., N. Walker, R. Bronson, M. Kaghad, M. Oosterwegel, J. Bonnin, C. Vagner, H. Bonnet, P. Dikkes, A. Sharpe, F. McKeon, and D. Caput.** 2000. p73-deficient mice have neurological, pheromonal and inflammatory defects but lack spontaneous tumours. Nature **404**:99–103.
60. **Zhang, W., L. Grasso, C. D. McClain, A. M. Gambel, Y. Cha, S. Travali, A. B. Deisseroth, and W. E. Mercer.** 1995. p53-independent induction of *WAF1/CIP1* in human leukemia cells is correlated with growth arrest accompanying monocyte/macrophage differentiation. Cancer Res. **55**:668–674.
61. **Ziegler, A., A. S. Jonason, D. J. Leffell, J. A. Simon, H. W. Sharma, J. Kimmelman, L. Remington, T. Jacks, and D. E. Brash.** 1994. Sunburn and p53 in the onset of skin cancer. Nature **372**:773–776.

MICROTUBULE DISRUPTION CAUSES PHOSPHORYLATION OF ΔNP63α BUT DOES NOT ALTER ΔNP63α SUBCELLULAR LOCALIZATION OR DNA BINDING ABILITY

Westfall, M.D., Pietenpol, J.A. Department of Biochemistry, Center in Molecular Toxicology, The Vanderbilt-Ingram Comprehensive Cancer Center, Vanderbilt University School of Medicine, Nashville, Tennessee 37232, USA.

Introduction

Cellular response to stress includes recognition of the cellular stress or DNA damage, cell cycle arrest and assessment of the damage, and implementation of the appropriate response such as DNA repair or apoptosis in the case of irreparable damage. A principal component of the response to DNA damage or other cellular stresses is the p53 protein (18). Central to the ability of p53 to function and regulate these responses is a complex set of posttranslational modifications including phosphorylation and acetylation (28, 32, 44). Since the identification of the p53 homologue p63, studies have attempted to examine the role that cellular stresses or chemotherapeutic agents would have on p63 regulation and function (21, 25, 31). Different TAp63 splice variant protein levels increased with DNA damaging agents or UV treatment of cells (Katoh et al., 2000; Okada et al.). Conversely, ΔNp63α protein and mRNA decreased with UV treatment of mouse keratinocytes (Liefer et al., 2000). However, these studies did not examine the effects such treatments have on ΔNp63α posttranslational modifications. Agents such as IR, UV, ADR, and Taxol induce posttranslational modifications of p53, the goal of this work was to determine if such agents would cause posttranslational modifications of ΔNp63α, and if so, what affect would they have on ΔNp63α function or regulation. The

goal of the research described herein was to determine if p63 is differentially phosphorylated after cellular stress, as is the case for p53.

We examined the effect of radiation and two anticancer agents on growth arrest and p63 in primary epithelial cells as well as in established cell lines. Our results indicate that ΔNp63α is phosphorylated in primary, immortalized, and tumor cell lines in response to agents that alter microtubule dynamics and arrest cells in mitosis. We also show that this phosphorylation does not affect ΔNp63α subcellular localization or DNA binding ability.

Materials and Methods

Cell Culture and Treatment. Second passage primary human epidermal keratinocytes (HEK) were obtained from the Vanderbilt Skin Disease Research Core. HEKs were isolated as previously described (13) and were cultured in EpiLife M-EPI-500 keratinocyte growth media (Cascade Biologics, Portland, OR) supplemented with human keratinocyte growth supplement S-001-5 (Cascade Biologics) and 0.06 mM CaCl2. Primary human mammary epithelial cells (HMEC) from two females (#1012 and #1016) were isolated and provided by S. Eltom (Meharry Medical College). HMEC-1016 and HMEC-1012 were grown in DMEM:F12 medium (1:1) (GibCoBRL, Grand Island, NY) supplemented with 1% FBS, 10 μg/ml ascorbic acid, 2 nM β-estradiol, 35 μg/ml bovine pituitary extract, 1 ng/ml cholera toxin, 12.5 ng/ml epidermal growth factor (EGF), 0.1 mM ethanolamine, 0.1 mM phospho-ethanolamine, 1 μg/ml hydrocortisone, 1 μg/ml insulin, 0.2 mM L-glutamine, 10 nM T3, 10 μg/ml transferrin, and 15 nM sodium selenite. The squamous cell carcinoma cell line SCC1 was provided by D. Sidransky (Johns Hopkins University, Baltimore, MD) and cultured in DMEM medium

supplemented with 10% FCS and 1% penicillin-streptomycin. The immortalized keratinocyte cell line HaCaT was provided by Petra Boukamp (German Cancer Research Center, Heidelberg Germany) and cultured in DMEM medium supplemented with 10% FCS and 1% penicillin-streptomycin. All cells were cultured at 37°C with 5% CO2. Where indicated, cells were treated as described in the text with ionizing radiation (IR), paclitaxel (Taxol, Tax, or T), ultraviolet radiation (UV), and adriamycin (ADR).

Protein Lysate Preparation and Western analysis. Cells were washed with ice-cold phosphate-buffered saline, and harvested in one of the following lysis buffers: Lysis Buffer (LB: 50 mM Tris-HCl pH 7.4, 150 mM NaCl, 0.1% Nonidet P-40 (v/v), 0.1% Triton X-100 (v/v), 4 mM EDTA, 1 mM dithiothreitol (DTT)), Radio Immunoprecipitation Assay buffer (RIPA: 150 mM NaCl, 1% Nonidet P-40 (v/v), 0.5% deoxycholate (v/v), 0.1% SDS (v/v), 50 mM Tris pH 8.0, 5 mM EDTA), or EBC (EBC: 50 mM Tris-HCl pH 7.5, 100 mM NaCl, 0.5% Nonidet P-40). Lysis buffers were supplemented with phosphatase inhibitors 50 mM NaF, 0.2 mM NaVanadate, 10 mM p-nitrophenyl phosphate, and 10 mM β-glycero-phosphate, and the protease inhibitors antipain (10 μg/ml), leupeptin (10 μg/ml), pepstatin A (10 μg/ml), chymostatin (10 μg/ml) (Sigma), and 4-(2-aminoethyl)-benzenesulfonylfluoride (200 μg/ml) (Calbiochem, San Diego, CA). Cells were incubated on ice 30-45 min, and the protein supernatant was clarified by centrifugation at 13,000 x *g* for 10 min at 4°C. Protein concentration was determined by the Bio-Rad Protein Quantification kit (Bio-Rad Laboratories, Hercules, CA). Protein lysates, 25 μg to 50 μg, were boiled in 1X Laemmli sample buffer, separated by SDS-Page, and transferred to Immobilon-P membrane (Millipore, Bedford, MA). Membranes were blocked with 5% non-fat dry milk (w/v) in

TTBS (100 mM Tris-HCl pH 7.5, 150 mM NaCl, 0.1% Tween-20 (v/v) and incubated with the following antibodies: α-p63 monoclonal antibody Ab-1 (Oncogene Research Products, Calbiochem), α-p53 monoclonal antibody Ab-2 (Oncogene Research Products, Calbiochem), α-p21Waf1 antibody Ab-1 (Oncogene Research Products, Calbiochem), α-14-3-3σ polyclonal antibody N-14 (Santa Cruz Biotechnology Inc., Santa Cruz, CA), α-β-actin polyclonal antibody I-19 (Santa Cruz Biotechnology Inc.), α-Gal4 monoclonal antibody DBD-RK5C1 (Santa Cruz Biotechnology Inc.), α-MPM2 antibody (Upstate Biologics. β-actin analyses as well as fast green staining of the membranes were used to assess uniformity of protein loading. Primary antibodies were detected using goat α-mouse, goat α-rabbit, or rabbit α-goat horseradish peroxidase-conjugated secondary antibody and enhanced chemiluminescence detection.

Phosphatase Assay. 63 was immunoprecipitated from HEK or HMEC protein lysates by rocking end over end at 4°C for 1 h in EBC using a p63 antibody (H-129, Santa Cruz) and 15 μl bed volume of protein A sepharose (PAS) (Amersham Biosciences Corp., Piscataway, NJ). Immunoprecipitates were washed once with EBC and twice with phosphatase buffer (50 mM Tris pH 8.0, 10% glycerol). Samples were resuspended in 20 μl phosphatase buffer with or without phosphatase inhibitors. Forty units (2 μl of 20U/μl) of calf intestinal alkaline phosphatase (Roche, Indianapolis, IN) were added and samples were incubated 37°C for 3 h. The phosphatase reaction was stopped by the addition of Laemmli SDS sample buffer. The control and phosphatase-treated lysates were analyzed by Western.

Formaldehyde cross-linking. Growth medium was aspirated from ~5 x 10^6 cells and cell cultures were washed with phosphate-buffered saline (PBS) and incubated with a

1.6% formaldehyde (EM Science) solution in PBS for 13 min at room temperature. The cross-linking was terminated by the addition of glycine to a final concentration of 0.144 M for 5 min. Monolayers were washed twice with PBS. Extracts were prepared by scraping cells in 1 ml of RIPA buffer (150 mM NaCl, 1% Nonidet P-40, 0.5% deoxycholate, 0.1% SDS, 50 mM Tris pH 8.0, 5 mM EDTA) containing the protease inhibitors antipain (10 μg/ml), leupeptin (10 μg/ml), pepstatin A (10 μg/ml), chymostatin (10 μg/ml), 4-(2-aminoethyl) benzenesulfonylfluoride (200 μg/ml), and the phosphatase inhibitors 50 mM NaF and 0.2 mM Na-vanadate. Cell lysates were sonicated to yield chromatin fragments of approximately 600 bp as assessed by agarose gel electrophoresis. Debris was pelleted by centrifugation for 15 min at 13,000 x *g*. The lysate was aliquoted and 0.8 mg of protein extract was precleared with 10 μg of mouse immunoglobulin G bound to PAS for p53 immunoprecipitation or 20 μg of rabbit immunoglobulin G bound to PAS for p63 immunoprecipitation. Protein lysates were precleared for 1 hr at 4°C. After centrifugation for 2 min at 13,000 x *g*, supernatants were transferred to a new tube. A 15 μl bed volume of PAS and 2 μg of α-p53 antibody (Ab-2 Oncogene Research Products) or α-p63 antibody (H129 Santa Cruz Biotechnology) were added to extracts precleared with non-specific antibodies, and immunoprecipitation was performed by rocking overnight at 4°C. To control for nonspecific binding during immunoprecipitation, cross-linked lysates were also immunoprecipitated with mouse monoclonal α-cyclin B1 (GNS1 Santa Cruz) or rabbit polyclonal α-Bax (N20 Santa Cruz) antibodies that did not cross-react with p53 or p63 respectively.

Immunocomplexes were washed twice with RIPA buffer, four times with IP wash buffer (100 mM Tris pH 8.5, 500 mM LiCl, 1% Nonidet P-40, 1% deoxycholic acid), and

twice more with RIPA buffer. Between washes, samples were rocked for 5 min at 4°C; 200 μl of cross-linking reversal buffer (125 mM Tris pH 6.8, 10% β-mercaptoethanol, 4% SDS) were added to the washed PAS pellet. Samples were boiled for 30 min to reverse the formaldehyde cross-links. DNA was phenol-chloroform extracted, the phenol-chloroform phase back extracted with 10mM Tris pH 8.3, ethanol precipitated, allowed to air dry, and dissolved in sterile H_2O.

PCR amplification. p21 Site 1 and 14-3-3σ Site 1 PCR amplifications were performed in 16.6 mM $(NH4)_2SO4$, 0.67 mM Tris pH 8.8, 6.7 mM $MgCl_2$, 10 mM β-mercaptoethanol, 10% dimethyl sulfoxide, 1.5 mM nucleotides, and 1.25 U Taq polymerase (Promega). 175 ng of each primer were used for each 25 μl reaction. Forty-five PCR cycles were performed for p21 site 1, each cycle consisting of 20 sec at 94°C, 45 sec at 61°C, and 25 sec at 72°C. 14-3-3σ site 1 was amplified using 45 PCR cycles each consisting of 20 sec at 94°C, 45 sec at 57.5°C, and 25 sec at 72°C. p21 Site 2 and 14-3-3σ site 2 PCR amplifications were performed using Ready-To-Go PCR beads (Amersham Biosciences, Piscataway, NJ) according to the manufacturer's directions with a final primer concentration of 0.4 μM. Thirty PCR cycles were performed for p21 site 2. Each cycle consisted of 30 sec at 95°C, 45 sec at 66°C, and 25 sec at 72°C. Thirty-eight PCR cycles were performed for 14-3-3σ site 2. Each cycle consisted of 20 sec at 94°C, 45 sec at 61°C, and 25 sec at 72°C. Glyceraldehyde phosphate dehydrogenase (GAPDH) PCR amplification was performed in 10 mM Tris pH 9.0, 50 mM KCl, 0.1% Triton-X, 0.5 mM $MgCl_2$, 0.25 mM nucleotides, and 1.25 U Taq polymerase (Promega). Each primer was used at 0.2 μM per 25 μl reaction. Thirty-five cycles of PCR were performed for GAPDH amplification, each cycle consisted of 20 sec at 94°C, 45 sec at 62°C and 25

sec at 72°C. Primers used for PCR amplifications were as follows: for p21 site 1: 5'-GCTT GGGCAGCAGGCTG-3' and 5'-AGCCCTGTCGCAAGGATCC-3'; p21 site 2: 5'-GCAGTG GGGCTTAGAGTGGGG-3' and 5'-CAGGCTTGGAGCAGCTACAATT AC-3'; 14-3-3σ site 1: 5'-CATTTAGGCAGTCTGATTCC-3' and 5'-GCTCACGCCTG TCATCTC-3'; 14-3 3σ site 2: 5'-CTCACTACCTCAAGATACCC-3' and 5'-CACAGG CCTGTGTCTCCC-3'. GAPDH was amplified using 5'-CACCAGCCATCCTGTCCTC C-3' and 5'-GTTCCTTCCCAGCCCCCACT-3' primers. PCR DNA products were resolved using 8% polyacrylamide gels (acrylamide:bis acrylamide, 19:1) in 1X Tris acetate-EDTA buffer. Gels were stained with ethidium bromide. Relative levels of DNA were determined using Quantity One® software (Bio-Rad Laboratories, Hercules, CA).

Flow cytometry. Control and treated cells were trypsinized, the trypsin was inactivated, and 10^6 cells were aliquoted for flow cytometry. The remaining cells were processed for protein analysis (see above). Cells were incubated with 20 μg of propidium iodide (Sigma) per ml, and the DNA content was measured with a FACSCaliber instrument (Becton-Dickson). Data were plotted with Cell Quest software (Becton-Dickson); 15,000 events were analyzed for each sample.

Subcellular Fractionation. For each timepoint analyzed, 5 x 10^7 cells were harvested by trypsinizing the cells and pelleting at 1000 rpm at 4^0C. The cells were washed one time with PBS and pelleted as above. After the PBS wash, the cells were resuspended in 1 ml of Hypotonic Lysis Buffer (HLB: 5 mM Tris-HCl pH 7.5, 5mM KCl, 1.5 mM $MgCl_2$, 0.1 mM EGTA, 1mM DTT) supplemented with the phosphatase inhibitors, 50 mM NaF, 0.2 mM NaVanadate, 10 mM p-nitrophenyl phosphate, and 10 mM β-glycero-phosphate and the protease inhibitors, antipain (10 μg/ml), leupeptin (10

μg/ml), pepstatin A (10 μg/ml), chymostatin (10 μg/ml) (Sigma), and 4-(2-aminoethyl)-benzenesulfonylfluoride (200 μg/ml). After resuspension in Hypotonic Lysis Buffer, cells were incubated on ice for 30 min. For isolation of nuclei, cells were transferred to a dounce homogenizer size AA (Thoma Scientific, Swedesboro, NJ) and dounced 20 times with douncing efficiency verified by trypan blue staining of a small aliquot of dounced cells. After douncing, samples were centrifuged for 5 min at 1000 x g at 4^0C to pellet the nuclei and the supernatant (cytoplasmic fraction) was transferred to a separate tube. The pelleted nuclei were washed once with Hypotonic Buffer and resuspended in EBC lysis buffer supplemented with the phosphatase inhibitors, 50 mM NaF, 0.2 mM NaVanadate, 10 mM p-nitrophenyl phosphate, and 10 mM β-glycero-phosphate and the protease inhibitors, antipain (10 μg/ml), leupeptin (10 μg/ml), pepstatin A (10 μg/ml), chymostatin (10 μg/ml) (Sigma), and 4-(2-aminoethyl)-benzenesulfonylfluoride (200 μg/ml). Isolated cellular fractions were quantified as described (see above) and analyzed by Western (see above).

Immunofluorescence Microscopy. Sub-confluent cells, grown on 22 mm^2 glass cover slips (VWR Scientific, Atlanta, GA), were treated for 12 h with 100 nM Taxol. After treatment, cells were washed one time with PBS and fixed with 100% cold methanol or 4% paraformaldehyde/PBS, for 20 min at room temperature. Cells were washed four times with PBS, permeabilized by incubation with 0.2% Triton X-100 (in PBS) for 10 min at room temperature, then washed two additional times with PBS. For p63 staining, non-specific binding sites were blocked by cellular incubation for 2 h with 5% horse serum in PBS, incubated in primary antibodies diluted in 5% serum/PBS (mouse p63 1:750) for 1 h at room temperature, followed by four washes with PBS.

Cells were incubated in biotinylated secondary antibody diluted in 5% serum/PBS (1:250) for 1 h at room temperature, washed four times with PBS, and incubated in streptavidin-conjugated Cy3 diluted in 5% serum/PBS (1:1000) for 1 h at room temperature. Cells were washed four times with PBS and nuclei were counterstained by incubation with DAPI for 5 min at room temperature. After DAPI staining, cells were washed three times with PBS and cover slips were mounted onto 25x75 mm microslides (Fisher Scientific, Pittsburgh, PA) using AquaPolyMount (Polysciences, Warrington, PA). Phase contrast images were captured using the Zeiss Epifluorescence inverted microscope and Zeiss AxioCam digital camera. Fluorescent images were captured using the Zeiss Axiophot upright microscope and the Princeton Instruments cooled CCD digital camera.

Results

ΔNp63α is phosphorylated in primary epidermal keratinocytes and mammary epithelial cells after Taxol treatment. As previously shown (48), ΔNp63α exists as a phosphoprotein in rapidly growing and differentiating primary HEKs. Since it is well established that p53 is phosphorylated after cells are treated with IR, ADR, UV, and microtubule inhibitors (43, 45), we determined what effect these treatments would have on ΔNp63α in HEKs and primary human mammary epithelial cells (HMECs) that express p63 (2). HEKs and HMECs were treated with UV, Taxol, IR, and ADR (Fig. 1A HEKs and 1B HMECs). Western analysis showed that UV, Taxol, IR, and ADR treatment resulted in an increase in the p53 protein and an increase in its downstream target p21 in UV, IR, and ADR treated cells (Fig. 1A and 1B). However, there was minimal, if any, increase in p21 levels in Taxol treated samples. These results coincided

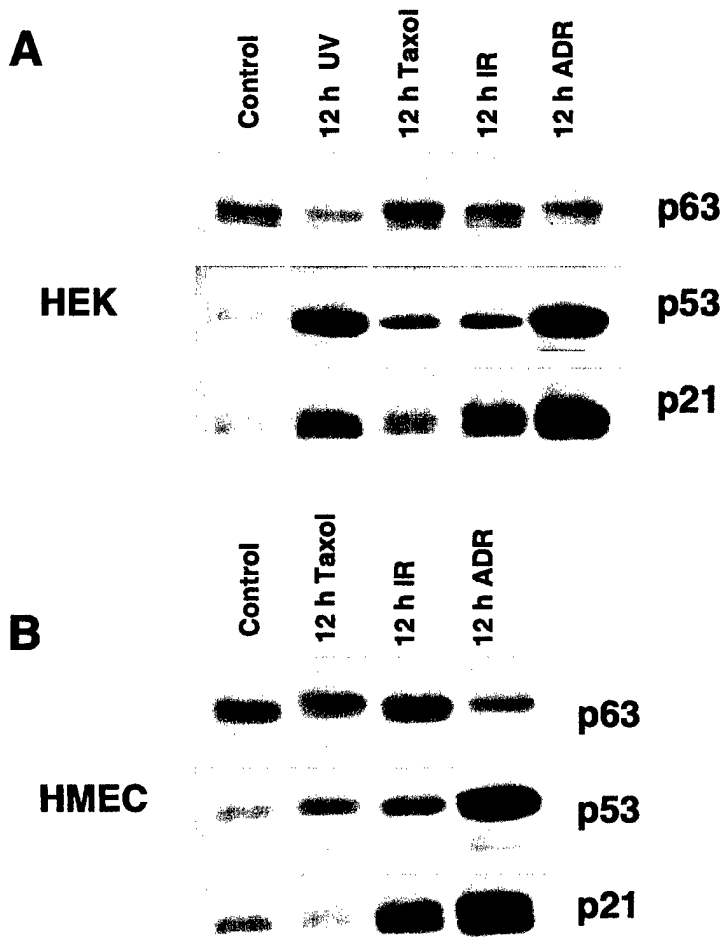

Figure 1. Analysis of HEKs and HMECs after treatment with radiation and chemotherapeutics. HEKs and HMECs were treated for 12 h with 50 J/m^2 UV, 100 nM Taxol, 8 Gy IR, or 0.4 μM ADR. A) Western analysis of p63, p53, and p21 on HEK lysates from treated cells B) Same as in A) but with HMECs. Results are representative of three independent experiments.

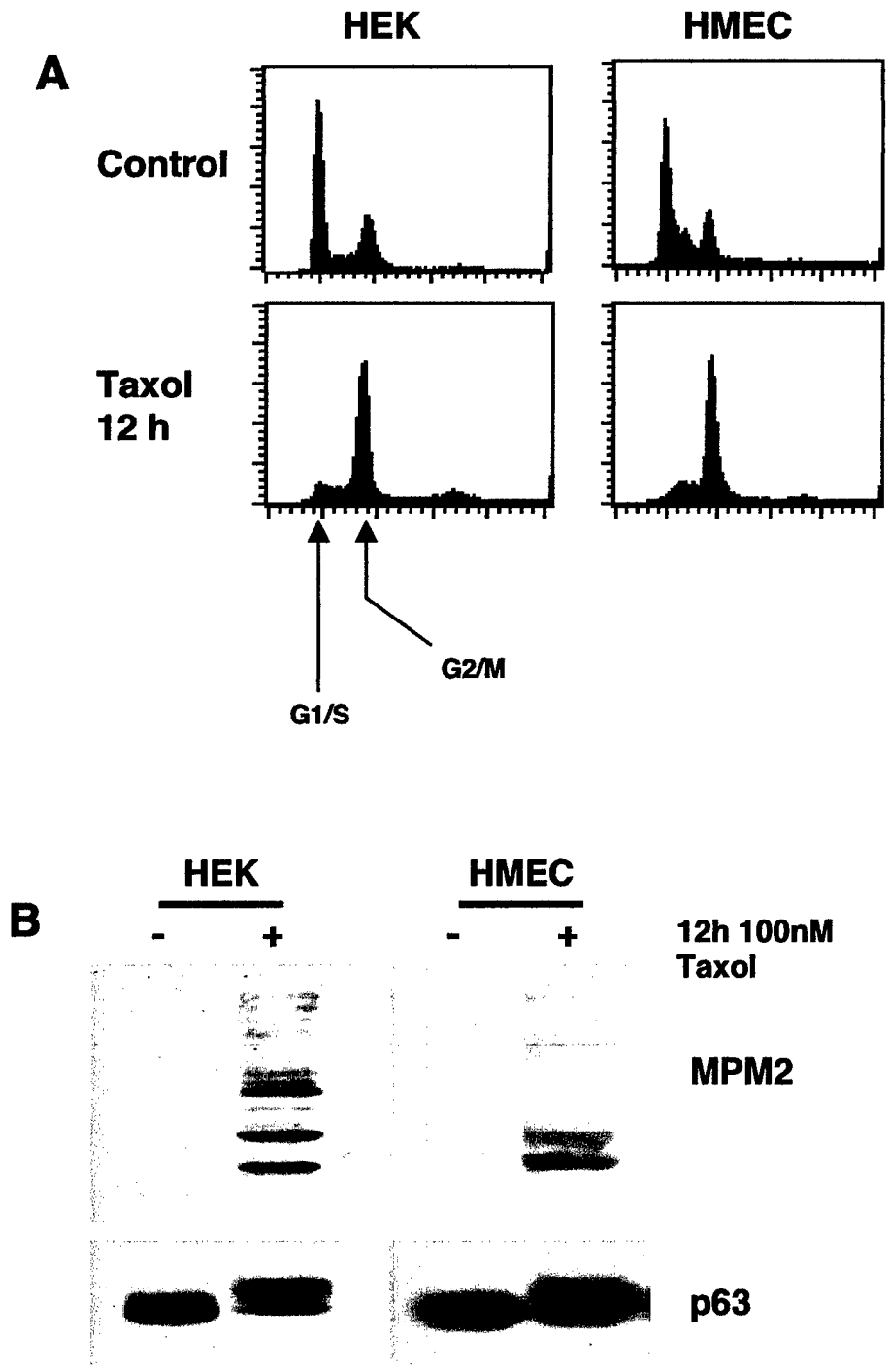

Figure 2. Taxol-induced mobility shift of ΔNp63α in HEKs and HMECs. HEKs and HMECs were treated for 12 h with 100 nM Taxol. A) Flow cytometric analysis of HEKs and HMECs treated with Taxol for analysis of cell cycle position. B) Western analysis of HEK and HMEC lysates from 100 nM Taxol treated cells for expression of p63 and the mitotic marker MPM2. Results are representative of three independent experiments.

with an altered mobility of ΔNp63α in the Taxol treated samples suggesting that Taxol treatment caused posttranslational modifications of the ΔNp63α protein. Flow cytometric analysis of both HEKs and HMECs showed a G2/M arrest after a 12 h Taxol treatment. This arrest correlated with a shift in ΔNp63α mobility to a slower migrating form. Western analysis of the same cell lysates in was performed with MPM2, an antibody that recognizes mitotic phospho-epitopes, indicated that ΔNp63α phosphorylation occurred during mitosis (Fig. 2B).

To determine if the reduced mobility of ΔNp63α after Taxol treatment was due to phosphorylation, p63 was immunoprecipitated from HEK and HMEC protein lysates prepared from control and Taxol treated cells and incubated with calf intestinal alkaline phosphatase (CIAP) in the presence and absence of phosphatase inhibitors (Fig. 3). Western analysis of HEK (Fig. 3A) or HMEC (Fig. 3B) lysates revealed a change of the slower migrating ΔNp63α protein form(s) to faster migrating form(s) after CIAP treatment in the absence of phosphatase inhibitors, consistent with the conclusion that ΔNp63α is a phosphorylated protein. In addition, phosphatase treatment revealed that total ΔNp63α protein from control and Taxol treated cells exists in a phosphorylated state as ΔNp63α from both control and Taxol treated cells migrated as a single, faster migrating band after phosphatase treatment (Fig. 3A and 3B).

ΔNp63α phosphorylation is microtubule inhibitor specific and dose-dependent. Chemicals that alter microtubule dynamics are classified into two categories: microtubule-destabilizers (microtubule depolymerization enhanced) and microtubule-stabilizers (microtubule polymerization enhanced). To determine if ΔNp63α was differentially affected by microtubule depolymerization versus polymerization, we

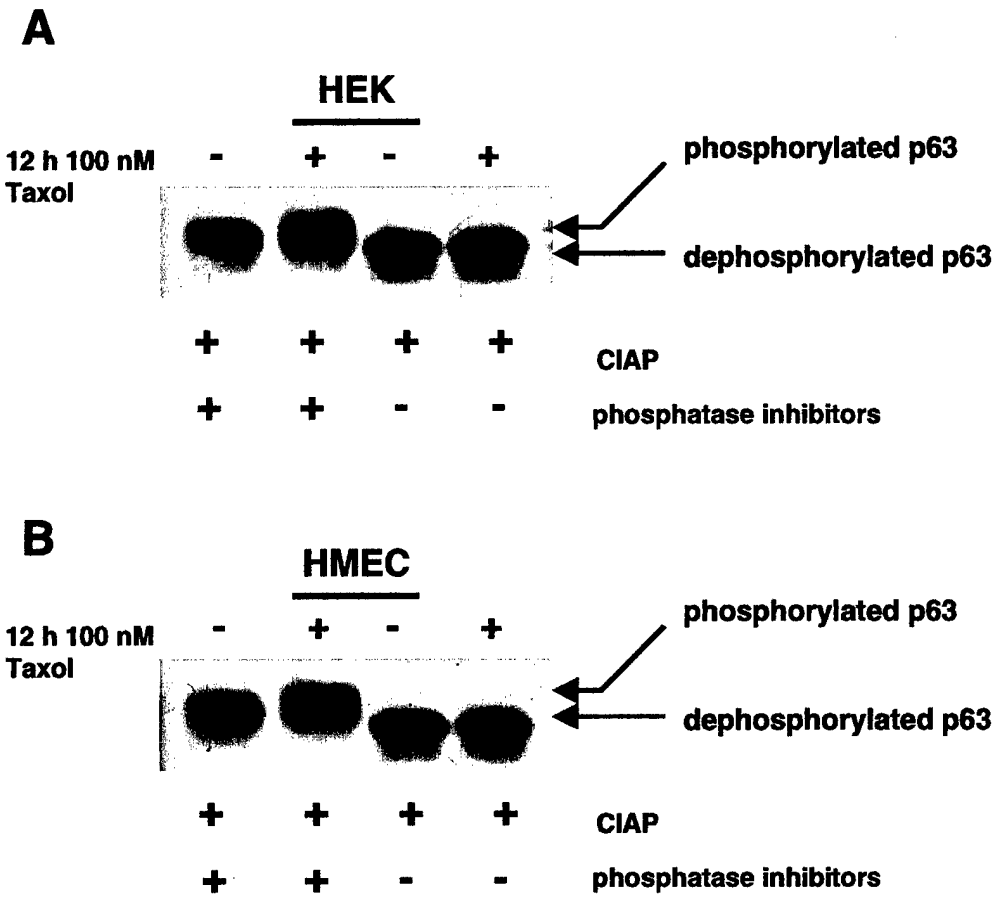

Figure 3. ΔNp63α is phosphorylated after 12 h 100 nM Taxol treatment. A) Protein lysates were prepared from control and Taxol treated HEKs and p63 was immunoprecipitated with a rabbit polyclonal antibody. Immunoprecipitates were treated with calf intestinal alkaline phosphatase (CIAP) in the presence or absence of phosphatase inhibitors and immunoprecipitated protein was analyzed by Western for p63 using a mouse monoclonal antibody. Arrows denote differentially migrating ΔNp63α forms. B) Same as in A) but with HMECs. Results are representative of three independent experiments.

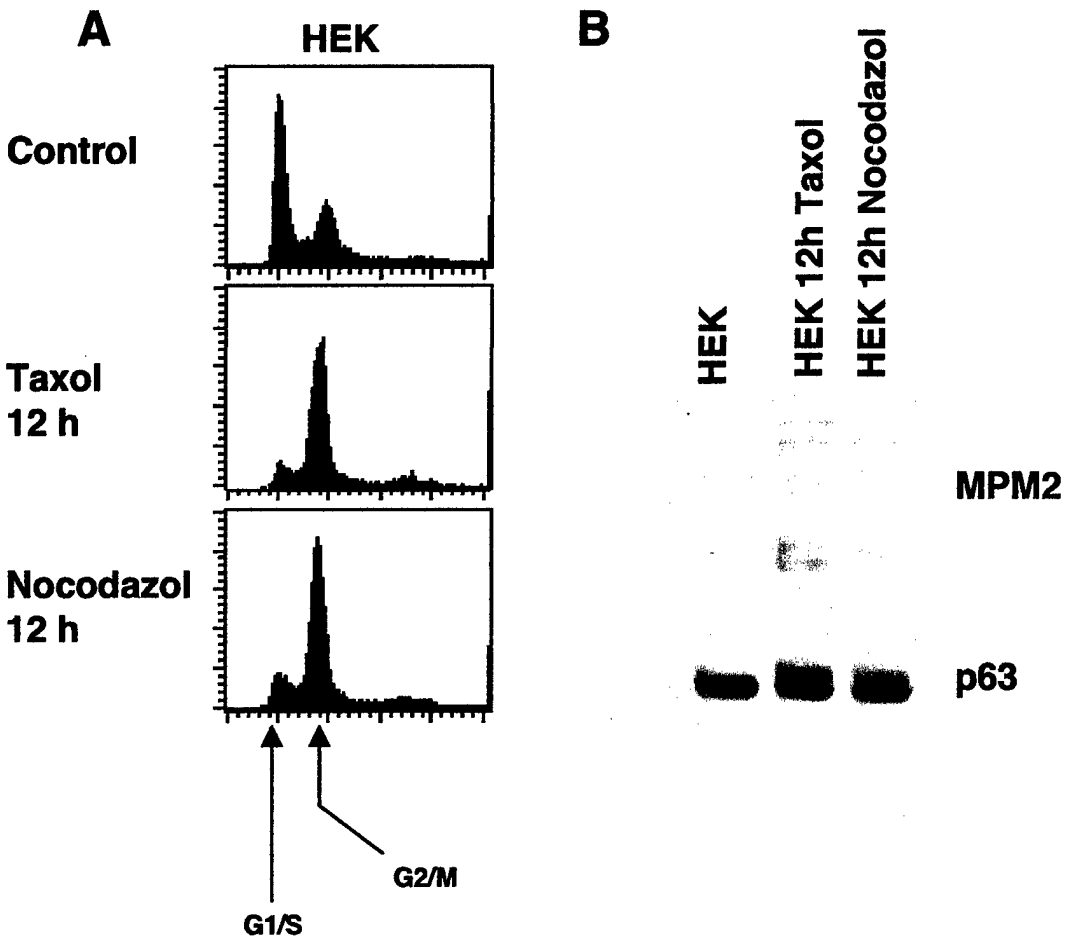

Figure 4. ΔNp63α phosphorylation is microtubule inhibitor specific. HEKs were treated for 12 h with 100 nM Taxol or 83 nM nocodazol. A) Flow cytometric analysis of HEKs treated with Taxol or nocodazol for analysis of cell cycle position. B) Western analysis of HEK lysates from 100 nM Taxol and 83 nM nocodazol treated cells for expression of p63 and the mitotic marker MPM2. Results are representative of three independent experiments.

compared the effect of Taxol, a microtubule-stabilizing drug (36-38), with nocodazol, a microtubule-destabilizing drug (6, 40). Flow cytometric analysis of HEK cells demonstrated that nocodazol arrested cells with a 4N DNA content with similar kinetics to Taxol (Fig. 4A). Furthermore, Western analysis showed that nocodazol, like Taxol, caused phosphorylation and a decreased mobility of ΔNp63α (Fig. 4B). MPM2 detection by Western again indicated that the phosphorylation correlated with cell entry into mitosis (Fig. 4B).

In addition to determining that phosphorylation was microtubule inhibitor-dependent, we determined if the effect was dose-dependent. Using a squamous cell carcinoma cell line, SCC1, we treated cells with 25, 50, and 100 nM Taxol and analyzed the cells by flow cytometry and Western at 12 h, 24 h, 48 h, and 72 h after Taxol treatment. All doses of Taxol induced growth inhibition by 12 h (Fig. 5A). However, at later time points, cultures treated with the lower doses of Taxol had an increased number of cells with a DNA content <2N (Fig. 5A, note Sub-G_1 population). This is consistent with a previous report demonstrating a reversible mitotic arrest at lower concentrations of Taxol treatment, subsequent progression in the cell cycle, and ultimately cell death (39). Furthermore, prolonged cell exposure to Taxol will eventually result in mitotic slippage, a process where cells biochemically reenter the G_1 phase of the cell cycle without going through cytokinesis, and subsequent apoptosis (Fig. 5A 24 h, 48 h, and 72 h) (5, 9, 42). The higher Taxol dose (100 nM) likely prevented this mitotic slippage until later time points that were not examined (Fig. 5A). Western analysis again showed a marked shift in ΔNp63α migration (Fig. 5B 12 h and 24 h). Interestingly, at later time points (Fig. 5B, compare 24 h with 12 h), the majority of the ΔNp63α protein was shifted to the slower

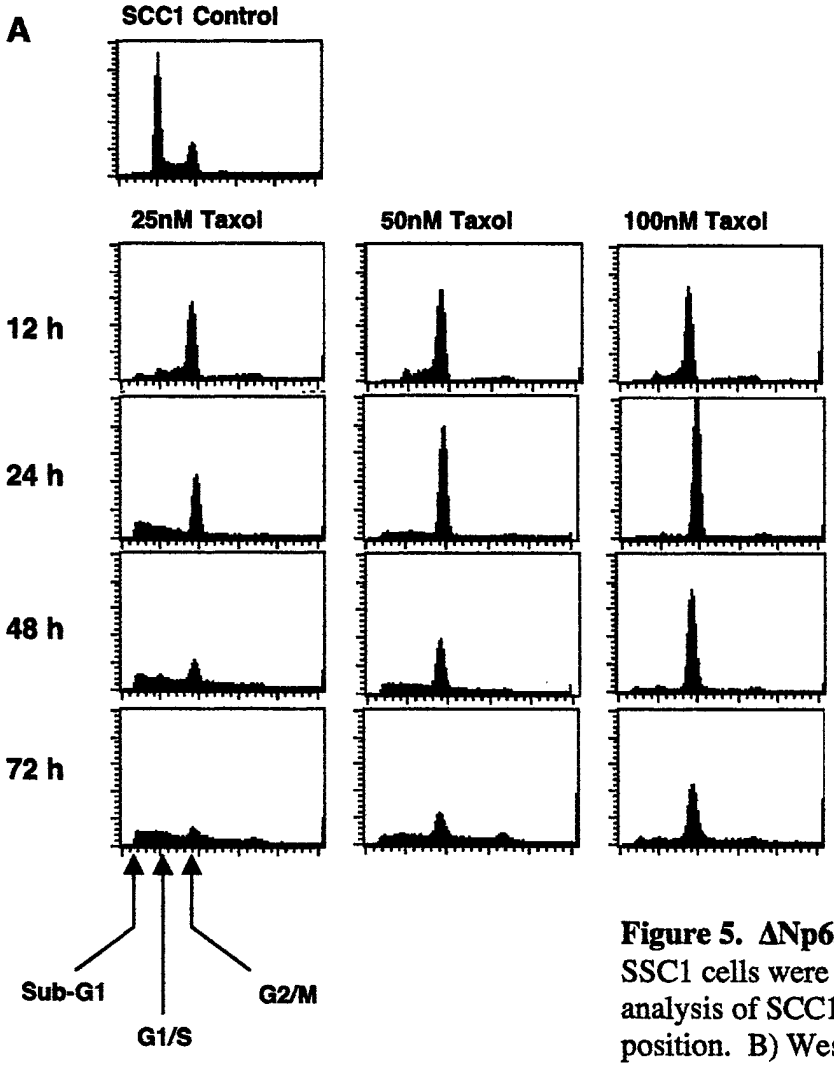

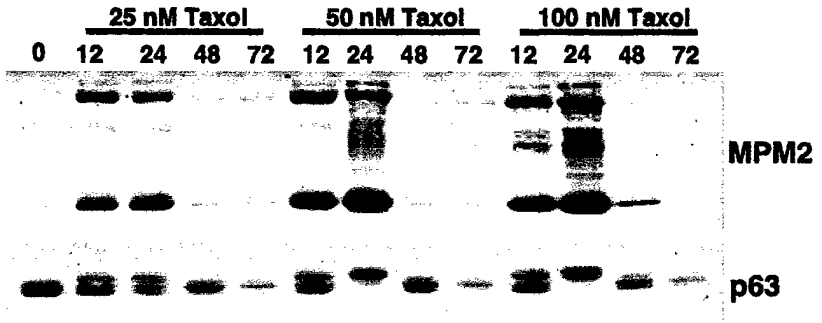

Figure 5. ΔNp63α phosphorylation after Taxol treatment is dose-dependent. SSC1 cells were treated for 12 h with 25, 50, or 100 nM Taxol. A) Flow cytometric analysis of SCC1 cells treated with Taxol or nocodazol for analysis of cell cycle position. B) Western analysis of SCC1 lysates from 100 nM Taxol treated cells for expression of p63 and the mitotic marker MPM2.

migrating form after Taxol treatment; however, experiments in SCC1 cells also showed a reduction in the phosphorylated ΔNp63α at the 48 h and 72 h time point (Fig. 5B). The results in Fig. 4 and Fig. 5 indicate that ΔNp63α phosphorylation is dose-dependent and microtubule disruption specific. Additionally, the kinetics and efficiency of microtubule inhibitor-induced ΔNp63α phosphorylation appear to differ depending on cell type as later Taxol timepoints (Fig. 5B, see 24 h 50 nM and 100 nM) in SCC1 cells showed a complete shift in ΔNp63α mobility, a trend not seen in HEKs or HMECs (data not shown).

Increased ΔNp63α phosphorylation occurs during mitosis after Taxol treatment. Since treatment of cells with agents that disrupt microtubule dynamics results in cell cycle arrest in mitosis, we determined if Taxol-mediated ΔNp63α phosphorylation was dependent on mitotic arrest. For this line of investigation, we synchronized cells and analyzed the effect of Taxol on p63 phosphorylation in G_1, S, G_2, and mitosis (22). The immortalized keratinocyte cell line, HaCaT, was serum-starved for 48 h to synchronize the cells in G_1 and cells were subsequently washed with PBS and released into complete medium supplemented with 100 nM Taxol. Cells were harvested at 6 h, 12 h, 24 h, 36 h, 48 h and 72 h after release. Flow cytometric analysis showed the cells reentering the cell cycle between 12 and 24 h as indicated by the decrease in G_1-phase and increase in S-phase (Fig. 6A). Cell entry into mitosis did not occur until 24 to 36 h as assessed by Western analysis with MPM2 signal marking the 36 time point (Fig. 6A and 6B). Additionally, while ΔNp63α protein levels decreased slightly after 48 h serum starvation, a change in mobility during the G_1 or S-phase of the cell cycle was not detected (Fig. 6B). More importantly, the phosphorylation of ΔNp63α did not occur until the cells entered

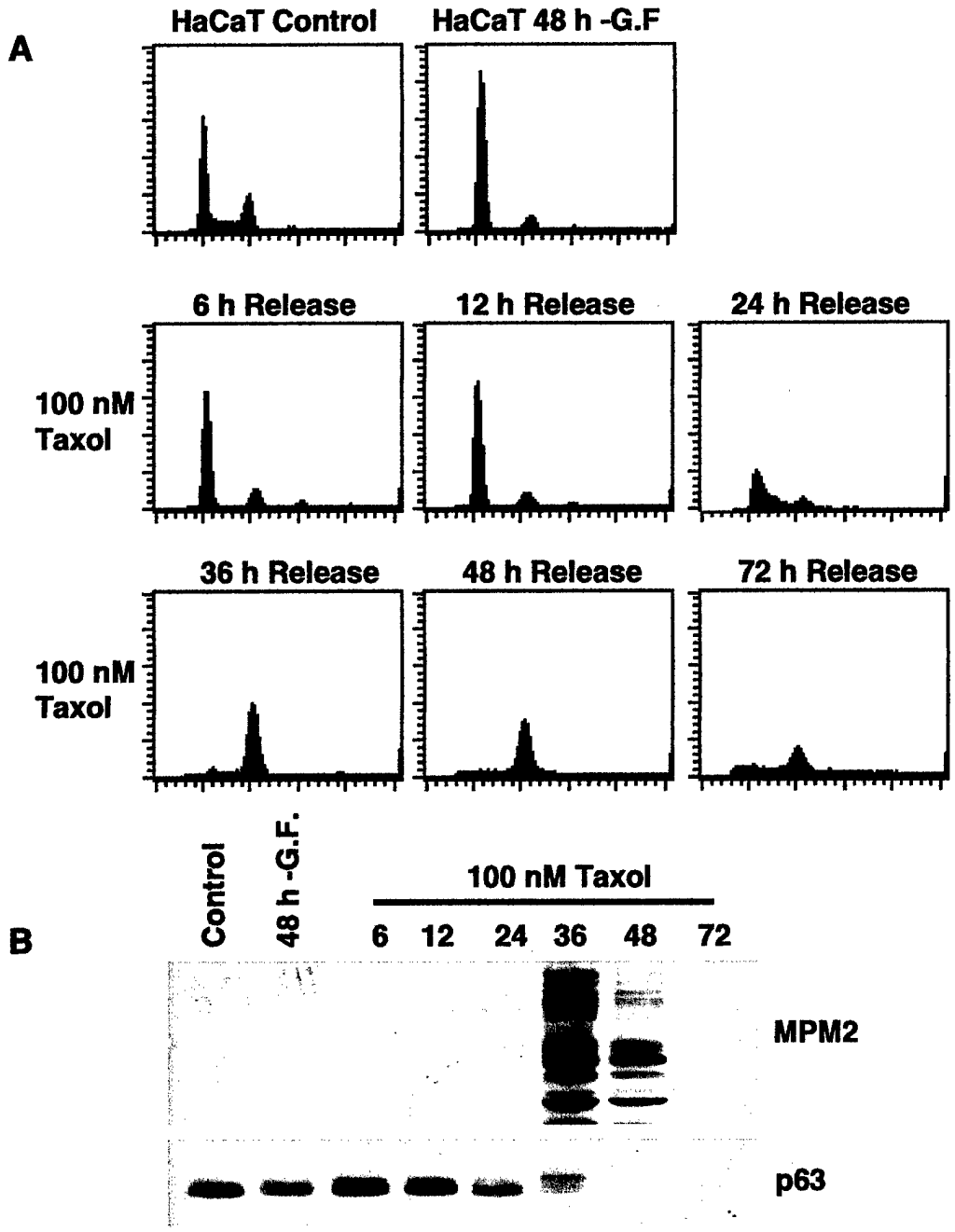

Figure 6. Increased ΔNp63α phosphorylation occurs during mitosis after Taxol treatment. HaCaT cells were synchronized by 48 h serum-starvation (-G.F. (growth factors)). Cells were washed twice with PBS and released into serum-containing media with 100 nM Taxol. A) Flow cytometric analysis of control, serum-starved, and released HaCaT cells. B) Western analysis of HaCaT lysates from control, serum-starved, and released HaCaT cells for expression of p63 and the mitotic marker MPM2. Results are representative of three independent experiments.

mitosis as indicated by the shift in protein mobility at 36 h (Fig. 6B). Of note, ΔNp63α protein levels significantly decreased by the 48 h time point and were below detectable levels at the 72 h time point after release (Fig. 6B). The decrease in ΔNp63α protein levels was due to the high percentage of apoptotic cells at the later time points resulting in degradation of the ΔNp63α protein. The hyperphosphorylated form of ΔNp63α may be targeted for degradation; however, determining protein stability in this cell system would not be possible due to the confounding effects of apoptosis. In sum, the data in Fig. 5 (see Fig. 5B 12 h and 24 h Taxol) and Fig. 6 (see Fig. 6B 36 h release) strongly suggest that ΔNp63α can be phosphorylated during mitosis in a Taxol-dependent manner.

Taxol-induced ΔNp63α phosphorylation does not affect subcellular localization. The dramatic shift in ΔNp63α phosphorylation after 12 h Taxol treatment prompted us to determine if this posttranslational modification affected the subcellular regulation or DNA binding activity of p63. p63 protein is localized to the nucleus of basal cells of stratified epithelia (7, 8, 49) and to determine if Taxol treatment would alter this localization of p63, we investigated ΔNp63α location by immunofluorescence staining and subcellular fractionation. For immunofluorescence studies, HEKs and HMECs were grown on glass cover slips in the absence or presence of Taxol for 12 h and p63 protein was analyzed. Cellular nuclei were counter-stained with DAPI. ΔNp63α immunofluorescence showed strong nuclear staining in control samples for HEKs and HMECs (Fig. 7A and 7C, α-p63 column). More importantly, p63 localization corresponded to DAPI stained nuclei in control samples (Fig. 7A and 7C, Merged column) consistent with p63 localization in human tissue samples (7, 8, 49). The subcellular localization of p63 did not change in Taxol treated HEKs and HMECs

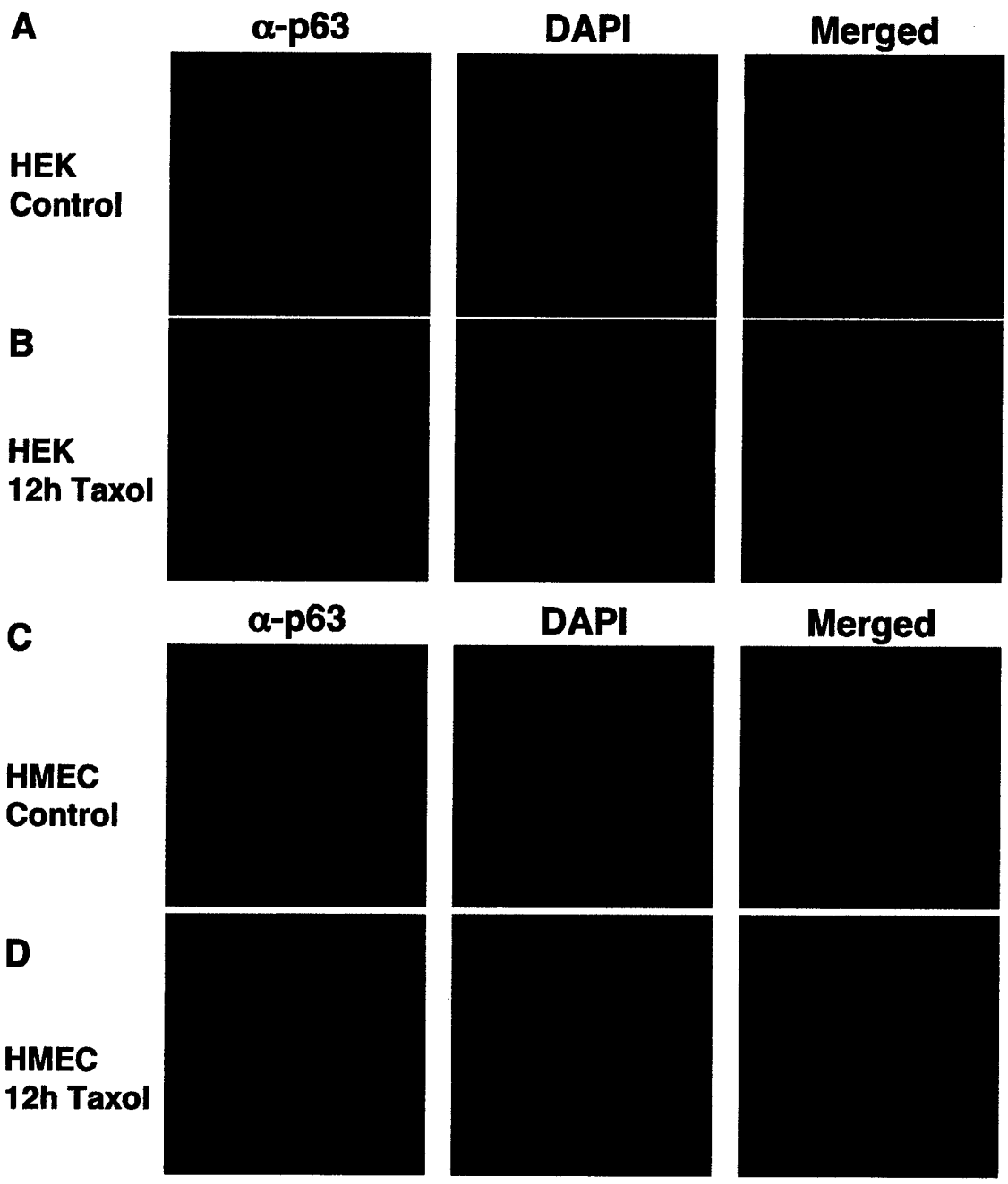

Figure 7. Taxol induced ΔNp63α phosphorylation does not affect subcellular localization. HEKs and HMECs were grown on glass coverslips in 6-well dishes. Cells were grown in the absence or presence of Taxol (100 nM 12 h) and fixed in 4% paraformaldehyde for immunofluorescence. A) HEK control cells were probed for p63 and stained with DAPI for nuclear localization. α-p63 and DAPI fields were merged in column three to show localization of p63. B) HEK cells were probed as in A) after 12 h 100 nM Taxol treatment. C and D) HMECs were probed as in A and B) respectively. Results are representative of three independent experiments.

(Fig. 7B and 7D, see α-p63 and Merged columns). To confirm the results seen in our immunofluorescence experiments, we also performed subcellular fractionation on control and 12 h Taxol treated HEKs and HMECs. Protein lysates were prepared by hypotonic lysing to generate nuclear and cytoplasmic fractions as described previously and we analyzed fractionated and total cell extracts by Western for ΔNp63α expression (Fig. 8B). The p53 and PIG3 proteins were analyzed to verify that our fractions were enriched for nuclear and cytoplasmic proteins, respectively (Fig. 8B) (12). ΔNp63α protein was in the same fraction as p53 in control and Taxol-treated samples confirming our immunofluorescent results. Cell cycle position was confirmed by flow cytometry (Fig. 8A) and MPM2 reactivity by Western analysis was used to verify cells arrested in mitosis (Fig. 8B).

Taxol-induced ΔNp63α phosphorylation does not affect DNA binding. As HEKs are induced to differentiate, p63 levels decrease with a corresponding decrease in DNA binding to select gene promoters (48) and a subsequent increase in transcript and protein levels of the cyclin dependent kinase inhibitor p21, a p53 target gene. However, when HEKs and HMECs were treated with 100 nM Taxol for 12 h there was not a statistically significant change in ΔNp63α or p21 protein levels, but there was a Taxol-induced increase in p53 levels similar to the IR-induced p53 levels (Fig. 1). Therefore, we evaluated if the Taxol-induced phosphorylation would alter binding of ΔNp63α to p53 consensus sites in the p21 promoter. Using ChIP methodology, we formaldehyde cross-linked control and 12 h Taxol treated HEKs and HMECs. After cross-linking, p63 was immunoprecipitated and the DNA to which the proteins were bound was purified. The DNA was PCR amplified using primers specific for sequences that flank the p53

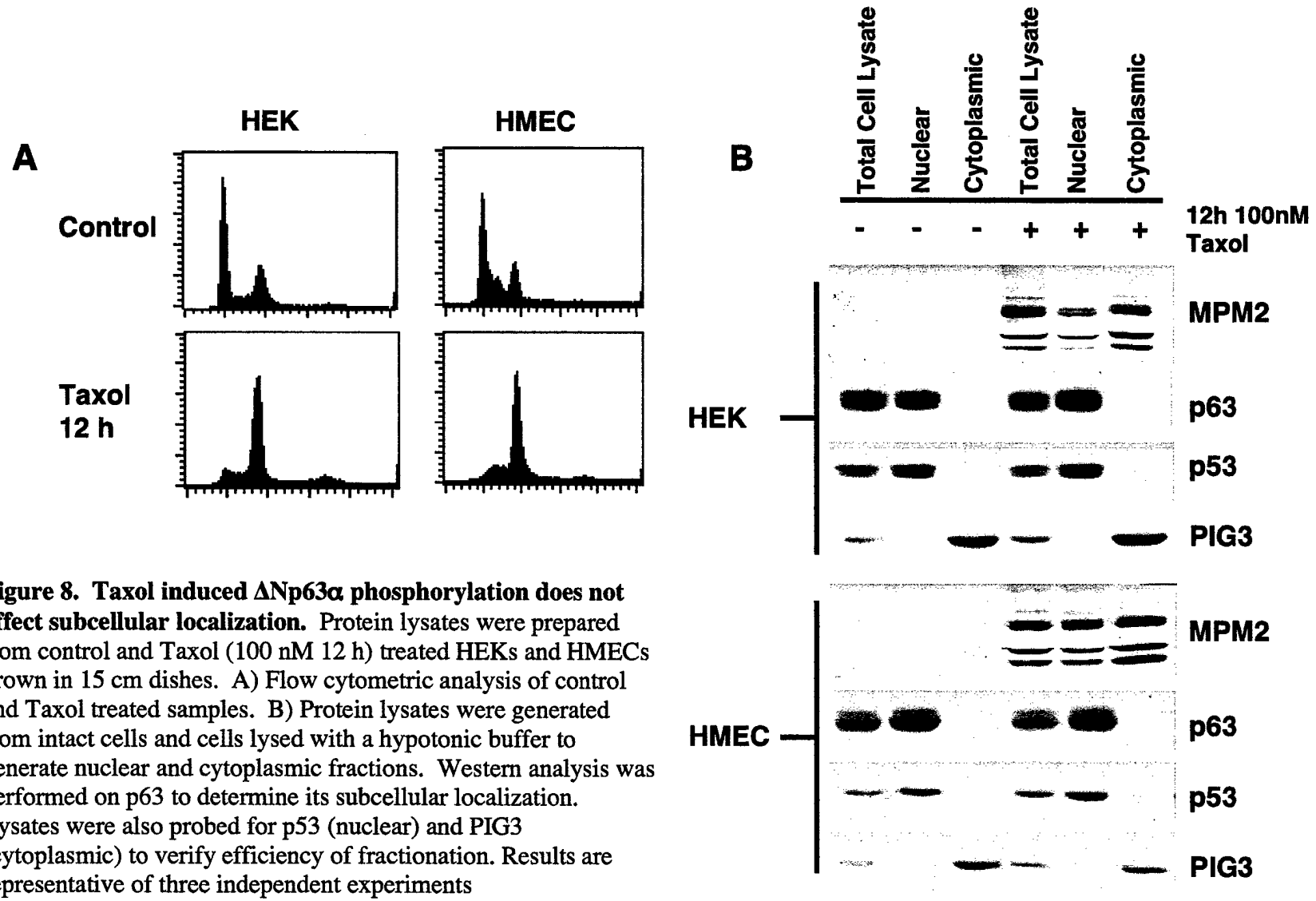

Figure 8. Taxol induced ΔNp63α phosphorylation does not affect subcellular localization. Protein lysates were prepared from control and Taxol (100 nM 12 h) treated HEKs and HMECs grown in 15 cm dishes. A) Flow cytometric analysis of control and Taxol treated samples. B) Protein lysates were generated from intact cells and cells lysed with a hypotonic buffer to generate nuclear and cytoplasmic fractions. Western analysis was performed on p63 to determine its subcellular localization. Lysates were also probed for p53 (nuclear) and PIG3 (cytoplasmic) to verify efficiency of fractionation. Results are representative of three independent experiments

response elements in the promoters studied. To assure that the amplified DNA was the correct size, control PCR reactions were performed with or without genomic HEK DNA (Fig. 9A and 9C "+" or "-" lanes respectively). To control for nonspecific binding during immunoprecipitation, cross-linked lysates were immunoprecipitated with rabbit polyclonal α-Bax antibodies that did not cross-react with p63 (Figs. 9A and 9C; lane C). The ChIP experiments revealed that p63 bound p21 promoter site 1 in rapidly growing (RG) and Taxol treated (Tax) HEKs (Fig. 9A). Occupancy at p21 site 1 did not change significantly between rapidly growing and Taxol treated cells (Fig. 9A). ChIP experiments performed in the HMECs yielded the same results as the HEKs with p63 binding to the p21 promoter site 1 (Fig. 9C). Quantification of the PCR reactions showed no change in occupancy of ΔNp63α between rapidly growing and Taxol treated HMECs at the p21 promoter (Fig. 9B and 9D). These data indicate that Taxol induced ΔNp63α phosphorylation does not affect DNA binding at the consensus site we assayed in the p21 promoter.

Discussion

Using HEKs and HMECs as a model system, we demonstrated by Western that the ΔNp63α protein shifted to a slower migrating band after 12 h Taxol treatment. We did not observe this shift in IR, UV, or ADR treated cells, however the experiments presented cannot rule out IR, UV, or ADR-induced ΔNp63α phosphorylation. Similar to previous assays, phosphatase experiments determined that this change in mobility in SDS-PAGE was due to phosphorylation. Similar to our previous findings in HEKs, ΔNp63α is phosphorylated in rapidly proliferating HMECs. Using a second microtubule inhibitor, nocodazol, we found that ΔNp63α phosphorylation is not Taxol specific but

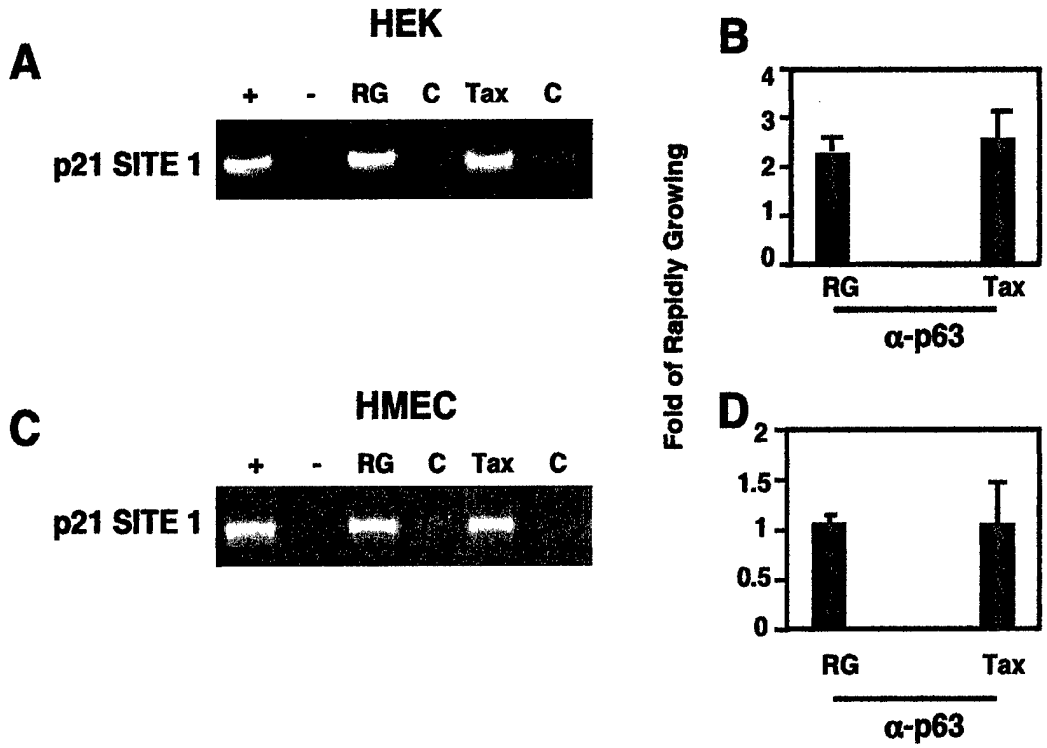

Figure 9. Taxol-induced ΔNp63α phosphorylation does not affect DNA binding. Abbreviations are (RG), Rapidly Growing; (Tax), 12 h 100 nM Taxol treatment; C, control. HEKs and HMECs were treated with 100 nM Taxol and at the time of harvest were treated with formaldehyde (X-Link) and processed as described in Chapter III. The DNA immunoprecipitated with p63-specific antibodies was PCR amplified using primers flanking the p53 binding sites in the p21 promoter (A and C). The lanes marked "+" indicate PCR products that were generated using DNA template derived from total genomic DNA harvested from rapidly growing HEKs. The lanes marked "–" indicate absence of DNA input for the PCR reaction. The lanes marked "C" indicate PCR reactions performed with templates immunoprecipitated with antibodies specific to Bax. Each ethidium bromide-stained gel shows one representative result of at least three independent experiments that are quantified and displayed with standard deviation in panels B and D.

specific to disruption of microtubule dynamics and mitotic arrest. The phosphorylation ΔNp63α is phosphorylated in rapidly proliferating HMECs. Using a second microtubule inhibitor, nocodazol, we found that ΔNp63α phosphorylation is not Taxol specific but specific to disruption of microtubule dynamics and mitotic arrest. The phosphorylation of ΔNp63α did not alter subcellular localization as immunofluorescence and subcellular fractionation experiments showed ΔNp63α remained in the nucleus after Taxol treatment. In addition, *in vivo* DNA-binding assays demonstrated that Taxol induced phosphorylation did not affect ΔNp63α binding to a p53 response element in the p21 promoter.

Due to the increased use of drugs that alter microtubule dynamics in cancer therapy it is important to understand the role of Taxol in altering intracellular signal transduction events. Taxol treatment of normal and tumor-derived cells causes increases in p53 phosphorylation after microtubule disruption (45), but the effect, if any, of microtubule inhibitors on the p53 family member p63 was not known prior to the studies presented within. This is an important avenue of research as Taxol is used as a first line therapy in the treatment of cancers arising from tissues in which p63 is expressed, including breast, ovarian, lung, and head and neck cancer. In fact, p63 is amplified in squamous cell carcinoma of the head and neck (20, 46) where Taxol has shown a 20-40% response rate when used as a single-agent (14, 17, 41). Additionally, clinical trials of Taxol in combination with various cytotoxic agents including cisplatin, 5-fluorouracil, carboplatin, and gemcitabine have been reported with various response rates in head and neck cancer (3, 15, 16, 24). However, several questions regarding p63 in tumorigenesis remain, such as: What is the role of p63 overexpression in tumors? How does p63

expression affect p53 activity in tumors? What role does Taxol-induced p63 phosphorylation play in p63 function? These and other questions need to be addressed to gain a better understanding of the role p63 plays in tumorigenesis.

The data presented demonstrating ΔNp63α phosphorylation, although provocative, has not been connected to a functional role for regulation of ΔNp63α *in vivo*. Due to the extensive analysis of p53 regulation by phosphorylation and other posttranslational modifications, it is likely that posttranslational modification of p63 will also play a role in its regulation and function. However, ΔNp63α lacks a transactivation domain where many of the regulatory phosphorylation sites are found in p53. Additionally, the carboxy terminal regulatory phosphorylation sites in p53 are not in regions that are conserved in ΔNp63α. Despite the lack in conserved sites between p53 and ΔNp63α, recent work shows the p53 family member p73 is regulated by several posttranslational modifications that are conserved in ΔNp63α, again suggesting that p63 is regulated in this fashion.

TAp73α is phosphorylated on Tyr-99, a residue conserved in ΔNp63α, by the c-Abl kinase in response to DNA damage (1, 50). Phosphorylation of Tyr-99 stimulates p73-mediated transactivation and apoptosis; however, the ΔNp63α protein acts as a transcriptional repressor. If ΔNp63α is also phosphorylated by c-Abl in response to DNA damage this modification may function to inhibit the repressive activity of ΔNp63α. Other studies show that TAp73β is phosphorylated by Protein Kinase Cδ at Ser-289 subsequently stimulating transactivation (33). In addition, numerous TAp73 splice-variants are phosphorylated at Thr-86 by cyclin A-CDK1/2, cyclin B-CDK1/2, and cyclin E-CDK2 causing inhibition of TAp73 transactivation activity. While these later

residues are not conserved within ΔNp63α, the data indicate that ΔNp63α may be phosphorylated by kinases that regulate p73, and possibly p53, with both positive and negative effects on ΔNp63α activity.

In addition to phosphorylation, p73 is modified by acetylation as well as sumolation. The histone acetyl transferase enzymes p300 and CREB binding protein (CBP) acetylated TAp73α stimulating its transactivation activity (Costanzo et al., 2002; Lu et al., 2001). Moreover, the acetylated residues on TAp73α are lys-321, 327, and 331 with lys-321 and 327 being conserved in ΔNp63α. Interestingly, a nonacetylatable p73 is defective in transactivating the proapoptotic gene p53AIP1 but retains the ability to transactivate other target genes such as p21 (4). Lys-627 of TAp73α, (lys-582 in ΔNp63α) is a sumo-1 modification site (29). In contrast to p53 sumolation, which is associated with increased transactivation activity (19, 34), p73 sumolation resulted in an increased rate of proteasome mediated degradation (29). Combined with phosphorylation, the studies on acetylation and sumolation of p53 and p73 strongly suggest a role for these posttranslational modifications in regulating ΔNp63α activity in either a positive or negative fashion.

What are the possible roles of p63 posttranslational modifications? Studies on p53 and p73 suggest that posttranslational modifications could regulate subcellular localization, protein stability, co-associated proteins, and activity. Our results indicate that a shift in distribution of phospho-forms or an increase in phosphorylation regulates protein stability, but an effect on activity or subcellular localization cannot be ruled out. Another alternative role for p63 phosphorylation could be regulation of subsequent posttranslational modifications after initial phosphorylation. This hypothesis is supported

by findings that p53 phosphorylation is required for subsequent acetylation by PCAF (35) and amino-terminal p53 phosphorylation enhances interaction with p300 (10, 11, 23). Additionally, p300-mediated p73 acetylation requires the kinase c-abl (4). Perhaps more importantly, the p53 phosphorylation-acetylation cascade appears to regulate p53 interactions with different histone deacetylase complexes (26, 27, 30, 47). Since ΔNp63α can function as a transcriptional repressor, it is likely to interact with co-repressor complexes that contain histone deacetylase, or other chromatin modifying enzymes, that repress transcription when associated with DNA bound ΔNp63α.

Determining types of modifications that occur on ΔNp63α is a primary objective of our research with continuing focus on residues that are modified differentially in rapidly proliferating versus differentiated or stressed cells. Continuing this line of investigation will ultimately lead to identification of modified residues that can be evaluated for their role in ΔNp63α regulation. Using techniques such as mass spectrometry and two-dimensional gel electrophoresis will undoubtedly advance this research and allow a better understanding of ΔNp63α function.

1. **Agami, R., G. Blandino, M. Oren, and Y. Shaul.** 1999. Interaction of c-Abl and p73alpha and their collaboration to induce apoptosis. Nature **399:**809-13.
2. **Barbareschi, M., L. Pecciarini, M. G. Cangi, E. Macrì, A. Rizzo, G. Viale, and C. Doglioni.** 2001. p63, a p53 homologue, is a selective nuclear marker of myoepithelial cells of the human breast. Am.J.Surg.Pathol. **25:**1054-1060.
3. **Benasso, M., G. Numico, R. Rosso, M. Merlano, I. Ricci, and A. Gentile.** 1997. Chemotherapy for relapsed head and neck cancer: paclitaxel, cisplatin, and 5-fluorouracil in chemotherapy-naive patients. A dose-finding study. Semin Oncol **24:**S19-46-S19-50.
4. **Costanzo, A., P. Merlo, N. Pediconi, M. Fulco, V. Sartorelli, P. A. Cole, G. Fontemaggi, M. Fanciulli, L. Schiltz, G. Blandino, C. Balsano, and M. Levrero.** 2002. DNA damage-dependent acetylation of p73 dictates the selective activation of apoptotic target genes. Mol Cell **9:**175-86.
5. **Cross, S. M., C. A. Sanchez, C. A. Morgan, M. K. Schimke, S. Ramel, R. L. Idzerda, W. H. Raskind, and B. J. Reid.** 1995. A p53-dependent mouse spindle checkpoint. Science **267:**1353-1356.
6. **De Brabander, M., J. De May, M. Joniau, and G. Geuens.** 1977. Ultrastructural immunocytochemical distribution of tubulin in cultured cells treated with microtubule inhibitors. Cell Biol Int Rep **1:**177-83.
7. **Dellavalle, R. P., T. B. Egbert, A. Marchbank, L. J. Su, L. A. Lee, and P. Walsh.** 2001. CUSP/p63 expression in rat and human tissues. Journal of Dermatological Science **27:**82-87.
8. **Di Como, C. J., M. J. Urist, I. Babayan, M. Drobnjak, C. V. Hedvat, J. Teruya-Feldstein, K. Pohar, A. Hoos, and C. Cordon-Cardo.** 2002. p63 expression profiles in human normal and tumor tissues. Clincal Cancer Res **8:**494-501.
9. **Di Leonardo, A., S. H. Khan, S. P. Linke, V. Greco, G. Seidita, and G. M. Wahl.** 1997. DNA rereplication in the presence of mitotic spindle inhibitors in human and mouse fibroblasts lacking either p53 or pRb function. Cancer Res **57:**1013-9.
10. **Dornan, D., and T. R. Hupp.** 2001. Inhibition of p53-dependent transcription by BOX-I phospho-peptide mimetics that bind to p300. EMBO Rep **2:**139-44.
11. **Dumaz, N., and D. W. Meek.** 1999. Serine15 phosphorylation stimulates p53 transactivation but does not directly influence interaction with HDM2. EMBO J. **18:**7002-7010.
12. **Flatt, P. M., K. Polyak, L. J. Tang, C. D. Scatena, M. D. Westfall, L. A. Rubinstein, J. Yu, K. W. Kinzler, B. Vogelstein, D. E. Hill, and J. A. Pietenpol.** 2000. p53-dependent expression of PIG3 during proliferation, genotoxic stress, and reversible growth arrest. Cancer Lett **156:**63-72.
13. **Flatt, P. M., J. O. Price, A. Shaw, and J. A. Pietenpol.** 1998. Differential cell cycle checkpoint response in normal human keratinocytes and fibroblasts. Cell Growth and Differentiation **9:**535-543.
14. **Forastiere, A. A., D. Shank, D. Neuberg, S. G. t. Taylor, R. C. DeConti, and G. Adams.** 1998. Final report of a phase II evaluation of paclitaxel in patients with advanced squamous cell carcinoma of the head and neck: an Eastern Cooperative Oncology Group trial (PA390). Cancer **82:**2270-4.

15. **Fountzilas, G., G. Stathopoulos, C. Nicolaides, A. Kalogera-Fountzila, H. Kalofonos, A. Nikolaou, C. Bacoyiannis, E. Samantas, C. Papadimitriou, P. Kosmidis, J. Daniilidis, and N. Pavlidis.** 1999. Paclitaxel and gemcitabine in advanced non-nasopharyngeal head and neck cancer: a phase II study conducted by the Hellenic Cooperative Oncology Group. Ann Oncol **10:**475-8.
16. **Frasci, G., P. Comella, A. Parziale, R. Casaretti, A. Daponte, A. Gravina, L. De Rosa, A. Gallipoli, and G. Comella.** 1997. Cisplatin-paclitaxel weekly schedule in advanced solid tumors: a phase I study. Ann Oncol **8:**291-3.
17. **Gebbia, V., A. Testa, G. Cannata, and N. Gebbia.** 1996. Single agent paclitaxel in advanced squamous cell head and neck carcinoma. Eur J Cancer **32A:**901-2.
18. **Giaccia, A. J., and M. B. Kastan.** 1998. The complexity of p53 modulation: emerging patterns from divergent signals. Genes Dev **12:**2973-83.
19. **Gostissa, M., A. Hengstermann, V. Fogal, P. Sandy, S. E. Schwarz, M. Scheffner, and G. Del Sal.** 1999. Activation of p53 by conjugation to the ubiquitin-like protein SUMO-1. EMBO J **18:**6462-71.
20. **Hibi, K., B. Trink, M. Patturajan, W. Westra, O. Caballero, D. Hill, E. Ratovitski, J. Jen, and D. Sidransky.** 2000. AIS is an oncogene amplified in squamous cell carcinoma. PNAS. **97:**5462-5467.
21. **Katoh, I., K. I. Aisaki, S. I. Kurata, S. Ikawa, and Y. Ikawa.** 2000. p51A (TAp63gamma), a p53 homolog, accumulates in response to DNA damage for cell regulation. Oncogene **19:**3126-30.
22. **Lam, M. H., S. L. Olsen, W. A. Rankin, P. W. Ho, T. J. Martin, M. T. Gillespie, and J. M. Moseley.** 1997. PTHrP and cell division: expression and localization of PTHrP in a keratinocyte cell line (HaCaT) during the cell cycle. J Cell Physiol **173:**433-46.
23. **Lambert, P. F., F. Kashanchi, M. F. Radonovich, R. Shiekhattar, and J. N. Brady.** 1998. Phosphorylation of p53 serine 15 increases interaction with CBP. J.Biol.Chem. **273:**-32488--32483.
24. **Licitra, L., G. Capri, F. Fulfaro, C. Grandi, E. Tarenzi, R. Cavina, and L. Gianni.** 1997. Biweekly paclitaxel and cisplatin in patients with advanced head and neck carcinoma. A phase II trial. Ann Oncol **8:**1157-8.
25. **Liefer, K., M. Koster, X. Wang, A. Yang, F. McKeon, and D. Roop.** 2000. Down-regulation of p63 is required for epidermal UV-B-induced apoptosis. Cancer Research **60:**4016-4020.
26. **Luo, J., A. Y. Nikolaev, S. Imai, D. Chen, F. Su, A. Shiloh, L. Guarente, and W. Gu.** 2001. Negative control of p53 by Sir2alpha promotes cell survival under stress. Cell **107:**137-48.
27. **Luo, J., F. Su, D. Chen, A. Shiloh, and W. Gu.** 2000. Deacetylation of p53 modulates its effect on cell growth and apoptosis. Nature **408:**377-81.
28. **Meek, D. W.** 1998. Multisite phosphorylation and the integration of stress signals at p53. Cell Signal **10:**159-166.
29. **Minty, A., X. Dumont, M. Kaghad, and D. Caput.** 2000. Covalent modification of p73α by SUMO-1 - Two-hybrid screening with p73 identifies novel SUMO-1-interacting proteins and a SUMO-1 interaction motif. J Biol Chem **275:**29220-29213.

30. **Murphy, M., J. Ahn, K. K. Walker, W. H. Hoffman, R. M. Evans, A. J. Levine, and D. L. George.** 1999. Transcriptional repression by wild-type p53 utilizes histone deacetylases, mediated by interaction with mSin3a. Genes and Development **13:**2490-2501.
31. **Okada, Y., M. Osada, S. Kurata, S. Sato, K. Aisaki, Y. Kageyama, K. Kihara, Y. Ikawa, and I. Katoh.** 2002. p53 gene family p51(p63)-encoded, secondary transactivator p51B(TAp63alpha) occurs without forming an immunoprecipitable complex with MDM2, but responds to genotoxic stress by accumulation. Exp Cell Res **276:**194-200.
32. **Prives, C., and P. A. Hall.** 1999. The P53 pathway. J.Pathol. **187:**112-126.
33. **Ren, J., R. Datta, H. Shioya, Y. Li, E. Oki, V. Biedermann, A. Bharti, and D. Kufe.** 2002. p73beta is regulated by protein kinase Cdelta catalytic fragment generated in the apoptotic response to DNA damage. J Biol Chem **277:**33758-65.
34. **Rodriguez, M. S., J. M. Desterro, S. Lain, C. A. Midgley, D. P. Lane, and R. T. Hay.** 1999. SUMO-1 modification activates the transcriptional response of p53. EMBO J **18:**6455-61.
35. **Sakaguchi, K., J. E. Herrera, S. Saito, T. Miki, M. Bustin, A. Vassilev, C. W. Anderson, and E. Appella.** 1998. DNA damage activates p53 through a phosphorylation-acetylation cascade. Genes and Development **12:**2831-2841.
36. **Schiff, P. B., J. Fant, and S. B. Horwitz.** 1979. Promotion of microtubule assembly in vitro by Taxol. Nature **22:**665-667.
37. **Schiff, P. B., and S. B. Horowitz.** 1981. Taxol assembles tubulin in the absence of exogenous guanosine 5' triphosphate or microtubule-associated proteins. Biochemistry **20:**3247-3252.
38. **Schiff, P. B., and S. B. Horwitz.** 1980. Taxol stabilizes micrtubules in mouse fibroblasts cells. Proc Natl Acad Sci **77:**1561-1565.
39. **Sena, G., C. Onado, P. Cappella, F. Montalenti, and P. Ubezio.** 1999. Measuring the complexity of cell cycle arrest and killing of drugs: kinetics of phase-specific effects induced by taxol. Cytometry **37:**113-24.
40. **Sentein, P.** 1977. Action of nocodazole on the mechanisms of segmentation mitosis. Cell Biol Int Rep **1:**503-9.
41. **Smith, R. E., D. E. Thornton, and J. Allen.** 1995. A phase II trial of paclitaxel in squamous cell carcinoma of the head and neck with correlative laboratory studies. Semin Oncol **22:**41-6.
42. **Stewart, Z. A., S. D. Leach, and J. A. Pietenpol.** 1999. $p21^{Waf1/Cip1}$ inhibition of cyclin E/Cdk2 activity prevents endoreduplication after mitotic spindle disruption. Mol Cell Biol **19:**205-215.
43. **Stewart, Z. A., and J. A. Pietenpol.** 1999. Cell cycle checkpoints as therapeutic targets. Journal of Mammary Biology and Neoplasia **4:**389-400.
44. **Stewart, Z. A., and J. A. Pietenpol.** 2001. p53 signaling and cell cycle checkpoints. Chemical Research in Toxicology **14:**243-263.
45. **Stewart, Z. A., L. Tang, and J. A. Pietenpol.** 2001. Increased p53 phosphorylation after microtubule disruption is mediated in a microtubule inhibitor- and cell-specific manner. Oncogene **20:**113-124.
46. **Tanière, P., G. Martel-Planche, J. C. Saurin, C. Lombard-Bohas, F. Berger, J. Y. Scoazec, and P. Hainaut.** 2001. *TP53* mutations, amplification of *P63* and

expression of cell cycle proteins in squamous cell carcinoma of the oesophagus from a low incidence area in Western Europe. Br J Cancer **85:**721-726.

47. **Vaziri, H., S. K. Dessain, E. Ng Eaton, S. I. Imai, R. A. Frye, T. K. Pandita, L. Guarente, and R. A. Weinberg.** 2001. hSIR2(SIRT1) functions as an NAD-dependent p53 deacetylase. Cell **107:**149-59.
48. **Westfall, M. D., D. J. Mays, J. C. Sniezek, and J. A. Pietenpol.** 2003. The ΔNp63 alpha phosphoprotein binds the p21 and 14-3-3σ promoters in vivo and has transcriptional repressor activity that is reduced by Hay-Wells syndrome-derived mutations. Mol Cell Biol **23:**2264-76.
49. **Yang, A., M. Kaghad, Y. Wang, E. Gillet, M. Fleming, V. Dotsch, N. Andrews, D. Caput, and F. McKeon.** 1998. p63, a p53 homolog at 3q27-29, encodes multiple products with transactivating, death-inducing, and dominant-negative activities. Mol Cell **2:**305-316.
50. **Yuan, Z. M., H. Shioya, T. Ishiko, X. Sun, J. Gu, Y. Y. Huang, H. Lu, S. Kharbanda, R. Weichselbaum, and D. Kufe.** 1999. p73 is regulated by tyrosine kinase c-Abl in the apoptotic response to DNA damage. Nature **399:**814-7.

Virology 295, 74–85 (2002)
doi:10.1006/viro.2002.1375, available online at http://www.idealibrary.com on IDEAL®

Stabilization and Functional Impairment of the Tumor Suppressor p53 by the Human Papillomavirus Type 16 E7 Oncoprotein

Alexandra Eichten,* Matthew Westfall,† Jennifer A. Pietenpol,† and Karl Münger*,[1]

*Department of Pathology and Harvard Center for Cancer Biology, Harvard Medical School, Boston, Massachusetts 02115; and †Department of Biochemistry, Vanderbilt-Ingram Cancer Center, Nashville, Tennessee 37232

Received November 29, 2001; returned to author for revision December 19, 2001; accepted January 15, 2002

The p53 tumor suppressor is stabilized in cells expressing the human papillomavirus type 16 (HPV-16) E7 oncoprotein. In contrast, expression of the HPV-16 E6 protein inactivates p53 by targeting it for proteasomal degradation. Since p53 activation is associated with protein accumulation we investigated the biochemical mechanisms and biological consequences of p53 stabilization in HPV-16 E7-expressing cells. Transcriptional reporter assays, expression profiling studies using cDNA arrays, and immunoblot analyses of known p53 target genes suggest that p53 remains transcriptionally inert in E7-expressing cells. The stabilized p53 in E7-expressing cells is in a wild-type conformation and the same number of phospho-forms is present. Furthermore, E7 expression does not alter p53 localization or generally block nuclear export or proteasomal degradation of p53. Moreover, the stabilized p53 remains susceptible to mdm2-induced proteasome-mediated degradation, and exogenous transfected p53 is transcriptionally active in E7-expressing cells. Taken together, these results suggest that E7 can interfere with the normal turnover of p53 but that the resulting increase of p53 has no detectable transcriptional consequences on the p53 targets that we investigated. © 2002 Elsevier Science (USA)

INTRODUCTION

Human papillomaviruses (HPVs) are small DNA viruses that infect epithelial cells. More than 100 different HPV types have been described. The mucosal-associated HPVs are classified into two groups: Low-risk HPVs are found in benign hyperplasias with a low potential for malignant progression, whereas high-risk HPVs are associated with squamous intraepithelial lesions that have a propensity to progress to invasive squamous cell carcinoma (reviewed in Lowy and Howley, 2001). High-risk HPVs have been etiologically linked to more than 95% of all cervical cancers (reviewed in zur Hausen, 1996) and approximately 20% of oral cancers; in particular, oropharyngeal carcinomas are also associated with high-risk HPV infections (Gillison *et al.*, 2000). During carcinogenic progression of a high-risk HPV-infected cell the viral genome frequently integrates into a host chromosome. This event is quite random with respect to the host chromosome but follows a specific pattern with respect to the viral genome. As a consequence of integration, expression of the E6 and E7 genes is dysregulated due to the frequent disruption of the viral E2 transcription factor. The E6 and E7 genes of the high-risk HPVs have oncogenic activities. E7 functionally inactivates the retinoblastoma tumor suppressor protein (pRB) and the related "pocket proteins" p107 and p130 by destabilization (reviewed in Munger *et al.*, 2001). The E6 protein binds to (Werness *et al.*, 1990) and promotes the degradation of the tumor suppressor p53 (Scheffner *et al.*, 1990). Expression of high-risk HPV E6 and E7 results in the extension of the life span and immortalization of normal human genital epithelial cells, the normal host cell type of these viruses (Münger *et al.*, 1989; Hawley-Nelson *et al.*, 1989). Moreover, continuous expression of E6 and E7 in cervical cancer cell lines is required for the maintenance of the transformed state (Goodwin and DiMaio, 2000; Wells *et al.*, 2000).

Human keratinocytes or fibroblasts that express HPV-16 E7 contain elevated levels of the p53 tumor suppressor protein (Demers *et al.*, 1994b; Jones *et al.*, 1997b; Thomas and Laimins, 1998). This increase is not due to increased transcription of p53, but results from an extension of its half-life (Jones and Münger, 1997). In normal cells, the p53 tumor suppressor has a short half-life as it is rapidly turned over through ubiquitin-mediated proteasomal degradation. The p53-responsive mdm2 protein (Barak *et al.*, 1993) interacts with p53 (Momand *et al.*, 1992) and functions as a ubiquitin ligase (E3) in this process (Honda *et al.*, 1997). Upon various situations of cellular stress including DNA damage, p53 becomes resistant to mdm2-mediated degradation presumably through specific phosphorylation of serine/threonine residues mainly in the amino-terminal transactivation domain of the protein and is stabilized. In addition, p53 may become acetylated at the carboxyl-termi-

[1] To whom correspondence and reprint requests should be addressed at Department of Pathology, Harvard Medical School, Armenise Building, Room 544A, 200 Longwood Avenue, Boston, MA 02115-5701. Fax: (617) 432-0727. E-mail: karl_munger@hms.harvard.edu.

0042-6822/02 $35.00

nus. These modifications lead to stimulation of its specific DNA-binding activity (reviewed in Meek, 1999). Similarly, signals that cause aberrant cell cycle progression such as E2F or the oncoproteins c-myc and adenovirus E1A stabilize p53. In this case mdm2-mediated p53 degradation is abrogated by increased expression of $p14^{ARF}$ (Zindy *et al.,* 1998; de Stanchina *et al.,* 1998), which directly inhibits mdm2 (Stott *et al.,* 1998). The stabilized and activated p53 causes cells to undergo growth arrest or apoptosis by modulating expression of specific target genes like $p21^{CIP1/waf1}$, bax, and mdm2 (reviewed in Ryan *et al.,* 2001).

Previous studies indicate that in E7-expressing IMR90 human diploid lung fibroblasts p53 is activated upon DNA damage to a comparable extent as in control cells (Jones *et al.,* 1999). This indicates that the p53 in E7-expressing cells retains the ability to be functionally activated upon specific stimuli. It was not clear, however, whether the stabilized p53 in E7-expressing cells represents a transcriptionally active pool in the absence of additional stimuli such as DNA damage. It was recently reported that mdm2 transcription was increased through the p53-responsive P2 promoter in E7-expressing normal human fibroblasts (Seavey *et al.,* 1999), thereby suggesting that p53 is transcriptionally activated in E7-expressing cells. However, our own previous studies show that mRNA levels of $p21^{CIP1/waf1}$, a major transcriptional target of p53, are not significantly increased in E7-expressing IMR90 cells (Jones *et al.,* 1999).

Here we used reporter gene assays, transcriptional profiling using cDNA arrays, and immunoblot analyses of known p53 target genes, to show that E7-mediated p53 stabilization does not induce a concomitant enhancement of p53 transcriptional activity. To determine the mechanisms of E7-mediated p53 stabilization, we investigated p53 phosphorylation, nuclear export, and proteasomal degradation in E7-expressing cells. We did not detect changes in the number of p53 phospho-forms using two-dimensional gel electrophoresis, and immunoprecipitations with conformation-specific antibodies revealed that the stabilized p53 in E7-expressing cells is present in a wild-type conformation. Treatment with geldanamycin does not induce p53 destabilization, suggesting that it is not bound to hsp90. Moreover, the stabilized and transcriptionally inactive p53 in E7-expressing IMR90 cells is nuclear and remains bound to mdm2. Interestingly, however, ectopic expression of E6 or mdm2 decreased p53 levels in E7-expressing cells, and similarly the transcriptional activity of exogenous p53 is not impaired by E7.

RESULTS

The stabilized p53 in HPV-16 E7-expressing cells is transcriptionally impotent

It was reported previously that overexpression of the HPV-16 E7 oncogene results in the accumulation (Demers *et al.,* 1994b) and increased half-life of p53 (Jones *et al.,* 1997a,b) protein. To further analyze E7-mediated p53 stabilization we generated stable control and HPV-16 E7-expressing IMR90 human diploid lung fibroblasts. In agreement with our previous studies (Jones and Münger, 1997) the p53 steady state levels were consistently three to four times higher in E7-expressing IMR90 cells than in control cells (Fig. 1A, 0-h time points) and the half-life of p53 was extended in stable E7-expressing cells (Fig. 1A). Note that the decrease of p53 levels in both LX and E7 cells is greater between the 0- and 1-h time points than at subsequent times, suggesting that these cells may contain two p53 populations with different half-lives.

There is conflicting evidence concerning the transcriptional activity of the stabilized p53 in E7-expressing cells. Our own study demonstrated that transcription of $p21^{CIP1/waf1}$, a major transcriptional target of p53, was not significantly altered in E7-expressing cells (Jones *et al.,* 1999). Consistent with this finding it was also reported that E7 can dampen expression of p53-responsive reporter plasmids in transient assays (Massimi and Banks, 1997). In contrast, another study showed that stable HPV-16 E7-expressing fibroblasts contained elevated mdm2 mRNA levels derived from the p53-responsive P2 promoter (Seavey *et al.,* 1999), suggesting that p53 may be transcriptionally active in E7-expressing cells. To further investigate the transcriptional activity of p53 in E7-expressing cells, we performed expression profiling using a cDNA array. The array contained a total of 12 known p53-responsive genes. The basal level of expression of the p53-responsive genes was variable, but none of these genes was expressed at a significantly higher level in E7-expressing cells (Fig. 1B). As expected from earlier studies (Cheng *et al.,* 1995), expression of PCNA was higher in E7-expressing cells than in control cells (Fig. 1B).

To more directly determine the transcriptional activity of p53, we transfected control and E7-expressing IMR90 cells with a constant amount of firefly luciferase reporter plasmid under the control of an artificial p53-responsive promoter consisting of 17 p53-binding sites (pRGC-luc). Activity was determined and normalized against the expression of the non-p53-responsive renilla luciferase reporter pRL-TK that was cotransfected as a transfection control. Expression of the p53-responsive reporter construct was decreased in E7-expressing cells to a level that was approximately 40% of that of control cells (Fig. 1C) even though this E7-expressing cell population contains 3.6-fold higher p53 levels than control cells (Fig. 1D, top). Activity of the renilla luciferase reporter was not affected by E7 expression (data not shown).

We also determined the protein levels of some p53 target genes on the cDNA array by immunoblot analysis (Fig. 1D). Steady state levels of the pro-apoptotic p53 target genes bax (Miyashita and Reed, 1995) and DR5 (alias TRAIL-R2/Apo2/Killer) (Wu *et al.,* 1997) were only

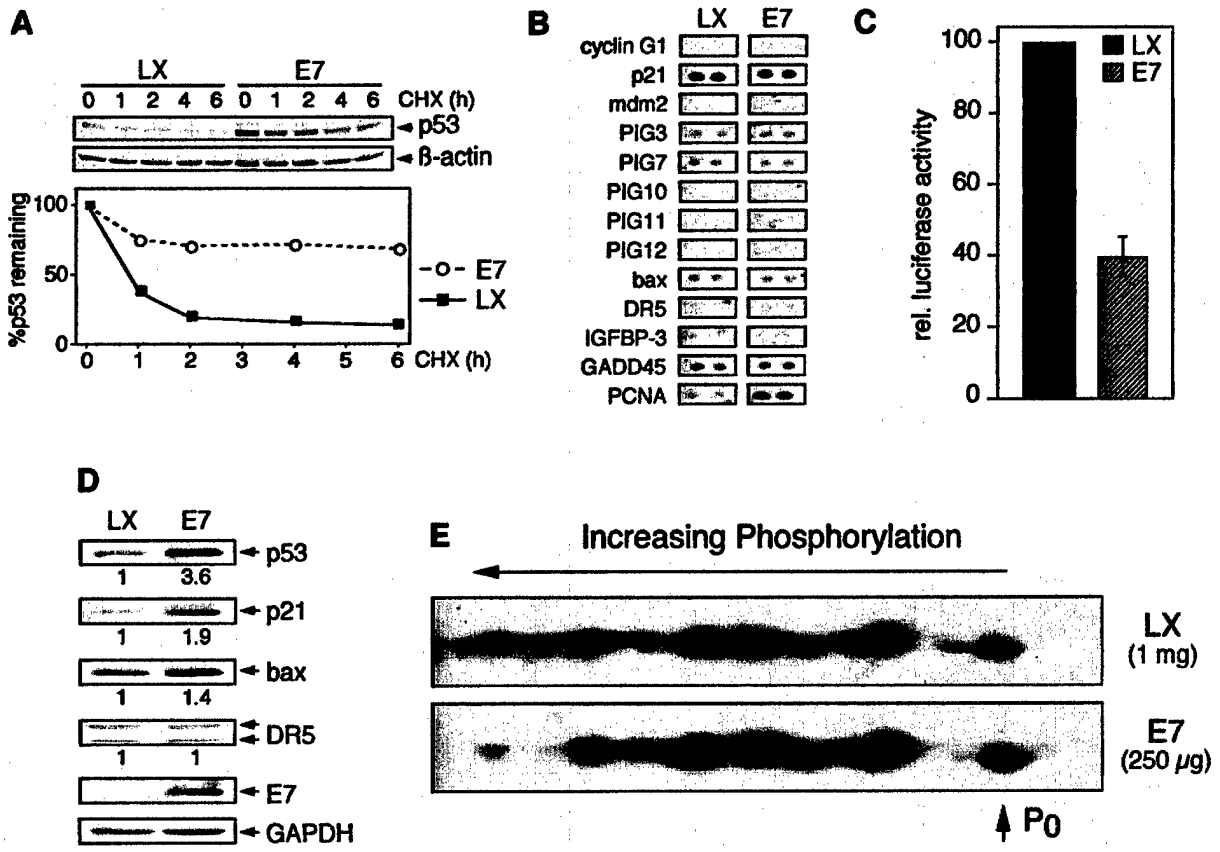

FIG. 1. Biochemical and functional characterization of p53 in control (LX) and HPV-16 E7-expressing (E7) IMR90 cells. (A) Estimation of p53 half-life. Cultures were treated with cycloheximide (CHX) for the indicated periods of time and 100 µg aliquots of protein lysates were analyzed by SDS–PAGE and immunoblotting. Quantification was performed after normalization for β-actin expression and is shown at the bottom. (B) Expression analysis of a set of p53 responsive genes by transcriptional profiling. A "Human Apoptosis ATLAS" cDNA nylon array (Clontech) was analyzed by sequential hybridization with ^{32}P-labeled single-stranded cDNA probes. PCNA is a known E7-responsive gene and was used as a positive control. (C) Decreased transcriptional activity of the stabilized p53 in E7-expressing IMR90 cells. Cells were transfected with the artificial p53-responsive firefly luciferase reporter plasmid pRGC-luc. Activity values were normalized for expression of a nonresponsive renilla luciferase reporter. Values represent averages and standard deviations of an experiment performed in triplicate. (D) Immunoblot analysis of p53, and the p53 transcriptional targets p21$^{CIP1/waf1}$ (p21), bax, and DR5 (alias TRAIL-R2/Apo2/Killer). Expression of HPV-16 E7 is also shown. Relative expression levels of each protein were determined after correction for GAPDH and are indicated below the panels in arbitrary units. (E) Two-dimensional SDS–PAGE analysis of p53. Aliquots containing similar amounts of p53 (1 mg LX; 250 µg E7) were analyzed. P_0 denotes unphosphorylated p53. See text for details.

slightly increased or were unchanged, respectively (Fig. 1D). Increased levels of p21$^{CIP1/waf1}$ have been observed in E7-expressing cells and are a consequence of increased protein stability (Jones *et al.*, 1997a) and there is no comparable increase in mRNA levels (Fig. 1B). Taken together these results indicate that p53 stabilization in E7-expressing cells does not lead to a concomitant increase in transcriptional activity.

No significant changes in the number of p53 phospho-forms in E7-expressing cells

In normal cells p53 is maintained at low levels primarily through mdm2-mediated ubiquitination and proteasomal degradation (Haupt *et al.*, 1997; Kubbutat *et al.*, 1997). However, various forms of cellular stress result in stabilization and accumulation of the p53 protein as a consequence of posttranslational modifications. Changes in p53 phosphorylation status have been implicated in both stabilization and activation of the protein (reviewed in Stewart and Pietenpol, 2001). To determine if increased p53 levels in HPV-16 E7 cells were associated with changes in p53 phosphorylation we performed two-dimensional gel electrophoresis. To adjust for the different p53 levels in the two cell lines, 1 mg of protein lysate from control cells and 250 µg protein from E7-expressing IMR90 cells were analyzed (Fig. 1E). A recombinant carboxyl-terminal truncated human p53 protein (amino acids 1–353) was added to the isoelectric focusing (IEF) sample buffer to serve as an internal standard for alignment of the indicated phospho-forms (Stewart *et al.*, 2001). Although several phosphorylated p53 species were detected, with the exception of the most highly phosphorylated isoform, a significant difference in p53 phosphorylation was not observed between the control and E7-expressing cells.

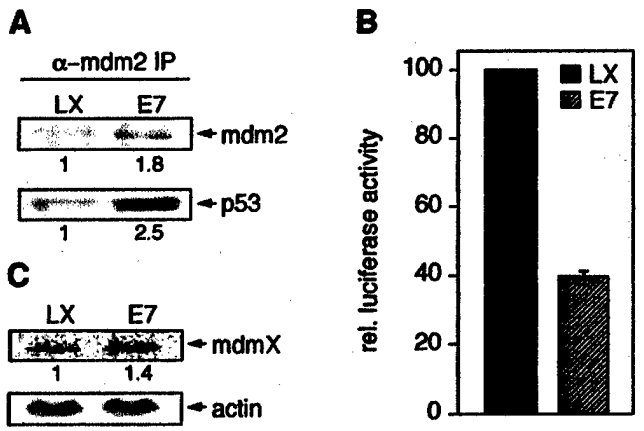

FIG. 2. Expression of mdm2 and the mdm2 homologue mdmX in control (LX) and HPV-16 E7 expressing (E7) IMR90 cells. (A) p53 is in complex with mdm2 in E7-expressing cells. Equal amounts of protein lysates were immunoprecipitated with mdm2-specific antibodies followed by immunoblot analysis for mdm2 (top) and coprecipitated p53 (bottom). Quantitation of the signals is shown below the panels. (B) Activity of the p53-responsive P2 promoter of human mdm2. Cells were transfected with the corresponding firefly luciferase reporter construct. Activity values were normalized for expression of a nonresponsive renilla luciferase reporter. Values represent averages and standard deviations of an experiment performed in triplicate. (C) Northern blot analysis of mdmX RNA expression. Relative levels of mdmX mRNA are shown below the top panel and have been corrected for equal loading as determined by actin mRNA.

p53 is bound to mdm2 in HPV-16 E7-expressing cells

It has been reported previously that E7-expressing cells contain higher mdm2 levels (Thomas and Laimins, 1998; Seavey *et al.*, 1999). In our cells steady state levels of mdm2 mRNA and protein in control and E7-expressing cells were too low to detect by transcriptional profiling (Fig. 1B) or direct immunoblot analysis (data not shown), respectively. Hence, we performed coupled immunoprecipitation/immunoblot analyses and found that mdm2 levels were increased approximately 1.8-fold in E7-expressing cells compared to control cells (Fig. 2A, top). This is a less dramatic increase than previously reported in other cell systems (Thomas and Laimins, 1998; Seavey *et al.*, 1999). Since a previous study reported that E7 could interfere with the interaction of mdm2 and p53 (Seavey *et al.*, 1999), we also determined the amount of p53 bound to mdm2 by coimmunoprecipitation experiments. Approximately 2.5-fold more p53 was coimmunoprecipitated with mdm2 in E7-expressing cells, which parallels the increase of mdm2 (1.8-fold) in these cells (Fig. 2A). These results suggest that mdm2 is effectively bound to p53 in E7-expressing IMR90 cells.

To determine whether the transcriptional activity of the mdm2 promoter is increased in E7-expressing cells a luciferase reporter plasmid under the control of the p53-responsive element of the human mdm2 P2 promoter was transfected into control and E7-expressing IMR90 cells. Similar to the synthetic p53-responsive reporter construct (Fig. 1C), the expression of the mdm2 reporter plasmid was decreased in E7-expressing cells to a level that was approximately 40% of that of control cells (Fig. 2B). These experiments further support the notion that E7-mediated p53 stabilization does not lead to a concomitant increase of transcriptional activity.

The recently described mdm2 homologue, mdmX, was reported to bind and stabilize p53 by protecting it from mdm2-mediated degradation (Jackson and Berberich, 2000). Interestingly, mdmX-bound p53 is transcriptionally inert (Shvarts *et al.*, 1997). Furthermore, mdmX can bind and stabilize mdm2 and inhibit its ability to degrade p53 (Sharp *et al.*, 1999). Hence mdmX appeared to be an attractive candidate to mediate the effects of E7 on p53. Analysis of mdmX protein levels in E7-expressing cells has not been conclusive due to limitations of the existing antibodies. Northern blot analyses revealed a slight, 1.4-fold increase of mdmX mRNA in E7-expressing cells (Fig. 2C). Hence it is possible that mdmX may be involved in p53 stabilization in E7-expressing cells.

Wild-type conformation of p53 in HPV-16 E7-expressing IMR90 cells

To investigate whether the stabilized p53 in E7-expressing cells is in a mutant conformation we performed immunoprecipitation experiments with conformation-specific antibodies. The antibody PAb1620 preferentially recognizes wild-type conformation p53 and the antibody PAb240 preferentially detects p53 with a mutant conformation (Gannon *et al.*, 1990). HaCaT cells, which carry a p53 with a mutant conformation (Lehman *et al.*, 1993), and C33A cells, which carry a p53 with a point mutation at codon 273 (Scheffner *et al.*, 1991) that has a wild-type conformation (Medcalf and Milner, 1993), were used as controls. Since these are mutant forms of p53 they do not exactly comigrate with the wild-type p53 in IMR90 cells. Precipitation with the wild-type conformation-specific PAb1620 but not with mutant conformation-specific PAb240 yielded a detectable signal in E7-expressing cells (Fig. 3A). These results suggest that the majority of p53 in E7-expressing cells is retained in a wild-type conformation.

To corroborate this result we next determined whether the stabilized p53 in E7-expressing cells is bound to hsp90. Hsp90 can bind to p53 that is in a mutant conformation and stabilize it by preventing proteasome-mediated degradation (Blagosklonny *et al.*, 1996). Geldanamycin is a drug that disrupts the interaction of mutant conformation p53 with hsp90 and renders is susceptible for proteasomal degradation (Blagosklonny *et al.*, 1996; Nagata *et al.*, 1999; Whitesell *et al.*, 1997). Control and E7-expressing cells were treated with geldanamycin and p53 steady state levels were determined by immunoblotting. The breast cancer cell line SK-Br-3 contains hsp90-bound p53 and was used as a positive control (Whitesell

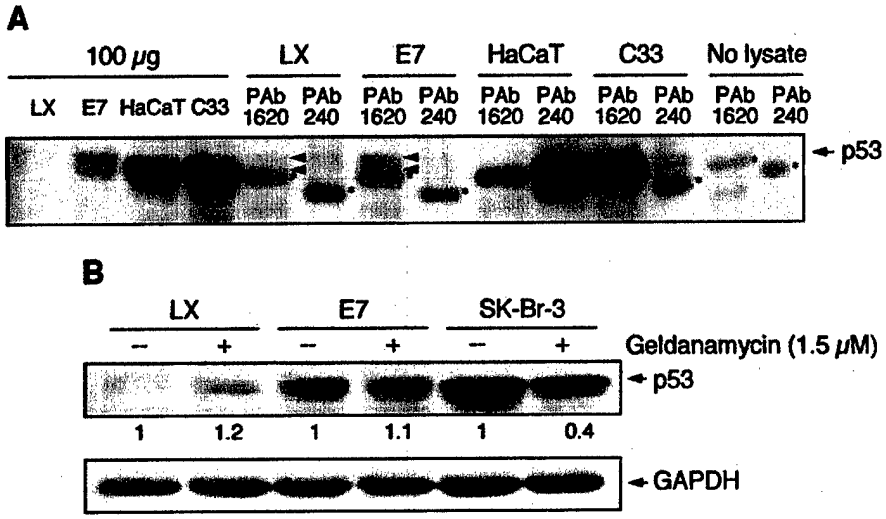

FIG. 3. The stabilized p53 in E7-expressing cells is in a wild-type conformation. (A) Immunoprecipitations with p53 antibodies PAb1620 and PAb240 were performed with lysates of control (LX) and HPV-16 E7-expressing (E7) IMR90 cells (1 mg) and HaCaT and C33A (C33) cells (500 μg) followed by p53 immunoblot analysis. PAb1620 preferentially recognizes wild-type conformation p53, whereas PAb240 preferentially precipitates mutant conformation p53. Samples containing 100 μg total protein were used as controls for direct Western blots. Background bands specific to each of the antibodies used were detected in the "No lysate" control lanes and are indicated by an asterisk; immunoprecipitated p53 is indicated by arrows. (B) Control (LX) and HPV-16 E7-expressing (E7) IMR90 cells were treated with geldanamycin, a compound that disrupts complexes of mutant p53 and hsp90 and renders p53 susceptible to proteasomal degradation. SK-Br-3 cells contain hsp90-bound mutant p53 and were used as a positive control. Levels of p53 were determined by immunoblot analysis normalized for GAPDH levels and are shown below the top panel.

et al., 1997). The p53 levels remained unchanged in control and E7-expressing cells upon geldanamycin treatment, while the p53 level in the SK-Br-3 cells decreased (Fig. 3B). These results suggest that the stabilized p53 in E7-expressing cells is not complexed to hsp90. Taken together these results indicate that the stabilized p53 in E7-expressing cells is in a wild-type conformation.

The stabilized p53 in HPV-16 E7-expressing cells is localized to the nucleus

p53 signaling can be inhibited by mechanisms other than mutations or conformational alterations. One such mechanism involves aberrant subcellular localization. We determined whether expression of E7 alters the subcellular localization of p53. Nuclear and cytoplasmic fractions were prepared from control and E7-expressing cells and subjected to SDS–PAGE and p53 immunoblot analysis. IκBα is an exclusively cytoplasmic protein and was used as a marker. Some p53 was detected in the cytoplasmic fractions in both control and E7-expressing cells, but the ratio between cytoplasmic and nuclear p53 was similar in both cell populations (Fig. 4A). Hence, the subcellular localization of p53 is not altered in E7-expressing cells.

Expression of E7 does not block nuclear export or proteasomal degradation of p53 per se

The finding that the stabilized p53 is mainly nuclear in E7-expressing cells led us to investigate whether E7 might block nuclear export of p53, which might result in its stabilization. Control and E7-expressing IMR90 cells were treated with the nuclear export inhibitor leptomycin B (LMB) and p53 steady state levels were determined by

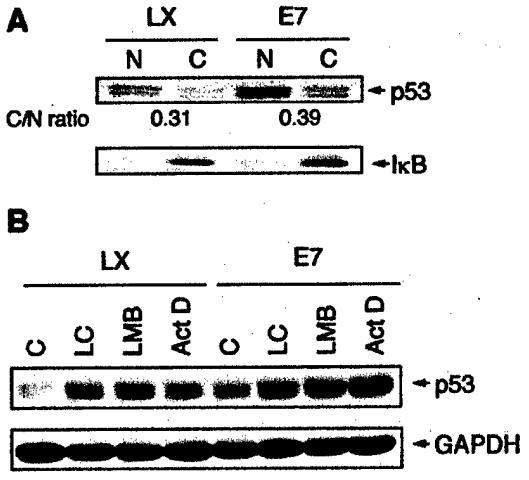

FIG. 4. p53 is nuclear in control (LX) and HPV-16 E7-expressing (E7) IMR90 cells and its nuclear export or proteasomal degradation is not generally impaired. (A) Nuclear (N) and cytoplasmic (C) fractions were subjected to p53 immunoblot analysis. IκB was used as a cytoplasmic marker. The ratio of cytoplasmic to nuclear p53 (C/N ratio) is indicated. (B) Cells were treated for 4 h with 40 μM lactacystin (LC, a proteasome inhibitor) or for 8 h with 40 ng/ml leptomycin B (LMB, a nuclear export inhibitor) and p53 levels were determined by immunoblot analyses. Treatment with a radiomimetic dose (2.5 nM) of actinomycin (Act D) for 24 h was used as a positive control. GAPDH is shown to document equal loading.

immunoblotting. p53 steady state levels increased to a similar extent in control and E7-expressing cells (Fig. 4B). This result indicates that E7 expression does not block the nuclear export of p53. Since it has been reported that E7 can interact with the S4 subunit of the 26S proteasome (Berezutskaya and Bagchi, 1997) we determined whether E7 might stabilize p53 by generally interfering with the proteasomal degradation machinery. Control and E7-expressing IMR90 cells were treated with the proteasome inhibitor lactacystin. Similar increases in p53 steady state levels were observed in control and E7-expressing cells, indicating that E7 does not generally interfere with the proteasomal degradation machinery (Fig. 4B). Treatment with the DNA-damaging agent actinomycin D, which results in p53 stabilization in both control and E7-expressing cells (Demers *et al.*, 1994a; Slebos *et al.*, 1994), was used as a control in these experiments (Fig. 4B).

Stabilized p53 in E7-expressing cells is susceptible to degradation by exogenous mdm2

To determine whether E7 can protect p53 from degradation by exogenous mdm2, mdm2 was transiently expressed in stable E7-expressing IMR90 cells and changes in p53 levels were determined by immunofluorescence. Transfection of HPV-16 E6, which induces E6AP-mediated p53 degradation, was used as a positive control. The DS-red plasmid encodes a fluorescent protein and was used as a transfection marker for these experiments. Like E6, expression of mdm2 decreased p53 levels in stable E7-expressing cells (Fig. 5). This indicates that E7-stabilized p53 is still susceptible to degradation by exogenous mdm2.

Exogenous p53 is transcriptionally active in E7-expressing cells

To investigate whether E7 can interfere with the transcriptional activity of exogenous p53 we transiently transfected control and E7-expressing IMR90 cells with increasing amounts of p53 and the p53-responsive luciferase reporter plasmid pRGC-luc and determined its transcriptional activity by using luciferase assays. In agreement with our previous results (Fig. 1C) transcriptional activity of endogenous p53 is diminished by approximately 60% in E7-expressing cells compared to the control population. Exogenous p53, however, was able to efficiently activate reporter gene expression in E7-expressing cells to a similar level as in control cells. This indicates that in IMR90 cells, E7 does not impair the transcriptional activity of exogenous p53.

DISCUSSION

The tumor suppressor protein p53 has a short half-life in normal cells. Its half-life is determined by mdm2-mediated proteasomal degradation (Honda *et al.*, 1997). The ubiquitin ligase (E3) mdm2 is a transcriptional target of p53 and is thought to play a role as a feedback regulator to keep p53 activity in check (Wu *et al.*, 1993). E7-expressing keratinocytes or fibroblasts contain increased p53 levels (Demers *et al.*, 1994b; Jones *et al.*, 1997b; Thomas and Laimins, 1998). Upregulation of p53 is an important component of the cellular response to oncogenic insults that can culminate in cellular growth arrest or apoptosis (reviewed in Levine, 1997). It is thought that the ability of the high-risk HPV E6 proteins to inactivate p53 by targeting it for proteasomal degradation (Scheffner *et al.*, 1990) is to negate this cellular reaction. Consistent with this model, a mutational analysis revealed that the ability of HPV-16 E7 to stabilize p53 correlates with cellular transformation and pRB degradation (Jones *et al.*, 1997b). Other oncoproteins including SV40 large tumor antigen (SV40 Tag) (Tiemann and Deppert, 1994), adenovirus E1A (Ad E1A) (Lowe and Ruley, 1993), and c-myc (Hermeking and Eick, 1994) can each stabilize p53. Since each of these oncoproteins results in dysregulating the G1/S transition it is plausible that aberrant activation of the pRB-regulated transcription factor E2F may cause p53 stabilization. One potential mechanistic link between E2F activation and p53 stabilization was suggested by the finding that $p14^{ARF}$, an inhibitor of mdm2-mediated p53 degradation (Zhang *et al.*, 1998), was E2F responsive (Bates *et al.*, 1998), and its cellular levels increased in response to Ad E1A and c-myc expression (de Stanchina *et al.*, 1998; Zindy *et al.*, 1998). Surprisingly, however, $p14^{ARF}$ levels do not rapidly increase upon HPV-16 E7 expression, and E7-mediated p53 stabilization was observed in $p19^{ARF}$-deficient mouse embryo fibroblasts (Seavey *et al.*, 1999). Hence other pathways must exist that can interfere with the ability of mdm2 to ubiquitinate p53 or the process of proteasomal p53 degradation. As a first step toward the identification of the biochemical pathways that may contribute to p53 stabilization in E7-expressing cells we analyzed p53 in E7-expressing cells on a biochemical and cell biological level. Our studies revealed no major differences between short-lived p53 in normal cells and stabilized p53 in HPV-16 E7-expressing IMR90 cells.

It has been reported that wild-type p53 can be functionally inactivated by nuclear exclusion. This has been documented in different carcinomas (Moll *et al.*, 1992, 1995; Bosari *et al.*, 1995; Ueda *et al.*, 1995; Schlamp *et al.*, 1997), and in addition, some viral oncoproteins such as the Ad E1B-55 kDa protein and the hepatitis B virus X protein can mislocalize p53 to the cytoplasm, thereby inhibiting its transcriptional activities (van den Heuvel *et al.*, 1993; Elmore *et al.*, 1997). Subcellular fractionation studies showed that p53 in E7-expressing cells remains nuclear (Figs. 4A and 5) and immunoprecipitation studies with conformation-specific antibodies (Fig. 3A) as well as treatment with geldanamycin (Fig. 3B) demonstrated that

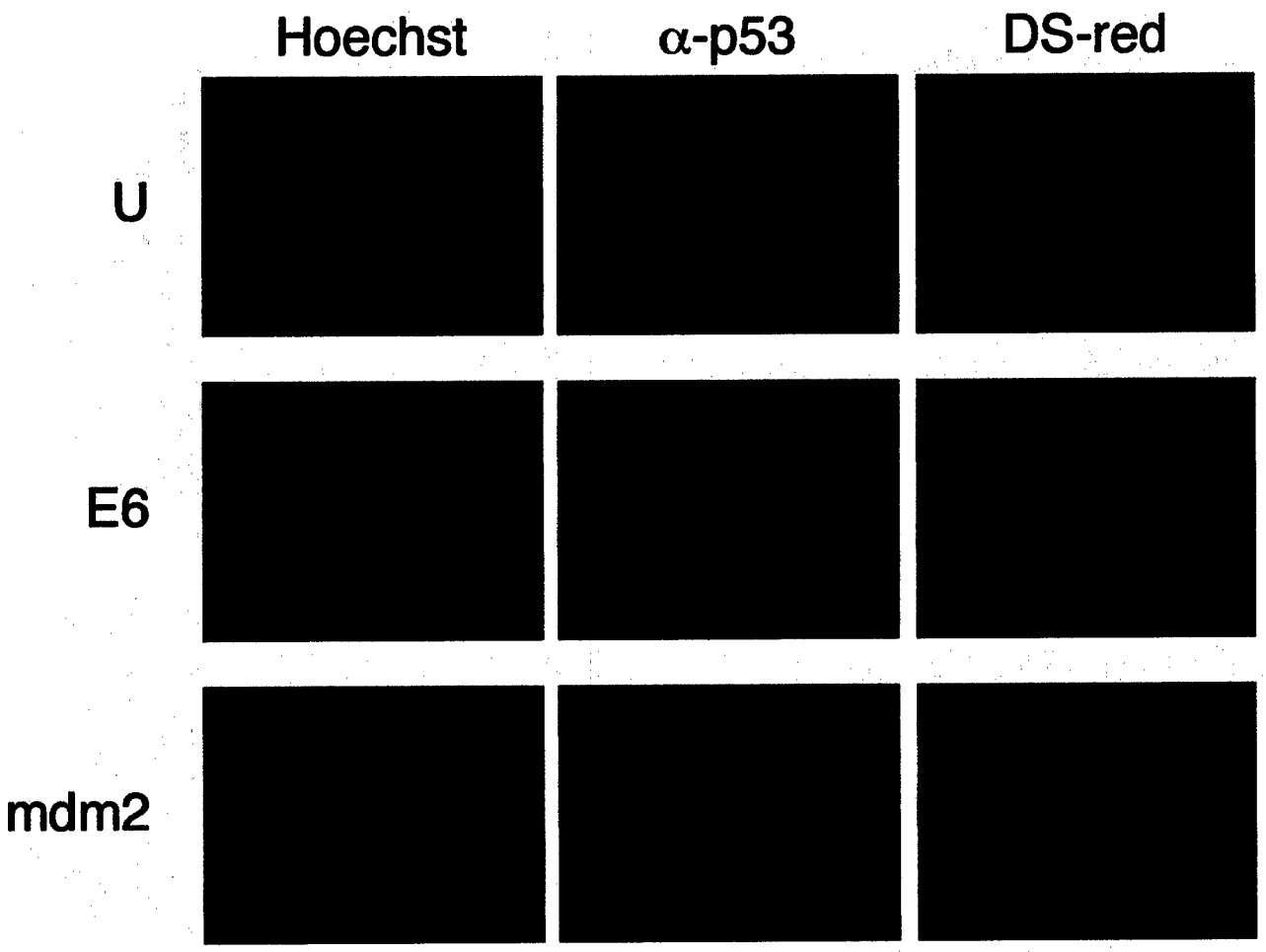

FIG. 5. Stabilized p53 in HPV-16 E7-expressing cells remains susceptible to degradation by exogenous mdm2. HPV-16 E7-expressing IMR90 cells were transiently transfected with mdm2 or HPV-16 E6 as a positive control. Untransfected E7-expressing IMR90 cells (U) are shown as controls. The fluorescent protein DS-red was cotransfected to allow specific identification of the transfected cells. p53 was detected by immunofluorescence. Nuclei were visualized by Hoechst staining.

the stabilized p53 in E7-expressing cells remains in a wild-type conformation. An analysis of the phosphorylation state of p53 by two-dimensional gel electrophoresis displayed no major differences in the number of phospho-forms in control or E7-expressing cells (Fig. 1E).

In contrast to another study (Seavey *et al.*, 1999), our analyses revealed no evidence for a disruption of the mdm2/p53 interaction in normal or E7-expressing cells (Fig. 2A), suggesting that the interaction of mdm2 and p53 is not generally decreased in E7-expressing cells. The two studies were performed with different strains of diploid normal human fibroblasts and it is of note that in the IMR90 cells used in this study, we did not observe a dramatic upregulation of mdm2 expression (Figs. 1B and 2A), suggesting that either there are differences in the expression levels of E7 in the two studies or there may be differences in the susceptibility to p53 activation between these strains of human fibroblasts.

Interestingly, however, our experiments revealed that the stabilized p53 in E7-expressing cells remains susceptible to proteasomal degradation by exogenous mdm2 as well as by the HPV-16 E6/E6-AP complex (Fig. 5). These results further support the notion that the stabilized p53 in these cells is in a wild-type conformation and is not inherently resistant to proteasomal degradation.

In addition, treatment of E7-expressing cells with the nuclear export inhibitor leptomycin B led to a further increase in cellular p53 levels, demonstrating that nuclear export of p53 is not generally abrogated in E7-expressing cells (Fig. 4B). Similar results were obtained when cells were treated with the proteasome inhibitor lactacystin, suggesting that proteasomal p53 degradation is not completely blocked in E7-expressing cells (Fig. 4B).

Additional studies will be necessary to delineate whether E7 interferes with mdm2-mediated ubiquitination of p53 or whether E7 affects the turnover of ubiquitinated p53. Interestingly, mdmX, a cellular homologue of mdm2 that may act as dominant negative inhibitor of mdm2, has been described. MdmX can bind p53 and stabilize it by preventing mdm2-mediated degradation

through the proteasome (Jackson and Berberich, 2000; Sharp *et al.,* 1999). MdmX-bound p53 was reported to be transcriptionally inactive (Shvarts *et al.,* 1997), which made it an attractive candidate. Our preliminary analyses revealed a 1.4-fold increase in mdmX mRNA levels in E7-expressing cells (Fig. 2C), but due to antibody limitations we could not determine whether mdmX or a related protein may be present at higher levels in E7-expressing cells and may contribute to p53 stabilization in E7-expressing IMR90 cells. Alternatively, E7 may interfere with a step that involves recognition of ubiquitinated forms of p53 by the proteasome. This process has not yet been studied in great detail; however, it has been postulated that ubiquitin-binding proteins such as hPLIC that are associated with the proteasome may play a role in this process (Kleijnen *et al.,* 2000).

In normal cells, stabilization of p53 is generally observed in response to genotoxic insults. Under these conditions, p53 stabilization leads to a corresponding increase of its transcriptional activation potential and transcriptional induction of downstream target genes (reviewed in Meek, 1999). Many of these genes encode growth suppressive and cytotoxic proteins, and activation of p53 generally leads to growth arrest or apoptosis (reviewed in Levine, 1997). In contrast, E7-expressing IMR90 cells grow rapidly and the rate of spontaneous apoptosis is similar to that in control cells. Our previous work has indicated that expression of E7, while it mimics a p53-dependent DNA damage response, does not fully activate p53 (Jones *et al.,* 1999). Most dramatically, $p21^{CIP1/waf1}$ protein levels but not mRNA levels are increased in E7-expressing cells (see Figs. 1B and 1D), consistent with an effect on protein stabilization rather than p53-dependent transcriptional induction (Jones *et al.,* 1999). Hence we analyzed in more detail whether the stabilized p53 in E7-expressing cells is activated as a transcription factor. Transcriptional profiling of matched control and E7-expressing cells showed no marked increases in the mRNA levels of any of the known p53-responsive genes present on this array (Fig. 1B). Similarly, immunoblot analyses showed that levels of the pro-apoptotic p53 targets bax (Miyashita and Reed, 1995) and DR5 (alias TRAIL-R2/Apo2/Killer) (Wu *et al.,* 1997) were not increased in rapidly growing E7-expressing IMR90 cells (Fig. 1D). Consistent with these findings, analysis of the transcriptional activity of an artificial p53-responsive reporter construct in a matched pair of control and E7-expressing IMR90 cells suggested that, despite the higher steady state levels (Figs. 1A and 1D), the transcriptional activity of p53 was decreased in E7-expressing cells (Figs. 1C, 2B, and 6). In particular, our analysis did not reveal any evidence for increased mdm2 RNA expression in E7-expressing cells (Fig. 1B), as suggested by a previous study that reported increased transcription from the p53-responsive mdm2 promoter P2 in E7-expressing cells (Seavey *et al.,* 1999). Consistent with this, mdm2 protein levels were only slightly increased in E7-expressing cells (Fig. 2A). Hence we measured the transcriptional activity of an mdm2 P2 promoter-driven reporter construct in a matched pair of control and E7-expressing IMR90 cells. Consistent with the results obtained with the artificial p53-responsive reporter (Fig. 1C), we did not detect increased activity of this reporter in E7-expressing cells; in fact, the transcriptional activity of the mdm2 P2 promoter construct was decreased in E7-expressing cells (Fig. 2B).

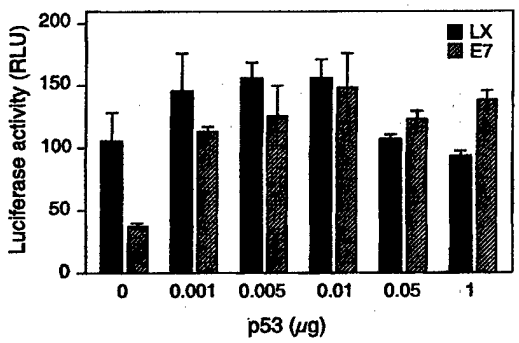

FIG. 6. Transcriptional activity of exogenous p53 in control (LX) and HPV-16 E7-expressing (E7) IMR90 populations. Cells were cotransfected with 500 ng of the p53-responsive firefly luciferase reporter pRGC-luc and the indicated amounts of p53. Activity values were normalized for expression of a nonresponsive renilla luciferase reporter. Values represent averages and standard deviations of an experiment performed in triplicate.

The decreased activity of the p53-responsive luciferase reporters (Figs. 1C and 2B) appears at variance with the unchanged levels of p53 target genes as determined by transcriptional profiling (Fig. 1B) and may suggest that other transcriptional elements are also involved in regulating the expression of these genes. Regardless, our results demonstrate that expression of E7 results in stabilization but not activation of p53.

Hence it is possible that the different mechanisms that lead to p53 stabilization in E7-expressing cells and during DNA damage are fundamentally different and that additional modifications such as phosphorylation and/or acetylation events are necessary to trigger transcriptional activation of p53. Alternatively, E7 may interfere with the transcriptional activation of p53. This has been suggested by earlier studies demonstrating that expression of E7 could interfere with p53-dependent activation of reporter plasmids in transient assays. These experiments suggested that the ability of E7 to interfere with p53-mediated transcriptional activation might be correlated with the capacity of E7 to interact with TATA-box-binding protein, TBP (Massimi and Banks, 1997). Additional studies will be necessary to further address these issues. To address whether E7 could also interfere with transcriptional activity of exogenous p53, we performed reporter assays with increasing amounts of exogenous p53 in a matched pair of control and E7-expressing

IMR90 cells using an artificial p53-responsive reporter. These studies showed that exogenous p53 is transcriptionally active in E7-expressing cells (Fig. 6).

It is remarkable that many viruses have developed multiple strategies to interfere with the activities of p53. This has been best demonstrated in the case of adenoviruses that encode multiple proteins that impinge on p53 functions. The Ad E1A protein can stabilize p53 through a mechanism that involves E2F-dependent activation of $p14^{ARF}$ (de Stanchina *et al.,* 1998; Bates *et al.,* 1998). The Ad E1B protein can inactivate p53 by binding directly to its transcriptional activation domain (Sarnow *et al.,* 1982; Kao *et al.,* 1990; Yew *et al.,* 1994). In addition the E4orf6 protein can enhance the destabilization of p53 through its interaction with E1B-55 kDa. Both E4orf6 and E1B-55 kDa bind independently to p53 without inducing its degradation. Concomitant expression of the two oncogenes leads to rapid turnover of p53 (Querido *et al.,* 1997; Steegenga *et al.,* 1998). In contrast, E4orf3 can relieve the inhibition of p53 activity by Ad E1B (Konig *et al.,* 1999). Hence it is not surprising that high-risk HPVs encode multiple proteins that impinge on p53 function. HPV-16 E7 expression leads to p53 stabilization, but the stabilized p53 is retained in a transcriptionally impotent state. In concert with the ubiquitin ligase E6-AP, the HPV-16 E6 protein can interact with p53 and target it for proteasomal degradation (Scheffner *et al.,* 1993, 1995). It has recently been reported that mdm2-mediated p53 degradation is also abrogated in HPV-positive cervical cancer cells and critically depends on E6/E6-AP (Hengstermann *et al.,* 2001). Given our results and the fact that the only other viral protein consistently expressed in cervical cancer cells is HPV E7 it is thus conceivable that E7 is responsible for blocking mdm2-mediated p53 degradation in these cells.

MATERIALS AND METHODS

Cell lines, retroviral infection, and transfection

Low-passage normal human diploid lung fibroblasts (IMR90), the keratinocyte cell line HaCaT, the HPV-negative cervical cancer cell line C33A, and the breast cancer cell line SK-Br-3 were maintained in Dulbecco's modified Eagle's medium (DMEM) supplemented with 10% fetal bovine serum (FBS), 50 U/ml penicillin, and 50 μg/ml streptomycin.

Recombinant retroviruses LXSN and LXSN-HPV-16 E7 were obtained from D. Galloway and used for retroviral transduction of IMR90 cells. Cells were incubated for 4 h with virus-containing supernatant in the presence of 4 μg/ml hexadimethrine bromide (polybrene) (Sigma). Pooled stable cell populations were obtained by selection with 300 μg/ml G418 (Gemini Bio-Products) for 8 days.

Transient transfection of IMR90 cell populations were performed by incubating the cells in 6-well plates for 4 h at 37°C in 1 ml Opti MEM I (Gibco) containing 4 μg DNA and 10 μg/ml polybrene followed by incubation with 24% DMSO (ICN Biomedicals Inc.) in Opti MEM I for 4 min at room temperature. The cells were washed three times with PBS, supplemented with DMEM with 10% FBS, and processed 24 h posttransfection.

RNA isolation, cDNA arrays, and Northern blotting

Total RNA was isolated using the RNeasy kit (Qiagen) according to the manufacturer's recommendations, followed by treatment with 1 U/μl DNase I (Roche) for 1 h at 37°C. To test for DNA contamination, RNA samples were subjected to PCR analysis using GAPDH primers. mRNA was isolated from total RNA by using the OligoTex kit (Qiagen) according to the manufacturer's manual and used as a template to prepare a ^{32}P-labeled single-stranded cDNA hybridization probe. A Human Apoptosis ATLAS cDNA array (Clontech) was used. The signals were visualized with a STORM PhosphoImager and the results were quantitated using ATLAS Image 1.5 software (Clontech). For Northern blot analyses 10 μg total RNA was separated on a 1% formaldehyde/agarose gel, transferred to a NYTRAN SuPerCharge nylon membrane (Schleicher & Schuell), and crosslinked with a Stratalinker (Stratagene). The cDNA probes were ^{32}P-labeled using the STRIP-EZ DNA kit (Ambion) following the manufacturer's instructions and hybridized in ExpressHyb (Clontech) according to the manufacturer's manual. The signals were visualized with a STORM PhosphoImager and quantitated using ImageQuant software.

Immunological methods

For immunoblot analyses cells were lysed in 1% NP-40 buffer (150 mM NaCl, 50 mM Tris-HCl pH 7.5, 1% Nonidet-P-40, 0.01% PMSF, 1 μg/ml aprotinin, 1 μg/ml leupeptin), immediately scraped off the plates, incubated on ice for 20 min, and centrifuged for 10 min at 4°C at 16,000*g* in a microcentrifuge. Protein concentrations of the lysates were determined by the Bradford method (Bio-Rad). Samples containing 100 μg of protein were separated by SDS–PAGE and transferred to a PVDF membrane (Immobilion P, Millipore). Antibody complexes were detected by enhanced chemiluminescence (Renaissance Enhanced Luminol Reagent, NEN Life Science Products). Primary antibodies were used at the following dilutions: p53 (Ab-6, 1:1000, Calbiochem), $p21^{CIP1/waf1}$ (Ab-1, 1:1000, Calbiochem), bax (1:500, Pharmingen), β-actin (1:10,000, CHEMICON), GAPDH (1:600, CHEMICON), E7 (mixture of 8C9, 1:100, Zymed and ED17, 1:1000, Santa Cruz), mdm2 (N-20, 1:300, Santa Cruz), DR5 (1:500, IMGENEX), IκBα (1:200, Santa Cruz). Secondary HRP-conjugated antibodies were used at 1:10,000 dilutions (Amersham). ECL images were acquired using a Fluoro-S MultiImage MAX (Bio-Rad) with a supercooled digital camera (Nikon) and quantitated using QuantityOne software (Bio-Rad). Equal

loading was controlled using GAPDH or β-actin immunoblots.

For immunoprecipitations cells were lysed and processed as described above. Samples containing 0.5–1 mg total protein were incubated for 1.5 h at 4°C with 2 μg of specific antibody, followed by protein A–Sepharose beads (Pharmacia) or protein G PLUS-agarose beads (Santa Cruz) for 1 h at 4°C at constant rotation. The p53 antibodies used were PAb1620 (Calbiochem) and PAb240 (Calbiochem), and for mdm2 Ab-1 (Calbiochem) was used. Immunocomplexes were washed four to six times in 1% NP-40 lysis buffer and subjected to SDS–PAGE and immunoblot analysis. An anti-mouse κ light-chain-specific secondary antibody (1:10,000, Southern Biotechnology Associates) was used to facilitate detection of immunoprecipitated p53.

For half-life determinations, control and E7-expressing IMR90 cells were treated with 30 μg/ml of the translation inhibitor cycloheximide (Sigma) for the indicated time periods. The cells were lysed and the p53 steady state levels were determined by immunoblot analysis. Images were digitally acquired using a Bio-Rad Fluoro-S-Max Multi-imager and quantitated using the manufacturer's software. The levels of p53 were normalized for β-actin expression.

For immunofluorescence analyses the cells were transiently transfected as described above. After 36 h the cells were fixed in 2% paraformaldehyde for 30 min at 25°C, washed in PBS, permeabilized with 100% methanol for 10 min at −20°C, and washed with PBS. After that the cells were incubated with 2.5% donkey serum in PBS for 5 min at 37°C, washed with PBS, incubated with primary antibody (p53, Ab-6, Calbiochem, 1:100) for 1 h at 37°C, and washed twice in PBS followed by an incubation with the FITC-coupled secondary donkey anti-mouse antibody (1:200) for 1 h at 37°C. The nuclei were stained with Hoechst (1:2000 in H_2O).

Drug treatments

Geldanamycin (Sigma) was dissolved in DMSO at a concentration of 1.5 mM. IMR90 control and E7-expressing cells and SK-Br-3 cells were treated for 4 h with 1.5 μM geldanamycin or mock-treated with an equal volume of DMSO. Leptomycin B (Sigma) was dissolved in ethanol at a concentration of 10 μg/ml. IMR90 control and E7-expressing cells were treated for 8 h with 40 ng/ml leptomycin B. Lactacystin (BIOMOL) was dissolved in water at a concentration of 40 mM. IMR90 control and E7-expressing cells were treated for 4 h with 40 μM lactacystin. Actinomycin D (Sigma) was dissolved in ethanol at a concentration of 2.5 μM. IMR90 control and E7-expressing cells were treated for 24 h with 2.5 nM actinomycin D.

Luciferase assays

Stable control and E7-expressing human diploid lung fibroblasts (IMR90) were transfected in 6-well plates with 500 ng of firefly luciferase reporter plasmid either under the control of an artificial p53-responsive promoter carrying 17 tandem repeats of the p53 consensus DNA-binding sequence derived from the ribosomal gene cluster (Kern *et al.*, 1991) (pRGC-luc) or under the control of the p53-responsive human mdm2 promoter (pGL2-mdm2-luc) (Zauberman *et al.*, 1995) (kind gifts from M. Oren). Twenty nanograms of the noninducible renilla luciferase reporter plasmid (pRL-TK) was cotransfected as a transfection control. The cells were lysed after 24 h in 30 μl lysis buffer (Dual-Luciferase Reporter Kit, Promega) per well, scraped off the plate, and centrifuged for 10 min at 4°C at 16,000*g*. The supernatants were subjected to the dual luciferase assay and the firefly luciferase activity was normalized for renilla luciferase expression.

Subcellular fractionation

Stable control and E7-expressing IMR90 cells were washed in PBS and scraped in sucrose buffer (250 mM sucrose, 10 mM MOPS, pH 7.2, 1 mM EDTA, 0.01% PMSF, 1 μg/ml aprotinin, 1 μg/ml leupeptin). The cells were then homogenized by 30 strokes of a Teflon tissue homogenizer (Glas-Col, Terre Haute, IN). Nuclei were pelleted at 700*g* at 4°C for 10 min. The supernatant is the cytoplasmic protein fraction. The pellet was resuspended in 1% NP-40 buffer and the nuclear lysate was cleared by centrifugation for 10 min at 4°C at 16,000*g*. Equal amounts of protein from the cytoplasmic and nuclear fraction were separated by SDS–PAGE and p53 levels were determined by immunoblotting.

Two-dimensional gel electrophoresis

For two-dimensional gel analyses of endogenous p53 (Stewart *et al.*, 2001), 1 mg of protein lysate from LXSN cells or 250 μg of protein lysate from E7 cells was prepared in a final volume of 600 μl of IEF sample buffer [9.5 M urea (Pharmacia), 2% NP-40, 2% β-mercaptoethanol, 0.2% ampholytes, pH 5–8 (Pharmacia), 0.001% bromophenol blue]. A truncated form of recombinant human p53 (amino acids 1–353) was incubated in each sample as an internal standard to permit alignment of p53 phospho-forms; the truncated human p53 was prepared as previously described (Szak and Pietenpol, 1999). IEF was performed using the PROTEAN IEF system (Bio-Rad) and 17-cm isoelectric strip gels, pH 5–8 (Bio-Rad). The isoelectric gels were passively rehydrated for 10 h in IEF sample buffer containing the protein lysate prior to focusing for 60,000 V-h. After IEF, gels were incubated for 15 min in equilibration buffer I [6 M urea, 2% SDS, 0.375 M Tris (pH 8.8), 20% glycerol, 130 mM DTT] and 15 min in

equilibration buffer II [6 M urea, 2% SDS, 0.375 M Tris (pH 8.8), 20% glycerol, 135 mM iodoacetamide (Sigma)] prior to separation by SDS–PAGE. Detection of p53 was by immunoblot using PAb1801 (1 μg/ml; Calbiochem).

ACKNOWLEDGMENTS

We thank Denise Galloway and Moshe Oren for their kind gifts of reagents; Joseph Growney for technical advice; Martin Scheffner, Philip Hinds, and Carl Maki for critical comments on the manuscript; Dieter Paul for encouragement; and J. Daniel for spiritual support. This work was supported by NIH Grants R01 CA66980 (K.M.) and CA70856 (J.A.P.). A.E. is supported by a "DAAD Doktorandenstipendium im Rahmen des gemeinsamen HSP III von Bund und Ländern."

REFERENCES

Barak, Y., Juven, T., Haffner, R., and Oren, M. (1993). mdm2 expression is induced by wild type p53 activity. *EMBO J.* **12,** 46146–46148.

Bates, S., Phillips, A. C., Clark, P. A., Stott, F., Peters, G., Ludwig, R. L., and Vousden, K. H. (1998). p14ARF links the tumour suppressors RB and p53. *Nature* **395,** 124–125.

Berezutskaya, E., and Bagchi, S. (1997). The human papillomavirus E7 oncoprotein functionally interacts with the S4 subunit of the 26 S proteasome. *J. Biol. Chem.* **272**(48), 30135–30140.

Blagosklonny, M. V., Toretsky, J., Bohen, S., and Neckers, L. (1996). Mutant conformation of p53 translated in vitro or in vivo requires functional HSP90. *Proc. Natl. Acad. Sci. USA* **93**(16), 8379–8383.

Bosari, S., Viale, G., Roncalli, M., Graziani, D., Borsani, G., Lee, A. K., and Coggi, G. (1995). p53 gene mutations, p53 protein accumulation and compartmentalization in colorectal adenocarcinoma. *Am. J. Pathol.* **147**(3), 790–798.

Cheng, S., Schmidt-Grimminger, D. C., Murant, T., Broker, T. R., and Chow, L. T. (1995). Differentiation-dependent up-regulation of the human papillomavirus E7 gene reactivates cellular DNA replication in suprabasal differentiated keratinocytes. *Genes Dev.* **9,** 2335–2349.

Demers, G. W., Foster, S. A., Halbert, C. L., and Galloway, D. A. (1994a). Growth arrest by induction of p53 in DNA damaged keratinocytes is bypassed by human papillomavirus 16 E7. *Proc. Natl. Acad. Sci. USA* **91,** 4382–4386.

Demers, G. W., Halbert, C. L., and Galloway, D. A. (1994b). Elevated wild-type p53 protein levels in human epithelial cell lines immortalized by the human papillomavirus type 16 E7 gene. *Virology* **198,** 169–174.

De Stanchina, E., McCurrach, M. E., Zindy, F., Shieh, S. Y., Ferbeyre, G., Samuelson, A. V., Prives, C., Roussel, M. F., Sherr, C. J., and Lowe, S. W. (1998). E1A signaling to p53 involves the p19(ARF) tumor suppressor. *Genes Dev.* **12,** 2434–2442.

Elmore, L. W., Hancock, A. R., Chang, S. F., Wang, X. W., Chang, S., Callahan, C. P., Geller, D. A., Will, H., and Harris, C. C. (1997). Hepatitis B virus X protein and p53 tumor suppressor interactions in the modulation of apoptosis. *Proc. Natl. Acad. Sci. USA* **94**(26), 14707–14712.

Gannon, J. V., Greaves, R., Iggo, R., and Lane, D. P. (1990). Activating mutations in p53 produce a common conformational effect: A monoclonal antibody specific for the mutant form. *EMBO J.* **9,** 1595–1602.

Gillison, M. L., Koch, W. M., Capone, R. B., Spafford, M., Westra, W. H., Wu, L., Zahurak, M. L., Daniel, R. W., Viglione, M., Symer, D. E., Shah, K. V., and Sidransky, D. (2000). Evidence for a causal association between human papillomavirus and a subset of head and neck cancers. *J. Natl. Cancer Inst.* **92,** 709–720.

Goodwin, E. C., and DiMaio, D. (2000). Repression of human papillomavirus oncogenes in HeLa cervical carcinoma cells causes the orderly reactivation of dormant tumor suppressor pathways. *Proc. Natl. Acad. Sci. USA* **97**(23), 12513–12518.

Haupt, Y., Maya, R., Kazaz, A., and Oren, M. (1997). Mdm2 promotes the rapid degradation of p53. *Nature* **387,** 296–299.

Hawley-Nelson, P., Vousden, K. H., Hubbert, N. L., Lowy, D. R., and Schiller, J. T. (1989). HPV16 E6 and E7 proteins cooperate to immortalize human foreskin keratinocytes. *EMBO J.* **8,** 3905–3910.

Hengstermann, A., Linares, L. K., Ciechanover, A., Whitaker, N. J., and Scheffner, M. (2001). Complete switch from Mdm2 to human papillomavirus E6-mediated degradation of p53 in cervical cancer cells. *Proc. Natl. Acad. Sci. USA* **98**(3), 1218–1223.

Hermeking, H., and Eick, D. (1994). Mediation of c-Myc-induced apoptosis by p53. *Science* **265,** 2091–2093.

Honda, R., Tanaka, H., and Yasuda, H. (1997). Oncoprotein MDM2 is a ubiquitin ligase E3 for tumor suppressor p53. *FEBS Lett.* **420,** 25–27.

Jackson, M. W., and Berberich, S. J. (2000). MdmX protects p53 from Mdm2-mediated degradation. *Mol. Cell. Biol.* **20**(3), 1001–1007.

Jones, D. L., Alani, R. M., and Münger, K. (1997a). The human papillomavirus E7 oncoprotein can uncouple cellular differentiation and proliferation in human keratinocytes by abrogating $p21^{Cip1}$-mediated inhibition of cdk2. *Genes Dev.* **11,** 2101–2111.

Jones, D. L., and Münger, K. (1997). Analysis of the p53-mediated G1 growth arrest pathway in cells expressing the human papillomavirus type 16 E7 oncoprotein. *J. Virol.* **71,** 2905–2912.

Jones, D. L., Thompson, D. A., and Münger, K. (1997b). Destabilization of the RB tumor suppressor and stabilization of p53 contribute to HPV type 16 E7-induced apoptosis. *Virology* **239,** 97–107.

Jones, D. L., Thompson, D. A., Suh-Burgmann, E., Grace, M., and Münger, K. (1999). Expression of the HPV E7 oncoprotein mimics but does not evoke a p53-dependent cellular DNA damage response pathway. *Virology* **258,** 406–414.

Kao, C. C., Yew, P. R., and Berk, A. J. (1990). Domains required for in vitro association between the cellular p53 and the adenovirus 2 E1B 55K proteins. *Virology* **179,** 806–814.

Kern, S. E., Kinzler, K. W., Bruskin, A., Jarosz, D., Friedman, P., Prives, C., and Vogelstein, B. (1991). Identification of p53 as a sequence-specific DNA-binding protein. *Science* **252**(5013), 1708–1711.

Kleijnen, M. F., Shih, A. H., Zhou, P., Kumar, S., Soccio, R. E., Kedersha, N. L., Gill, G., and Howley, P. M. (2000). The hPLIC proteins may provide a link between the ubiquitination machinery and the proteasome. *Mol. Cell* **6**(2), 409–419.

Konig, C., Roth, J., and Dobbelstein, M. (1999). Adenovirus type 5 E4orf3 protein relieves p53 inhibition by E1B-55-kilodalton protein. *J. Virol.* **73**(3), 2253–2262.

Kubbutat, M. H., Jones, S. N., and Vousden, K. H. (1997). Regulation of p53 stability by Mdm2. *Nature* **387,** 299–303.

Lehman, T. A., Modali, R., Boukamp, P., Stanek, J., Bennett, W. P., Welsh, J. A., Metcalf, R. A., Stampfer, M. R., Fusenig, N., Rogan, E. M., *et al.* (1993). p53 mutations in human immortalized epithelial cell lines. *Carcinogenesis* **14**(5), 833–839.

Levine, A. J. (1997). p53, cellular gatekeeper for growth and division. *Cell* **88,** 323–331.

Lowe, S. W., and Ruley, H. E. (1993). Stabilization of the p53 tumor suppressor is induced by adenovirus 5 E1A and accompanies apoptosis. *Genes Dev.* **7,** 535–545.

Lowy, D. R., and Howley, P. M. (2001). Papillomaviruses. *In* "Virology" (B. N. Fields and P. M. Howley, Eds.), pp. 2197–2229. Lippincott Williams & Wilkins, Philadelphia.

Massimi, P., and Banks, L. (1997). Repression of p53 transcriptional activity by the HPV E7 proteins. *Virology* **227,** 255–259.

Medcalf, E. A., and Milner, J. (1993). Targeting and degradation of p53 by E6 of human papillomavirus type 16 is preferential for the 1620+ p53 conformation. *Oncogene* **8**(10), 2847–2851.

Meek, D. W. (1999). Mechanisms of switching on p53: A role for covalent modification? *Oncogene* **18**(53), 7666–7675.

Miyashita, T., and Reed, J. C. (1995). Tumor suppressor p53 is a direct transcriptional activator of the human bax gene. *Cell* **80**(2), 293–299.

Moll, U. M., Laquaglia, M., Benard, J., and Riou, G. (1995). Wild-type p53 protein undergoes cytoplasmic sequestration in undifferentiated

neuroblastomas but not in differentiated tumors. *Proc. Natl. Acad. Sci. USA* **92,** 4407–4411.

Moll, U. M., Riou, G., and Levine, A. J. (1992). Two distinct mechanisms alter p53 in breast cancer: Mutation and nuclear exclusion. *Proc. Natl. Acad. Sci. USA* **89,** 7262–7266.

Momand, J., Zambetti, G. P., Olson, D. C., George, D., and Levine, A. J. (1992). The mdm-2 oncogene product forms a complex with the p53 protein and inhibits p53-mediated transactivation. *Cell* **69**(7), 1237–1245.

Münger, K., Basile, J. R., Duensing, A., Eichten, A., Gonzalez, S. L., Grace, M., and Zacny, V. (2001) Biological activities and molecular targets of the human papillomavirus E7 oncoprotein. *Oncogene* **20,** 7888–7898.

Münger, K., Phelps, W. C., Bubb, V., Howley, P. M., and Schlegel, R. (1989). The E6 and E7 genes of the human papillomavirus type 16 together are necessary and sufficient for transformation of primary human keratinocytes. *J. Virol.* **63,** 4417–4421.

Nagata, Y., Anan, T., Yoshida, T., Mizukami, T., Taya, Y., Fujiwara, T., Kato, H., Saya, H., and Nakao, M. (1999). The stabilization mechanism of mutant-type p53 by impaired ubiquitination: The loss of wild-type p53 function and the hsp90 association. *Oncogene* **18**(44), 6037–6049.

Querido, E., Marcellus, R. C., Lai, A., Charbonneau, R., Teodoro, J. G., Ketner, G., and Branton, P. E. (1997). Regulation of p53 levels by the E1B 55-kilodalton protein and E4orf6 in adenovirus-infected cells. *J. Virol.* **71**(5), 3788–3798.

Ryan, K. M., Phillips, A. C., and Vousden, K. H. (2001). Regulation and function of the p53 tumor suppressor protein. *Curr. Opin. Cell. Biol.* **13**(3), 332–337.

Sarnow, P., Ho, Y. S., Williams, J., and Levine, A. J. (1982). Adenovirus E1b-58 kd tumor antigen and SV40 large tumor antigen are physically associated with the same 54 kd cellular protein in transformed cells. *Cell* **28,** 387–394.

Scheffner, M., Huibregtse, J. M., Vierstra, R. D., and Howley, P. M. (1993). The HPV-16 E6 and E6-AP complex functions as a ubiquitin-protein ligase in the ubiquitination of p53. *Cell* **75,** 495–505.

Scheffner, M., Münger, K., Byrne, J. C., and Howley, P. M. (1991). The state of the p53 and retinoblastoma genes in human cervical carcinoma cell lines. *Proc. Natl. Acad. Sci. USA* **88,** 5523–5527.

Scheffner, M., Nuber, U., and Huibregtse, J. M. (1995). Protein ubiquitination involving an E1–E2-E3 enzyme ubiquitin thioester cascade. *Nature* **373,** 81–83.

Scheffner, M., Werness, B. A., Huibregtse, J. M., Levine, A. J., and Howley, P. M. (1990). The E6 oncoprotein encoded by human papillomavirus types 16 and 18 promotes the degradation of p53. *Cell* **63,** 1129–1136.

Schlamp, C. L., Poulsen, G. L., Nork, T. M., and Nickells, R. W. (1997). Nuclear exclusion of wild-type p53 in immortalized human retinoblastoma cells. *J. Natl. Cancer Inst.* **89**(20), 1530–1536.

Seavey, S. E., Holubar, M., Saucedo, L. J., and Perry, M. E. (1999). The E7 oncoprotein of human papillomavirus type 16 stabilizes p53 through a mechanism independent of p19(ARF). *J. Virol.* **73,** 7590–7598.

Sharp, D. A., Kratowicz, S. A., Sank, M. J., and George, D. L. (1999). Stabilization of the MDM2 oncoprotein by interaction with the structurally related MDMX protein. *J. Biol. Chem.* **274**(53), 38189–38196.

Shvarts, A., Bazuine, M., Dekker, P., Ramos, Y. F., Steegenga, W. T., Merckx, G., van Ham, R. C., van der Houven van Oordt, W., van der Eb, A. J., and Jochemsen, A. G. (1997). Isolation and identification of the human homolog of a new p53-binding protein, Mdmx. *Genomics* **43,** 34–42.

Slebos, R. J. C., Lee, M. H., Plunkett, B. S., Kessis, T. D., Williams, B. O., Jacks, T., Hedrick, L., Kastan, M. B., and Cho, K. R. (1994). p53-dependent G(1) arrest involves pRB-related proteins and is disrupted by the human papillomavirus 16 E7 oncoprotein. *Proc. Natl. Acad. Sci. USA* **91,** 5320–5324.

Steegenga, W. T., Riteco, N., Jochemsen, A. G., Fallaux, F. J., and Bos, J. L. (1998). The large E1B protein together with the E4orf6 protein target p53 for active degradation in adenovirus infected cells. *Oncogene* **16**(3), 349–357.

Stewart, Z. A., and Pietenpol, J. A. (2001). p53 signaling and cell cycle checkpoints. *Chem. Res. Toxicol.* **14**(3), 243–263.

Stewart, Z. A., Tang, L. J., and Pietenpol, J. A. (2001). Increased p53 phosphorylation after microtubule disruption is mediated in a microtubule inhibitor- and cell-specific manner. *Oncogene* **20**(1), 113–124.

Stott, F. J., Bates, S., James, M. C., McConnell, B. B., Starborg, M., Brookes, S., Palmero, I., Ryan, K., Hara, E., Vousden, K. H., and Peters, G. (1998). The alternative product from the human CDKN2A locus, p14(ARF), participates in a regulatory feedback loop with p53 and MDM2. *EMBO J.* **17,** 5001–5014.

Szak, S. T., Pietenpol, J. A. (1999). High affinity insertion/deletion lesion binding by p53. Evidence for a role of the p53 central domain. *J. Biol. Chem.* **274**(6), 3904–3909.

Thomas, J. T., and Laimins, L. A. (1998). Human papillomavirus oncoproteins E6 and E7 independently abrogate the mitotic spindle checkpoint. *J. Virol.* **72**(2), 1131–1137.

Tiemann, F., and Deppert, W. (1994). Stabilization of the tumor suppressor p53 during cellular transformation by simian virus 40: Influence of viral and cellular factors and biological consequences. *J. Virol.* **68,** 2869–2878.

Ueda, H., Ullrich, S. J., Gangemi, J. D., Kappel, C. A., Ngo, L., Feitelson, M. A., and Jay, G. (1995). Functional inactivation but not structural mutation of p53 causes liver cancer. *Nat. Genet.* **9**(1), 41–47.

van den Heuvel, S. J., van Laar, T., The, I., and van der Eb, A. J. (1993). Large E1B proteins of adenovirus types 5 and 12 have different effects on p53 and distinct roles in cell transformation. *J. Virol.* **67**(9), 5226–5234.

Wells, S. I., Francis, D. A., Karpova, A. Y., Dowhanick, J. J., Benson, J. D., and Howley, P. M. (2000). Papillomavirus E2 induces senescence in HPV-positive cells via pRB- and p21(CIP)-dependent pathways. *EMBO J.* **19**(21), 5762–5771.

Werness, B. A., Levine, A. J., and Howley, P. M. (1990). Association of human papillomavirus types 16 and 18 E6 proteins with p53. *Science* **248,** 76–79.

Whitesell, L., Sutphin, P., An, W. G., Schulte, T., Blagosklonny, M. V., and Neckers, L. (1997). Geldanamycin-stimulated destabilization of mutated p53 is mediated by the proteasome in vivo. *Oncogene* **14**(23), 2809–2816.

Wu, G. S., Burns, T. F., McDonald, E. R., 3rd, Jiang, W., Meng, R., Krantz, I. D., Kao, G., Gan, D. D., Zhou, J. Y., Muschel, R., Hamilton, S. R., Spinner, N. B., Markowitz, S., Wu, G., and el-Deiry, W. S. (1997). KILLER/DR5 is a DNA damage-inducible p53-regulated death receptor gene. *Nat. Genet.* **17**(2), 141–143.

Wu, X. W., Bayle, J. H., Olson, D., and Levine, A. J. (1993). The p53 mdm-2 autoregulatory feedback loop. *Genes Dev.* **7,** 1126–1132.

Yew, P. R., Liu, X., and Berk, A. J. (1994). Adenovirus E1B oncoprotein tethers a transcriptional repression domain to p53. *Genes Dev.* **8,** 190–202.

Zauberman, A., Flusberg, D., Haupt, Y., Barak, Y., and Oren, M. (1995). A functional p53-responsive intronic promoter is contained within the human mdm2 gene. *Nucleic Acids Res.* **23**(14), 2584–2592.

Zhang, Y., Xiong, Y., and Yarbrough, W. G. (1998). ARF promotes MDM2 degradation and stabilizes p53: ARF-INK4a locus deletion impairs both the Rb and p53 tumor suppression pathways. *Cell* **92,** 725–734.

Zindy, F., Eischen, C. M., Randle, D. H., Kamijo, T., Cleveland, J. L., Sherr, C. J., and Roussel, M. F. (1998). Myc signaling via the ARF tumor suppressor regulates p53-dependent apoptosis and immortalization. *Genes Dev.* **12,** 2424–2433.

zur Hausen, H. (1996). Papillomavirus infections—A major cause of human cancers. *Biochim. Biophys. Acta* **1288**(2), F55–F78.